The American Mineralogist

Journal of the Mineralogical Society of America

Vol. 33 NOVEMBER-DECEMBER, 1948 Nos. 11 and 12

Contents

Published bi-monthly by the Society

Mineralogical Society of America

ASSOCIATED WITH THE GEOLOGICAL SOCIETY OF AMERICA

President: M. A. Peacock, University of Toronto, Toronto, Canada.
Vice President: Adolf Pabst, University of California, Berkeley, California.
Secretary: C. S. Hurlbut, Jr., Harvard University, Cambridge, Massachusetts.
Treasurer: Earl Ingerson, U. S. Geological Survey, Washington 25, D.C.
Editor: Walter F. Hunt, University of Michigan, Ann Arbor, Michigan.
Councilors: R. E. Grim, Illinois Geological Survey, Urbana, Illinois.
Joseph Murdoch, University of California at Los Angeles, Los Angeles, California.
H. H. Hess, Princeton University, Princeton, New Jersey.
Clifford Frondel, Harvard University, Cambridge, Massachusetts.
M. J. Buerger, Massachusetts Institute of Technology, Cambridge, Massachusetts.

The enlarged issues of this journal for 1948 are made possible by a grant from the Penrose Fund of the Geological Society of America.

The American Mineralogist—Journal of the Mineralogical Society of America

A journal containing articles on mineralogy, crystallography, petrography, and allied sciences, issued every two months. Contributions are invited from everyone.

Office of Publication, Mineralogical Laboratory, Ann Arbor, Mich.

The general conduct of the journal is in the hands of the Editor, Walter F. Hunt, Ann Arbor, Michigan. The council of the Mineralogical Society has appointed the following board of associate editors, to whom should be sent articles dealing with the special subjects indicated:

Michael Fleischer, U. S. Geological Survey, Washington, D.C., *New minerals.*
Samuel G. Gordon, Academy of Natural Science, Philadelphia, Pa., *Mineral museums.*
Esper S. Larsen, Harvard University, Cambridge, Mass., *Optical crystallography.*
Austin F. Rogers, Stanford University, California, *Geometrical crystallography.*
M. N. Short, University of Arizona, Tucson, Arizona, *Mineralography.*
George Tunell, University of California at Los Angeles, *Structural crystallography.*

Contributors of leading articles are given without charge 100 reprints (without covers) of their article. If additional reprints are desired these can be purchased at the following rates:

Pages	*1–4*	*5–8*	*9–12*	*13–16*	*17–20*	*21–24*	*25–28*	*29–32*	*Covers*
Copies									
25	$3.50	$5.00	$ 8.00	$ 9.50	$11.00	$13.00	$15.00	$16.00	$4.90
50	3.80	5.55	8.80	10.40	12.10	14.20	16.40	17.50	5.50
75	4.10	6.10	9.60	11.30	13.20	15.40	17.80	19.00	6.10
100	4.40	6.65	10.40	12.20	14.30	16.60	19.20	20.50	6.70
Addl. C's	1.20	2.20	3.20	3.60	4.40	4.80	5.60	6.00	2.40

Cover Composition $1.55.

Sent to all members and fellows of the Mineralogical Society of America. Subscription price, $3.00 per year (single copies of normal issues, 75¢ plus postage).

Entered as second class matter at the post office at Menasha Wis., under Act of March 3, 1879. Acceptance for mailing at the special rate of postage provided for in section 1103, Act of Oct. 3, 1917, paragraph 4 section 429 P. L. & R. authorized March 13, 1922.

Notices of change of address, orders, and remittances should be sent to Dr. Earl Ingerson, U.S. Geological Survey, Washington 25, D. C.

Printed by the George Banta Publishing Company, Menasha, Wisconsin

NEW Complete Line of BAUSCH & LOMB Stereoscopic WIDE FIELD MICROSCOPES

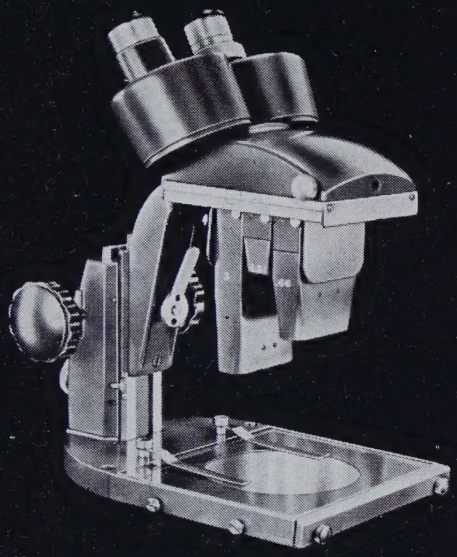

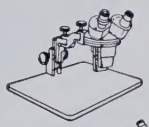

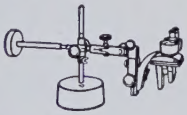

A truly *complete* line of different models. You can select to meet *your* specific needs. Revolutionary design and construction introduces new high standards of optical and mechanical performance.

WIDER FIELDS • HIGHER EYEPOINT
DUST-PROOF NOSEPIECE...Sealed-in Prisms
STURDIER MECHANICAL CONSTRUCTION

WRITE for complete information and a demonstration. Bausch & Lomb Optical Company, 676-Y St. Paul St., Rochester 2, New York.

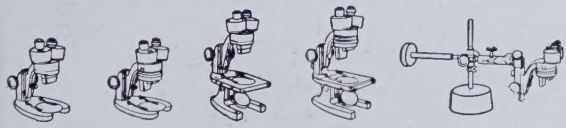

Designed **EXCLUSIVELY**

For MICROSCOPE ILLUMINATION!

NEW SPENCER No. 735 LAMP

Here is the illuminator for advanced microscopy you knew was bound to come . . . with convenient precise controls for critical adjustment . . . with essential optical and mechanical qualities to complement a fine microscope.

COOLER OPERATION. Sturdy die-cast housing dissipates heat.

CRITICAL FOCUSING FROM EITHER SIDE. Rack & pinion movement.

NO TRANSFORMER. Lamp operates from 110 volt outlet.

PRECISION REFLECTOR ADJUSTMENT. So quick, simple, and accurate.

RAPID BULB CHANGE. Lamphouse separates. Hinged lamp chimney opens to reveal bulb and reflector.

PRECISE TILTING. Screw adjustment maintains any angle.

QUALITY OPTICAL SYSTEM. Two plano-convex lens elements.

IRIS DIAPHRAGM. Knurled ring control.

FILTER HOLDER. Choice of single or multiple holder.

Correct illumination is essential for the best results from any microscope objective, eyepiece and condenser. Your instrument deserves the Spencer No. 735. For further details write Dept. L7.

American Optical
COMPANY
Scientific Instrument Division
Buffalo 15, New York

Manufacturers of the **SPENCER** *Scientific Instruments*

FOR SALE

Geological Atlas of the U. S. Geologic Folios, library edition, 18½ x 21½. Numbers 1-70 less numbers 7, 9, 19, 30, 36, 39, 48, 52, 57, 58, 60, 68; 58 in all. Price $95.00.

Kunz—Gems and Precious Stones of North America, 1890. $17.50

Kunz—Ivory and the Elephant, 1916. $15.00

Rosenthal—The Kingdom of the Pearl. Illustrated by Dulac. Number 194 of 675 numbered copies. $10.00

All are in good used condition and are sent postpaid.

COUNTRY BOOK SHOP, HIGHLAND MILLS, NEW YORK

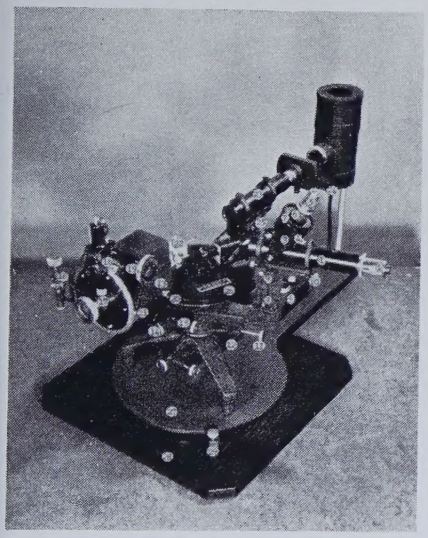

Two-Circle Goniometer

$1000

(without head)

Developed by Prof. C. W. Wolfe
Boston University

Manufactured and Sold
by
Laboratory Associates
60 White Street
Belmont, Mass.

For detailed information write to Laboratory Associates.

The Recently Prepared 200 page Author-Subject
INDEX TO VOLUMES 21-30, 1936-1945, of
THE AMERICAN MINERALOGIST
by
EARL INGERSON, Geophysical Laboratory
and
MICHAEL FLEISCHER, U.S. Geological Survey
is now available

The price is $2.00 to members and subscribers and $3.00 to non-members. The Treasurer will be glad to receive your order now. Address, Dr. Earl Ingerson, U.S. Geological Survey, Washington 25, D.C.

Grieger's

EXCITING *News*

ON SEPTEMBER 15TH WE RELEASED

The New 1948 Edition of our Encyclopedia and Super Catalog of the Lapidary & Jewelry Arts

THIS ENCYCLOPEDIA IS A HANDSOME VOLUME OF NEW AND VALUABLE INFORMATION INCLUDING MUCH THAT HAS NEVER BEFORE APPEARED IN PRINT

• IT IS AN OUTSTANDING NEW BOOK - NOT A CATALOG •

NEITHER TIME, COST OR RESEARCH HAVE BEEN SPARED TO MAINTAIN THE HIGHEST STANDARD OF USEFULNESS AND SCOPE. IT SUGGESTS THINGS TO DO - THE MOST APPROVED METHODS OF DOING THEM AND IS FILLED WITH ILLUSTRATIONS AND INSTRUCTIONS DESIGNED TO FULFILL YOUR EVERY REQUIREMENT.

HERE "IN A GEODE" IS WHAT THE ENCYCLOPEDIA CONTAINS. VERY IMPORTANT CONTRIBUTIONS ON ALL PHASES OF GEM CUTTING PROCEDURES BY SUCH NATIONALLY KNOWN AUTHORS AS - HOWARD - BAXTER - VAN LEUVEN - PEARL AND MERZ. YOU WILL FIND A COMPLETE ARRAY OF IMPORTANT INFORMATIVE BOOKS ON GEM CUTTING AND JEWELRYCRAFT WITH AN EXTENSIVE SECTION ON MINERAL SPECIMENS AND IDENTIFICATION. MATERIALS, TOOLS, SUPPLIES AND ALL THE MAJOR LINES OF LAPIDARY EQUIPMENT INCLUDING SUCH FAMOUS NAMES AS HILLQUIST - HIGHLAND PARK - VRECO - COVINGTON - ALLEN - FELKER - ORCUTT AND POLY PRODUCTS ARE DISPLAYED IN DETAIL.

WE SUPPLY RUF GEM MATERIAL AND PREFORMS
A GREAT CONVENIENCE AND SAVING TO THE GEM WORKER

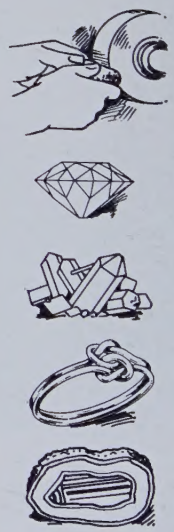

THE ENCYCLOPEDIA AND SUPER CATALOG IS 9"×12" IN SIZE, CONTAINS 160 PAGES AND HAS A SEWED BACK BINDING WITH A PLASTIC LAMINATED COVER. YOU HAVE NEVER BEEN ABLE TO BUY SO MUCH FOR A DOLLAR. OUR FIFTEENTH ANNIVERSARY CATALOG PUBLISHED IN SEPTEMBER 1947, TOGETHER WITH VARIOUS SUPPLEMENTS THAT COMPRISE 80 PAGES 9"×12", IS AVAILABLE FOR 35¢

IN CASE YOU ORDER THE ENCYCLOPEDIA DO NOT ORDER THE 35¢ CATALOG

Grieger's

1633 EAST WALNUT STREET
PASADENA 4, CALIFORNIA.
PHONE SY 6-6423

OPEN ON FRIDAY AND SATURDAY ONLY 8:30AM - 5:30 PM - MONDAY THRU THURSDAY OPEN BY APPOINTMENT ONLY

THE AMERICAN MINERALOGIST

JOURNAL OF THE MINERALOGICAL SOCIETY OF AMERICA

Vol. 33 NOVEMBER–DECEMBER, 1948 Nos. 11 and 12

VERMICULITE AND ITS RELATION TO BIOTITE AS REVEALED BY BASE EXCHANGE REACTIONS, X-RAY ANALYSES, DIFFERENTIAL THERMAL CURVES, AND WATER CONTENT

ISAAC BARSHAD

University of California, Berkeley, California.

TABLE OF CONTENTS

ABSTRACT

Vermiculite is a base-exchange mineral with a high base exchange capacity. The exchangeable bases are Mg exclusively, or Mg and Ca. Base exchange takes place readily without grinding the material. Upon replacing the naturally occurring exchangeable bases of vermiculite with Li, Na, K, NH_4, Rb, Cs, Mg, Ca and Ba, the resulting samples were subjected to *x*-ray and differential thermal analysis and water loss was determined at various temperatures. The results showed that the kind of adsorbed cation determines the expansion of the lattice, its hydration properties and the shape of the differential thermal curve. The properties of K saturated vermiculite closely approximate those of biotite.

By leaching Gruner's hydrobiotite with $MgCl_2$ solution, K ions are replaced by Mg ions with the resulting conversion of hydrobiotite into vermiculite, and by prolonged treatment of biotite with $MgCl_2$ solution, it was converted into a material closely resembling vermiculite.

The results of this investigation seem to justify the conclusion that the exchangeable bases of vermiculite occupy interlayer positions as do K ions in biotite, and that vermiculite is essentially a Mg or Mg plus Ca mica. A new formula for vermiculite with the exchangeable bases in interlayer positions is proposed.

Introduction

In a study of the colloids of California prairie soils, a vermiculite-like substance, or possibly Gruner's hydrobiotite, was found (1). The similarity to vermiculite lay chiefly in the x-ray diffraction pattern and the differential thermal curve. At the time, the soil colloids were thought to differ from vermiculite in that the former had pronounced base exchange property. The structural formula for vermiculite, as given by Gruner (2), does not provide for exchangeable cations. Accordingly, it was decided to investigate the base exchange property of vermiculite. As this work proceeded, other aspects of the subject seemed to need further study. This paper reports the results of this work.

Material Used

(1) Vermiculite from Union of South Africa. Large, pale yellow translucent sheets.
(2) Vermiculite called culsageeite or jefferisite from Culsagee Mine, Macon County, North Carolina. Bronze in color and in large flakes.
(3) Protovermiculite from Magnet Cove, Arkansas. Large golden yellow scales. (This apparently comes from the same source as Gruner's vermiculite no. 2.)
(4) Vermiculite from Libby, Montana. Dark greenish brown scales. (From the same source as Gruner's vermiculite no. 10.)
(5) Vermiculite from Lenni, Delaware County, Pennsylvania. Apple green, compact, and in small scales.
(6) Biotite (source unknown).
(7) Prochlorite from Chester, Vermont.
(8) Chlorite from Chester, Vermont.
(9) Ripidolite from West Chester, Pennsylvania.

Base Exchange Studies

The experimental work is based on the idea that base exchange is represented by the equation:

$$AX + B^{+} \rightleftarrows BX + A^{+}$$

where A^{+} and B^{+} represent solution cations of equal charge, and AX and BX represent the exchange material saturated with A^{+} and B^{+}, respectively. When the exchange material has only one kind of exchangeable cation, the material is said to be saturated with that ion. The total

amount of exchangeable cations is usually expressed as milliequivalents per 100 grams and this quantity is called base exchange capacity.

To demonstrate that a material possesses base exchange property, it is necessary to show that the material will undergo the above reaction. If one starts the reaction with an AX material and B^+ in solution and carries the reaction to completion, it should then be possible to demonstrate the presence of BX and of A^+ in the solution. If the reaction is reversible, it will be possible to reconvert BX into AX by means of a solution of A^+.

The method of effecting base exchange was as follows: A small amount of material (0.5–2.0 grams)—either unground or lightly ground by hand to pass a 100 mesh sieve—was placed in a small beaker containing a neutral normal solution of the desired cation and heated to about 70° C. for several hours. The material was then transferred to a sintered glass bottom crucible under suction. After the solution had passed through the filter completely, the material was transferred back to the beaker with fresh salt solution and the process was repeated two or three times daily for about 10 days. The filtered solutions were analyzed for bases. At the end of this treatment the material was washed free of the salt solution with neutral methanol and dried in the air.

Standard methods of analysis were used for determining the bases replaced from the sample and the bases adsorbed by the material from the solution.

NH_4 Exchange Capacity and the Exchangeable Bases in Natural Vermiculites

The results of leaching vermiculites 1, 2, 3, and 5 with N neutral NH_4Ac, the salt commonly used in the determination of replaceable bases, are given in Table 1. NH_4^+ taken up by exchange was determined by distillation in the presence of NaOH.

It is seen (Table 1) that the NH_4 exchange capacity of vermiculites 1, 2 and 3 is very high but that of vermiculite 5 is considerably smaller. The reason for this difference will appear later.

In the light of the structural formula of vermiculite, as given by Gruner, these results were difficult to explain, for the formula does not show any exchangeable bases. At first an explanation for the large exchange capacity was sought by an early theory for the cause of the base exchange property, which states that adsorbed water molecules dissociate into OH^- and H^+; the OH^- remains on the exchange material and H^+ exchanges for an NH_4^+ or any other cation. Since vermiculite is highly hydrated, this reaction was thought possible, and it was reasoned that if this reaction should take place, a large amount of acidity would de-

TABLE 1. BASES EXCHANGED FOR NH_4^+ BY UNGROUND AND LIGHTLY GROUND VERMICULITES WHEN LEACHED WITH N NEUTRAL NH_4Ac SOLUTION

Milliequivalents per 100 grams air dry material

Vermiculite	Exchangeable Bases					NH_4^+ Adsorbed
	Mg^{++}	Ca^{++}	Na^+	K^+	Σ	
1. Lightly ground	128.3	13.7	0.0	0.0	142.0	141.3
2. Lightly ground	146.0	0	0.0	0.0	146.0	145.5
3. Unground	144.5	0	0.0	0.0	144.5	145.9
4. Lightly ground	40.0	93.0	0.0	0.0	133.0	134.5
5. Lightly ground	65.5	0	0.0	0.0	65.5	64.8

velop in the leaching solution. The vermiculites were therefore leached with N neutral NaCl solution and the pH of the leachate was determined. It was found that the pH of the NaCl solution did not change by passing it through the samples. This led to the conclusion that H^+ was not replaced, and hence the foregoing explanation of the exchange is not acceptable. That the exchange property of the vermiculite was not due to the presence of water, was also shown by the fact that the exchange capacity did not change materially when the material was dehydrated to the extent of losing all the free water as seen in Table 2.

TABLE 2. NH_4^+ ADSORBED BY LIGHTLY GROUND VERMICULITES TREATED WITH H_2O_2 OR HEATED TO VARIOUS TEMPERATURES

Milliequivalents per 100 grams air dry material

Vermiculite	Treatment		
	H_2O_2	110° C.	255° C.
1	146.5	141.0	135.2
2	144.0	143.7	139.0
3	131.0	127.6	88.5
5	65.5	62.4	60.8

That the Mg^{++} and Ca^{++} found in the leachates were actually replaced by NH_4^+ is shown by the fact that Mg^{++}, or $Mg^{++}+Ca^{++}$ found in solution closely approximates NH_4^+ adsorbed. The exchangeable base of samples 2 and 5 is exclusively Mg^{++} whereas samples 1 and 3 contain exchangeable Mg^{++} and Ca^{++}; in sample 1, the base is chiefly Mg^{++}, but in no. 3 the Ca^{++} is more than twice the Mg^{++}.

The Effect of Particle Size on Base Exchange Capacity

To determine whether or not light grinding has any effect on the base exchange capacity of the vermiculites, the base exchange capacity and the exchangeable bases of an unground vermiculite (no. 2) were determined. The results reported in Table 1 show that the exchange capacity and the exchangeable bases were not affected by lightly grinding the material.

As the solution acted on the unground material, a visual picture was presented of the path the ions take in passing in and out of the crystal lattice. Vermiculite no. 2 upon exchanging its Mg^{++} for NH_4^+ changed color from bronze to dark gold. This color change was observed to proceed from the edges towards the center of the plates or sheets, indicating that the ions enter and leave by the edges, and travel in a plane parallel to the tetrahedral layers.

The effect of particle size on base exchange was further studied by treating the hand ground samples with hydrogen peroxide, which, as Gruner (3) showed, produces exfoliation, and this reduces the particles to extreme fineness. As shown by comparing Tables 1 and 2, base exchange capacity was not affected by treating the sample with H_2O_2. The conclusion seems to be warranted that particle size has no effect on the base exchange capacity of vermiculite.

The Reversibility of the Base Exchange Reaction

The reversibility of the base exchange reaction with the vermiculites is readily demonstrated in various ways: (1) by converting the NH_4 vermiculite to Na and Ca vermiculites and reconverting them back to the NH_4 vermiculite without any change in exchange capacity (Table 4); (2) by reconverting the NH_4 vermiculite, Na vermiculite and K vermiculite back to the original Mg vermiculite. These reconversions can best be observed by the use of the differential thermal curves and the *x*-ray diffraction patterns. In Figures 1 and 2 the differential thermal curves of the original Mg saturated vermiculites are given, as well as those of the Na, NH_4 and K forms and also those of the reconverted Mg vermiculites. These curves show that the original Mg vermiculites were reobtained by treating the sample with $MgCl_2$. The *x*-ray diffraction pattern of these vermiculites also give a clear picture of the changes which take place. These changes are most clearly brought out by the basal spacing (*d*002), as may be seen in Table 8. These results verify those of the differential thermal curves in showing that the original vermiculite was reobtained.

Vermiculites saturated with Na^+, K^+ and Ca^{++} were also prepared and the total content of these ions adsorbed was determined by the HF

method for total analysis of silicates (Table 3). Similar determination on the original vermiculites showed that none of these ions were present in sample 2, and only Ca in sample 1, the amount of which just equalled exchangeable Ca^{++}. It is seen in Table 3 that the amount of K^+ adsorbed is higher than Na^+, and Na^+ higher than Ca^{++}. These differences are due chiefly, as will be seen later, to different degrees of hydration of the K, Na, and Ca vermiculites and also, to a smaller extent, to the different molecular weight of these ions.

Table 3. Total Na^+, K^+, and Ca^{++} Adsorbed by Leaching Lightly Ground Vermiculites with N NaCl, KAc, and CaAc

Milliequivalents per 100 grams air dry material

Vermiculite	Na^+	K^+	Ca^{++}
1	155.6	180.0	143.0
2	154.5	177.5	145.0
5		68.0	

Table 4. Bases Exchanged for NH_4 by Vermiculites Saturated With Various Cations When Leached With N Neutral NH_4Ac Solution

Milliequivalents per 100 gram air dry material

Vermiculite	Saturated With	Base Replaced	NH_4 Adsorbed
1	K	K 49.4	50.8
	Mg	Mg 142.0	141.5
2	K	K 28.5	31.0
	Na	Na 146.5	147.0
	Mg	Mg 145.5	146.0
	Ca	Ca 143.0	145.5

The Nature of "K^+ Fixation"

The results given in Tables 3 and 4 show that only part of the K^+ taken up by exchange, was replaced by HN_4^+, whereas Na^+, Mg^{++} and Ca^{++} exchanged completely. The taking up of K^+ in excess of the amount replaceable by NH_4^+ has long been observed with soil colloids (6), and is known as K^+ fixation. The amount thus fixed by soil colloids is much less than by the vermiculites.

The nature of K^+ fixation by vermiculite was investigated (1) by thoroughly leaching K vermiculite with NaCl, $MgCl_2$ and NH_4Ac solu-

tions, and (2) by distillation of the NH_4 vermiculites with various bases until no further NH_3 appeared in the distillate. The results of the leaching experiment (Table 5) show clearly that the fixed K^+ is replaceable by Na^+ or Mg^{++} but to a limited extent only by the NH_4 ion. The distillation experiment (Table 6) shows that adsorbed NH_4^+ is likewise only partially replaceable by K^+ and to a lesser extent by Rb^+ and Cs^+, whereas NH_4^+ is readily replaced by Li^+, Na^+, Mg^{++}, Ca^{++}, and Ba^{++}. It is interesting to note that the amount of NH_4^+ replaced by K^+ is approximately equal to K^+ replaced by NH_4^+ (compare Tables 5 and 6).

TABLE 5. AMOUNTS OF K^+ REPLACED FROM K-SATURATED VERMICULITES BY PROLONGED LEACHING WITH N NEUTRAL NH_4Ac, NaCl, AND $MgCl_2$

Milliequivalents per 100 grams air dry material

Vermiculite	Replaced By		
	NH_4Ac	NaCl	$MgCl_2$
1	49.4	170.9	
2	28.5	166.9	170.5

TABLE 6. AMOUNTS OF NH_4^+ REPLACED FROM NH_4-SATURATED VERMICULITES BY DISTILLATION WITH DIFFERENT BASES

Milliequivalents per 100 grams air dry material

Vermiculite	LiOH	NaOH	KOH	RbOH	CsOH	$Mg(OH)_2$	$Ca(OH)_2$	$Ba(OH)_2$
1		163.2	45.3			164.0		
2	164.4	165.0	31.7	25.4	7.5	165.3	163.5	165.9

Having found that vermiculite has pronounced base exchange property, samples were saturated with different cations by treating them with neutral solutions of corresponding cations. The materials thus obtained were subjected to *x*-ray analysis, differential thermal study, and water content determination at various temperatures.

RESULTS OF *X*-RAY STUDY

An explanation of ion fixation appeared when the *x*-ray patterns of the variously saturated vermiculites were studied (Table 7). Those adsorbed cations which produce contracted lattices are more or less fixed against replacement by a cation which itself produces a contracted lattice, but ions which produce an expanded lattice can replace an ion adsorbed with-

in a contracted lattice apparently by being able to expand the lattice gradually as it enters the lattice from the edges.

As shown in Table 7, vermiculite exhibits remarkable differences when saturated with different cations. These differences are clearly revealed by the x-ray diffraction patterns and also by the differential thermal curves. In the light of this evidence, the moisture content of the

TABLE 7. BASAL REFLECTIONS (d002) FOR VERMICULITES AND BIOTITE SATURATED WITH VARIOUS CATIONS AND DRIED AT VARIOUS TEMPERATURES

Saturating Cation		Mg^{++}	Ca^{++}	Ba^{++}	Li^{+}	Na^{+}	K^{+}	NH_4^{+}	Rb^{+}	Cs^{+}	K^{+} 75% Ca & Mg 25%
Vermiculite No. 2	Air Dry	14.33	15.07	12.56	12.56	12.56	10.42	11.24	11.24	11.97	
Heated to	750° C.	9.40	9.55	10.27	9.55	9.55	10.27	9.25	10.46	11.22	
Heated to	255° C.		12.25 10.20			12.38 10.20					
Vermiculite No. 1	Air Dry	14.33	15.07			12.56	10.42	11.14			
Heated to	750° C.	9.50	9.50			9.60	10.27	9.25			
Heated to	450° C.	13.91 12.48 9.95				12.28 10.49	10.27				
Vermiculite No. 3	Air Dry	14.92									
Heated to	750° C.	9.60									
Vermiculite No. 4	Air Dry	14.33	15.07			12.48	10.34				11.77
Biotite	Air Dry	14.47					10.29				

TABLE 8. BASAL REFLECTIONS (d002) FOR VERMICULITE SAMPLES WHICH HAVE UNDERGONE THE FOLLOWING BASE EXCHANGE REACTIONS: NATURAL X→KX→NaX→MgX

Sample Air Dry	Natural (MgX)	KX	NaX	MgX
Vermiculite No. 1	14.33	10.42	12.56	14.33
Vermiculite No. 2	14.33	10.42	12.56	14.33

variously saturated vermiculite assumes special significance. Accordingly, samples were x-rayed after having been heated to various temperatures. The results show that the lattice contracts as water is expelled.

Measurements of the basal (d002) spacings show the following:

(1) The Mg saturated (natural) material—and Ca saturated materials have the widest spacing—the latter having a slightly wider spacing than the former.

(2) The NH_4, K, Rb, and Cs saturated materials have the narrowest spacing. The spacing of the K saturated material, however, is

identically the same as that of biotite. Not only the 00*l* spacing but also the rest of the spacings are the same as that of biotite.

(3) The Ba, Li, and Na saturated material gave a spacing which is narrower than that of the Mg and Ca saturated material, but wider than that of the NH_4, K, Rb, and Cs saturated material. The difference is approximately the width of one water molecule—2.60 Å.

It is interesting to note that the intensity of the reflections of the *d*002 spacing varied considerably with the exchangeable ion. Following is approximately the order of intensity for the different cations Ca = Mg > Ba = Li = Na = K > Rb > Cs, the last two giving weak, broad, and quite diffused lines.

(4) Upon complete dehydration, at 750° C., the spacings of the Mg, Ca, Na, Li, and NH_4 saturated materials approximate the spacing of talc. The spacing of the Ba and Rb saturated material altered to that of biotite and a small but significant change also took place in the Cs saturated material. On the other hand, heating to 750° C. produced but little change in the spacing of the K saturated material.

Differential Thermal Curves, and Water Content at Various Temperatures

The nature of hydration of the natural vermiculites as well as of vermiculites saturated with the various cations is most clearly revealed by the differential thermal curves shown in Figures 1, 2, 3, and 4. It is seen that three groups of curves were obtained which parallel the three groups of the *x*-ray diffraction patterns—namely, (1) the natural and Ca saturated vermiculites, (2) the Ba, Li and Na saturated vermiculites, and (3) the K, NH_4, Rb, and Cs saturated vermiculites. The significant portion of the curves is found in the endothermic trough, representing water losses, at the lower temperatures. These curves show the following:

(1) The curves for natural and Ca saturated materials have two troughs, the lowest point of the first being at about 150° C. and of the second at about 240° C. for Ca and at about 260° C. for natural vermiculites, the latter being largely saturated with Mg^{++}.

(2) The Ba, Li, and Na saturated vermiculites have only one trough the lowest points of which range from 140° C.–160° C.

(3) The NH_4, K, Rb, and Cs vermiculites have no trough at low temperatures and behave as if they are anhydrous.

Since these troughs represent water losses their significance appears when this water loss is determined for each trough separately.

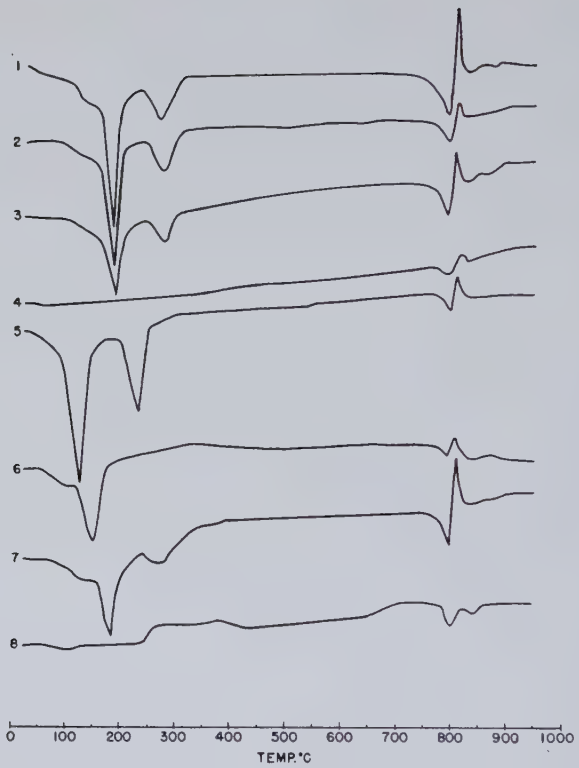

FIG. 1. Differential thermal curves of vermiculite no. 1.
1. natural
2. natural and H_2O_2 treated
3. natural and heated to 550°C. and then rehydrated
4. natural and heated to 800°C. and then rehydrated
5. Ca saturated
6. Na saturated
7. Mg saturated after being Na saturated
8. NH_4 saturated

The results of such determination are given in Tables 9 and 10. They show that the moisture loss corresponding to the first trough was about 12.85 per cent for Mg and Ca saturated material; for the second trough, it was 2.6 per cent, and between 250° C. and 500° C., 1.3 per cent. The moisture loss corresponding to the endothermic break in the curves for Ba, Li, and Na saturated materials was about 8.5 per cent and an additional 2.7 per cent moisture was lost between 150° to 500° C. The K, Rb, and Cs materials showed a loss of about 3 per cent between air temperature and 500° C.

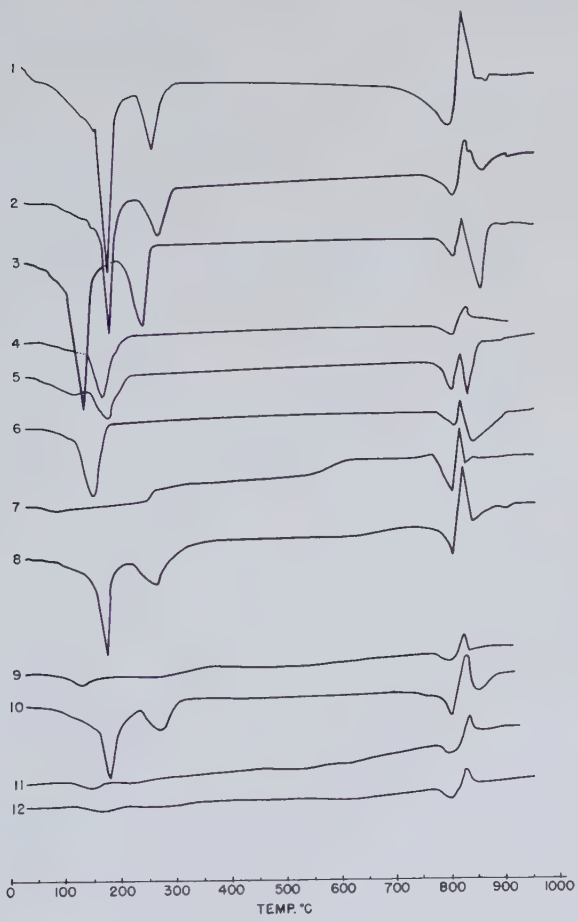

FIG. 2. Differential thermal curves of vermiculite no. 2.

1. natural
2. natural and H_2O_2 treated
3. Ca saturated
4. Ba saturated
5. Li saturated
6. Na saturated
7. NH_4 saturated
8. Mg saturated after being NH_4 saturated
9. K saturated
10. Mg saturated after being K saturated
11. Rb saturated
12. Cs saturated

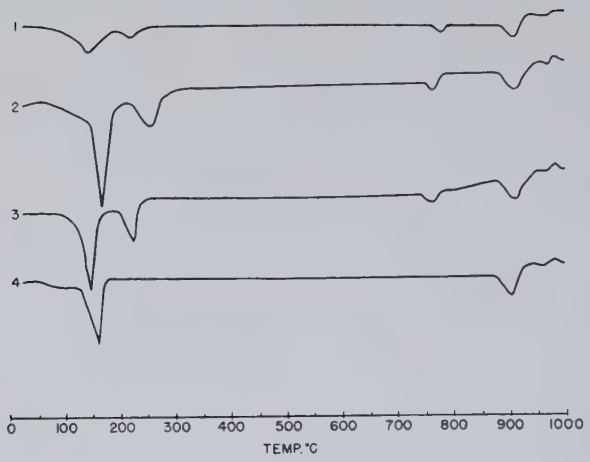

FIG. 3. Differential thermal curves of vermiculite no. 4.
1. natural
2. Mg saturated
3. Ca saturated
4. Na saturated

The moisture content assumes special significance when it is calculated as mols per exchangeable ion (Tables 9 and 10). It will be noted that Mg and Ca saturated vermiculite lost 10 mols H_2O per adsorbed cation when heated to 150° C., 2 mols between 150 and 250° C., and 1 mol between 250 and 500° C. When Ba saturated, 6 mols H_2O per Ba ion were driven off by heating to 150° C., and 2 additional mols upon heating from 150 to 600° C. When Li and Na saturated, 3 mols H_2O per adsorbed ion were driven off by heating to 150° C., and one additional mol upon heating from 150° to 500° C. On the other hand, the total water loss below 600° C. for K, Rb, and Cs saturated vermiculite was about one mol per adsorbed cation.

When the water content of the materials is compared with the expansion of the lattice, the results indicate that Mg and Ca saturated vermiculite expanded a distance equivalent to about two layers of water molecules and the expansion of the Ba, Li and Na vermiculite was approximately equal to one layer of water molecules.

The vermiculites rehydrate very rapidly after having been dehydrated by heating, even when heated to 550° C. Only when heated to 700° C. or higher, does vermiculite lose the property of rehydration. This is well illustrated by curves 1 and 3 of Figure 1, which have almost identical shapes for unheated (no. 1) and for a sample preheated to 550° C. and then exposed to the atmosphere (Curve 3). The rehydration is very rapid with material only slightly ground. This may account for the apparent

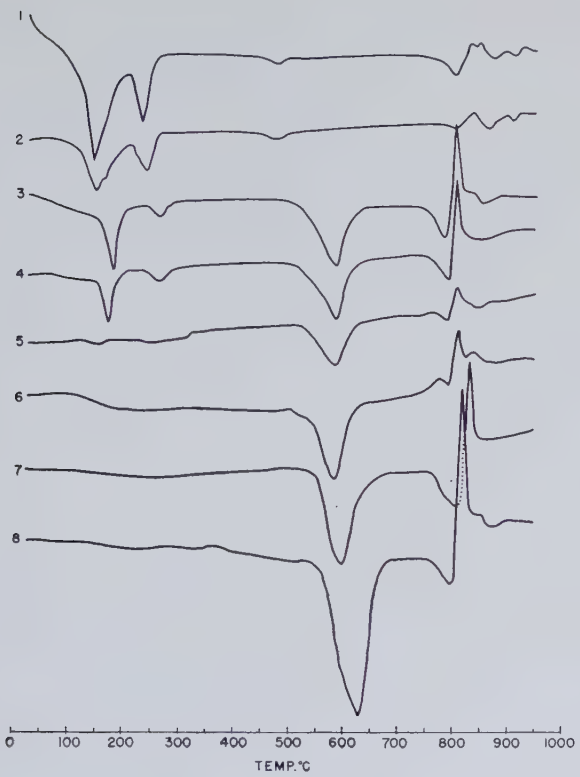

FIG. 4. Differential thermal curves of vermiculites no. 3 and no. 5, prochlorite, chlorite, and ripidolite.

1. natural vermiculite no. 3
2. vermiculite no. 3 H_2O_2 treated
3. natural vermiculite no. 5
4. natural and H_2O_2 treated vermiculite no. 5
5. K saturated vermiculite no. 5
6. prochlorite from Chester, Vermont
7. chlorite from Chester, Vermont
8. ripidolite from West Chester, Pa.

lack of contraction, as reported by Gruner, upon heating vermiculite to 300° or 400° C. It will be noted that samples heated to 255 and 400° C. and then *x*-rayed (Table 7), showed two or more 002 lines. This was probably due to rehydration of a part of the sample during the brief time required to pack the samples in tubes.

As is well known, one of the characteristic properties of vermiculite is that of exfoliation upon sudden heating to a high temperature. It was found, however, that vermiculite loses this property, if the water is driven off slowly by gradually heating to 250° C. The water is lost just

TABLE 9. LOSS IN WATER AT VARIOUS TEMPERATURES FROM VERMICULITE NO. 2 SATURATED WITH VARIOUS CATIONS

Temperatures	20–150° C.		150–250° C.		250–550° C.		150–550° C.		550–600° C.		550–800° C.	Total
Exchangeable Ion	%	Mols H_2O Per Adsorbed Cation	%	Mols H_2O Per Adsorbed Cation	%	Mols H_2O Per Adsorbed Cation	%	Mols H_2O Per Adsorbed Cation			%	%
Mg^{++}	12.85	10	2.65	2	1.32	1					4.59	21.31
Ca^{++}	12.90	10	2.68	2	1.32	1					4.85	21.75
Ba^{++}	8.50	6					2.73	2			3.31	14.54
Li^{+}	8.30	3					2.83	1			4.79	15.92
Na^{+}	8.50	3					2.92	1			4.92	16.34
K^{+}	1.21	0.3					2.46	0.8			2.73	6.40
Rb^{+}	1 50	0.5					1.60	0.5			2.62	5.72
Cs^{+}	1.71	0.5					2.29	0.7			2.26	6.26
							H_2O %	NH_3 %	H_2O %	NH_3 %		
NH_4^{+}	1.67						0.40	0.38	2.57	2.43	4.22	8.86

as readily by unground as by ground material. After being slowly dehydrated, unground vermiculite was then suddenly heated to high temperature, but it did not exhibit exfoliation. This suggests that the exfoliation depends on rapid formation of water vapor between lattice layers.

This property of exfoliation by vermiculite is also lost by saturation with K^{+}, Rb^{+} and Cs^{+}. The loss of this property in these cases is apparently for the same reasons as with the slowly heated natural vermiculites, that is, the absence of water between lattice layers.

TABLE 10. LOSS IN WATER AT VARIOUS TEMPERATURES FROM NATURAL VERMICULITES AND FROM VERMICULITES AND BIOTITE SATURATED WITH VARIOUS CATIONS

Temperatures		20–150° C.		150–250° C.		250–400° C.		400–600° C.	600–900° C.	Total
Vermiculite No.	Exch. ion	%	Mols H_2O per Adsorbed Cation	%	Mols H_2O per Adsorbed Cation	%	Mols H_2O per Adsorbed Cation	%	%	%
1 Natural	Ca, Mg	13.07	10	2.62	2	1.31	1		4.85	21.75
3 Natural	Ca, Mg	11 95	10	2.39	2	1.20	1	0.52	4.28	20.34
5 Natural	Mg	5.79	10	1.32	2	0.65	1	4.09	4.70	16.55
4 Natural	Mg, Ca, K	3.30	10	0.65	2	0.34	1		1.60	5.89
4	Mg	12.30	10	2.48	2	1.21	1		4.10	20.09
4	Ca	12.47	10	2.48	2	1.23	1		4.35	20.53
4	Na	7.46	3	2.35	1				4.50	14.31
4	K	1.20		0.25					1.60	3.05
Biotite 1μ	K	0.34							1.24	1.59
	Mg	12 77		2.70		1.45				

The Nature of the Hydration and the Expansion of the NH_4, K, Rb and Cs Vermiculites

The loss in weight of NH_4 saturated vermiculite is of special interest, because it represents the loss of both water and NH_3. To determine how much of the weight loss was due to NH_3 and how much to H_2O, the loss in NH_3 was determined by difference, that is, the amount of NH_4^+ left after each heating was determined and subtracted from the original amount present. The results show that (*a*) the loss in weight up to a temperature of 255° C. is of water alone, (*b*) the loss between 255° C.—550° C. is relatively small and consists of equal amounts of NH_3 and H_2O in terms of equivalents, (*c*) the loss between 550° C.–600° C. is considerable and also consists of equivalent amounts of NH_3 and H_2O, and (*d*) between 600° C.–800° C. the loss consists of water alone and is equal to the crystal lattice water i.e. OH^- of the octahedral layer. The total amounts of NH_3 lost per 100 grams of air dry NH_4 saturated material amounts to 2.81% or 165 m.e., which is the base exchange capacity of this sample. It is interesting to note that the loss in NH_3 is accompanied by the loss of an equivalent amount of water. This indicates that each NH_4^+ is closely associated with one water molecule and that the energy of binding between them must be large. The combined loss of NH_3 and water causes the unground NH_4 vermiculite to exfoliate upon rapid heating to a high temperature.

The strong association between NH_4^+ and water molecules may explain the slightly wider spacing of NH_4 vermiculite as compared with the heated K vermiculite, as shown in Table 7. Each K ion probably occupies the cavity formed by the hexagonal rings of oxygens in opposite lattice layers and the number of such cavities is about equal to the number of K^+ when fully K saturated. Each of these cavities in the NH_4 saturated material, however, must accommodate not only an NH_4^+ but also a water molecule. Since NH_4^+ is larger than the single cavity, it brings about a slight expansion (0.97Å) of the lattice. A similar situation possibly exists in the Rb, Cs, and K saturated samples, but differences in ion size must be taken into consideration in explaining the different degrees of expansion of the lattice of these materials.

Upon dehydration, the water molecules, which may possibly occupy the cavities formed by the hexagonal rings of oxygens opposite the exchangeable ions, are lost, and as a result, the exchangeable ions can extend into these cavities. If the radius of the exchangeable ion is larger than the radius of a sphere that can just fit into two opposite cavities when lattice layers are just in touch, the lattice will remain expanded. Calculations show that the radius of such a sphere is 1.67Å and that of the radii of K^+, Rb^+ and Cs^+ in a coordination number of twelve (7)

are 1.56Å, 1.67 Å, and 1.84 Å, respectively. It is seen that only the radius of Cs^+ is larger than the radius of the sphere just described and as a result the lattice in which Cs^+ is present remains expanded even after dehydration (Table 7).

Changes at Ignition in the Crystal Lattice of Vermiculite Saturated With Various Cations

An examination of the portion of the differential thermal curve in the neighborhood of ignition temperature reveals a small endothermic effect in the Ba, K, and Rb vermiculites followed by a small exothermic effect, whereas Mg, Ca, Li, and Na vermiculites showed a large endothermic effect followed by a still larger exothermic effect.

Moisture determinations showed that the endothermic effect is caused by loss in water, the magnitude of the effect being proportional to the amount of the water lost (Table 9).

The diffraction patterns of the moderately heated Mg, Ca and Na vermiculites reveal a contracted lattice with basal spacings of 9.95 Å, 10.20 Å and 10.20 Å respectively, which closely approximate the $d002$ spacings of biotite. However, these spacings contracted to 9.40 Å, 9.55 Å, 9.55 Å, respectively upon ignition. This contraction is believed to be responsible for the exothermic effect shown by the differential thermal curves. Since the contraction of the K vermiculite is small—about 0.15 Å—the exothermic effect is likewise small.

Calculations show that the thickness of a single lattice layer is about 10.20 Å. It seems, therefore, that the contraction at ignition represents a change within the lattice layer itself. The loss of the OH ions from the octahedral layer at high temperature is in harmony with this view. The still narrower basal spacing of the heated NH_4 vermiculite (after NH_3 was completely removed) is believed to be brought about by a further contraction. This contraction, however, may be explained by the manner of the superimposition of the hexagonal oxygen rings of the linked tetrahedra of opposite lattice layers. If the layers with a thickness of 9.47 Å are superimposed in a tetrahedral fashion, calculations show that the $d002$ spacing would be 9.15 Å, and this is about the basal spacing observed in the heated NH_4 vermiculite.

The Conversion of Hydrobiotite and Biotite to Vermiculite

Since the x-ray diffraction patterns and hydration properties indicate that K saturated vermiculite closely resembles true biotite, experiments were made to convert by base exchange, biotite and the "hydrobiotite" as described by Gruner (2), into vermiculite.

The materials used in these experiments were vermiculite no. 4, one of the hydrobiotites described by Gruner, and a true biotite.

The experimental procedure employed was similar to that used in reconverting the artificially prepared potassium vermiculite into true vermiculite (Mg saturated) as described previously. Vermiculite no. 4, the so-called hydrobiotite, was converted into Mg, Ca, and Na saturated forms, as well as completely saturated with K^+. The true biotite was converted only to the Mg saturated form.

The conversion of the vermiculite samples took place quite readily both when ground lightly by hand and with unground material exfoliated with H_2O_2. The conversion, however, of biotite was found to proceed very slowly with material only lightly ground. From the path the exchangeable ions take in entering or leaving the lattice of vermiculite, as was shown previously, it was anticipated that the conversion will be most rapid with small particles. This was verified by determining the amount of potassium exchanged in a given time for different particle size fractions as obtained by sedimentation (Table 13). Only material of particle size $< 1\mu$ was completely converted by leaching for a period of three months. Since only small amounts of biotite were used, only x-ray patterns and the water content were determined. The results are shown in Tables 7 and 10. These, however, amply demonstrate the conversion. Sufficient amounts of the converted hydrobiotite were obtained to determine the x-ray diffraction patterns (Table 7), differential thermal curves (Fig. 3), and moisture content (Table 10), and to make additional base exchange studies (Tables 11 and 12).

TABLE 11. BASES EXCHANGED FOR NH_4^+ BY LIGHTLY GROUND OR H_2O_2 TREATED UNGROUND VERMICULITE NO. 4 WHEN LEACHED WITH N NEUTRAL NH_4Ac FOR A PROLONGED PERIOD

Milliequivalents per 100 grams air dry material

Exchangeable Bases				NH_4^+ Adsorbed
Ca^{++}	Mg^{++}	K^+	Σ	
21.4	15.8	0.8	37.0	36.5

The x-ray diffraction patterns, the differential thermal curves, the water content, as well as its relation to the exchangeable ion, and the NH_4 exchange capacity of the converted hydrobiotites clearly show that this hydrobiotite was converted into vermiculite by simple base exchange.

The base exchange studies show that (1) the exchangeable bases of this natural hydrobiotite consist of about 75% K^+, 15% Ca^{++}, and 10% Mg^{++}, (2) that the water content of the natural material is due to the presence of the exchangeable Ca^{++} and Mg^{++}, and (3) that the K^+ exchanges for NH_4^+ to a very limited extent but quite readily for Mg^{++}, Ca^{++}, or Na^+.

TABLE 12. BASES REPLACED FROM NATURAL VERMICULITE NO. 4 WHEN LEACHED WITH N NEUTRAL $MgCl_2$ SOLUTION, AND NH_4^+ ADSORBED BY THE Mg SATURATED SAMPLE

Milliequivalent per 100 grams air dry material

Exchangeable Bases				NH_4^+ Adsorbed	
Replaced by Mg	Replaced by NH_4^+		Σ	On basis of natural material	On basis of Mg saturated material
K^+	Ca^{++}	Mg^{++}			
121.5	21.4	15.8	158.7	160.0	138.2

The *x*-ray diffraction patterns and the water content of biotite converted to the Mg saturated form, are also identical to that of Mg saturated vermiculites, as may be seen in Tables 7 and 10. It is interesting to point out that the amount of water that was gained by biotite upon leaching with a salt solution is proportional to the K^+ replaced and depends on the kind of ion which replaced it. For example, one sample of

TABLE 13. THE REPLACEMENT OF INTERLAYERED POTASSIUM FROM VARIOUS SIZED PARTICLES OF BIOTITE* BY LEACHING WITH SOLUTIONS OF $MgCl_2$, $CaCl_2$, AND NaCl

Milliequivalents per 100 gram air dry material

	$MgCl_2$	$CaCl_2$	NaCl
Fraction			
1–5μ	81.3		17.7
5–50μ	13.9	8.1	4.4
>50		3.3	

* These biotite fractions were leached for two months with the respective salt solutions prior to the additional three weeks of leaching during which the potassium replaced was determined.

biotite, when leached with a $MgCl_2$ solution, lost 82.8 m.e. K per 100 grams, and gained 9.34% water (at 250° C.), or about 12.5 water molecules per exchangeable ion; another biotite sample when leached with a $MgCl_2$ solution lost 57.5 m.e. K per 100 grams and gained 5.78% water (at 140° C.) or about 11 water molecules per exchangeable ion.

THE STRUCTURAL FORMULA OF VERMICULITE

The structural formula of vermiculite as given by Gruner and later by Hendricks and Jefferson is: $(OH)_2(Mg,Fe)_3(Si,Al,Fe)_4O_{10}.\ 4H_2O$.

Although this formula indicates isomorphous substitution of Al and Fe^{+++} for Si ions in the tetrahedral layer, the charge resulting from this substitution apparently was assumed to be balanced by the presence of Fe^{+++} in the octahedral layer, and not by cations between lattice layers. Essentially this structure is that of a neutral lattice similar to talc with water molecules between the layers. The first indication that this formula is not entirely satisfactory was Gruner's preparation of NH_4-micas from vermiculites (3). On the basis of his formula Gruner could not find a satisfactory explanation for the conversion of supposedly neutral talc-like layers of the vermiculite to charged layers of the mica type. The existence of charged water molecules was postulated but no further work was done to substantiate it.

The results reported in this paper show clearly that vermiculite is essentially a mica with Mg^{++} or Mg^{++} and Ca^{++} instead of K^+ occupying interlayer positions, and that these cations can readily be exchanged for other cations some of which produce the true mica structure. It has also been shown that biotite and Gruner's hydrobiotite can be converted into vermiculite.

These results indicate that the structural formula of vermiculite as proposed by Gruner needs modification. Some provision must be made for the interlayer exchangeable cations. Essentially the only structural difference between vermiculite and mica is that layers of water are present in the natural vermiculites or vermiculite artificially prepared from biotite, whereas such water is absent from ordinary mica.

Accordingly chemical formulas were calculated from the analyses of vermiculites listed by Gruner (2), using Harvey's (4) method. The amount of each cation found by analysis is calculated per 22 negative charges which corresponds to the summation of negative charges of a lattice half unit of mica. The cations were distributed as follows: (*a*) All the silica was placed in tetrahedral coordination, and enough Al^{+++} and Fe^{+++} to make a total of four. (*b*) the remaining Al^{+++} and Fe^{+++} together with Fe^{++}, Ti, Mn, Ni, Cr, and enough Mg ions to fill the three positions, were assigned to octahedral coordination. (*c*) The remaining Mg^{++} and all the Ca^{++} were assigned to interlayer positions. This manner of distributing the Mg ions between the octahedral and interlayer position results in a minimum of interlayer cations. The actual distribution, however, of the Mg ion may not necessarily be as indicated. There is no valid reason for filling all the three octahedral spaces and consequently Mg ions may be shifted from octahedral to interlayered position. The only means at our disposal of ascertaining the actual distribution of the Mg ions is by determining the interlayered cations by means of base exchange. Calculations, nevertheless, will indicate the degree of iso-

TABLE 14. CALCULATED DISTRIBUTION OF CATIONS IN A LATTICE LAYER OF VERMICULITE

Sample No. (Gruner 2)	Tetrahedral Coordination			Octahedral Coordination							Interlayered			Interlayered m.e./100 grams air dry basis	H_2O Mols
	Si	Al	Fe^{+3}	Al	Fe^{+3}	Fe^{+2}	Ni	Mn	Mg	Σ	Mg	Ca	Σ	Σ	
2	2.760	1.240		.145	.471	.010		.006	2.368	3.000	.153	.171	.324	133.1	4.73
3	2.655	1.345		.352	.288	.038			2.322	3.000	.360		.360	148.8	4.76
4	2.863	1.045	.092		.579	.055			2.366	3.000	.276	.036	.314	130.5	4.31
5	2.907	1.093		.498	.166	.063	.148		2.125	3.000	.218	.005	.223	93.4	4.45
8	2.721	1.279		.295	.450	.076			2.179	3.000	.271		.271	112.0	4.69

morphous substitution of Al and Fe^{+++} for Si ions and whether or not the remaining cations exceeds the number required to fill the three octahedral positions.

The calculated lattices are given in Table 14. It may be seen that the extent of the isomorphous substitution of Al and Fe^{+++} for Si ions is within the range found in the micas. It is interesting to note that some of the values obtained for the interlayer cations lie in the range obtained experimentally for vermiculite no. 1, 2, and 3 reported herein. The values for the interlayer cations which are considerably less than those obtained experimentally may indicate that Mg ions should be shifted from the octahedral to interlayer positions.

Regardless of the difficulty of determining by calculation the right amount of interlayer Mg, the calculations support the experimental findings that Mg and Ca ions are present in interlayer positions in vermiculite.

Taking into consideration the experimental results as well as the calculated results for interlayer cations, the formula for vermiculite may be written as follows:

$$(H_2O)_x(Mg,Ca)_y(Al,Fe,Mg)_z(Si,Al,Fe)_4O_{10}(OH)_2$$

where x represents mols of H_2O, y, the interlayer ions, which may range from 0.22–0.36, and z, the octahedral ions, 3 or less. The exact quantities of x, y, and z can only be determined experimentally.

Verification of the Existence of Vermiculite-Chlorite Mixtures

As a result of calculating the distribution of cations in the lattice for certain vermiculites, Hendricks and Jefferson (5) found that there are too many magnesium ions to fill the three octahedral spaces available for cations. Such a surplus also appears in Table 14. Hendricks and Jefferson concluded "that the surplus of atoms with octahedral coordination is that they are partially present in brucite-like layers, $R_3^{++}(OH)_6$ between the talc layers thus forming a chlorite-like structure." This conclusion has been only partially verified, for only in certain vermiculites does the excess of octahedral ions indicate a chlorite like structure, whereas in others, as has already been shown, the surplus ions are present as exchangeable ions, and therefore they occupy interlayer positions.

The existence of a vermiculite-chlorite like structure as proposed by Hendricks and Jefferson was verified experimentally, however, by x-ray and thermal methods. Base exchange determination and dehydration data also yielded supporting evidence. The sample of vermiculite from Lenni-Delaware Co., Pa., (sample no. 5) is apparently a vermiculite-

chlorite. The base exchange capacity of this sample was 65 m.e. as measured by the NH_4^+ adsorbed, and the exchangeable base was found to be Mg^{++} (Table 1). This low NH_4 capacity, as compared with the other vermiculites, was not due to the presence of K^+, as in the vermiculite from Libby, Montanta, for K^+ was absent from this sample, and the amount of K^+ the material was able to adsorb by exchange was equal to the NH_4 capacity as seen in Table 3.

The water content of this vermiculite at low temperature, as seen in Table 10, was less than in the true vermiculite but its relation to the exchangeable base was identical to that of the true vermiculites as seen in Tables 9 and 10.

Both of these properties indicate a similarity to the true vermiculites. They only differ in magnitude, being about half those of the true vermiculites.

The differential thermal curve of this sample together with those of two chlorites and a prochlorite are given in Figure 4. It is clearly seen that the portion of the curve at the lower temperature is similar to that of true vermiculite, whereas the portion of the curve at high temperatures is similar to that of the chlorites.

Table 15. Interplanar Spacings of Vermiculite, Mg-Saturated Biotite, and Natural and K-Saturated Vermiculite No. 5, and Ripidolite

Vermiculite No. 1 and No. 2	Mg-Saturated Biotite	Vermiculite No. 5 Natural	Vermiculite No. 5 K-Saturated[1]	Ripidolite Natural	Ripidolite K-Saturated[2]
14.33Å	14.47Å	14.47Å	14.47Å	14.47Å	14.47Å
			10.50	—	
		7.23	7.23	7.16	7.16
		4.77	4.77	4.76	4.76
4.55	4.55	4.55	4.55	4.55	4.55

[1] Intensity of the reflections were weak.

[2] No change in intensity of the reflections.

The x-ray diffraction patterns of the natural materials also reveals a very clear distinction between the true vermiculite and the true chlorites. The clearest distinction is shown by the wide spacings. The first and second spacings of vermiculites 1 and 2, and the vermiculites prepared from hydrobiotite and the biotite are found at about 14.33 Å and 4.55 Å, and no other spacings appear between these two (Table 15). The chlorites—ripidolite and prochlorite, however, have two additional spacings which lie between the 14.33 Å and the 4.55 Å spacings; namely at about 7.20 Å and at about 4.76 Å, with intensities about equal to

that of the 14.33 Å line. As was shown previously, when the true vermiculite is saturated with potassium, the x-ray pattern obtained is that of biotite. In contradistinction to vermiculite it was found that when ripidolite and prochlorite were leached with potassium salts no change took place in their x-ray diffraction pattern.

The x-ray diffraction pattern of the natural vermiculite-chlorite sample under discussion was similar to that of chlorite (Table 15) with the exception that the intensity of the 7.2 Å line was only about half that of the 14.47 Å line. The difference between the true chlorite and this vermiculite-chlorite was best brought out when the latter was saturated with K. The x-ray pattern of chlorite remained, but the intensities of the 14.47 Å, 7.23 Å and the 4.76 Å spacings were greatly weakened. A new spacing, that of biotite, appeared at about 10.4 Å the intensity of which was very weak.

The foregoing together with the results obtained by Gruner indicate that there are four general classes of vermiculite-like minerals found in the state of nature, namely, (1) true vermiculite in which Mg^{++} occupies interlayer positions corresponding to K^+ in biotite. This material contains water between lattice layers. (2) Vermiculite-biotite mixtures, (3) vermiculite-chlorite mixtures, and (4) biotite-chlorite mixtures. Gruner's sample 11 appears to belong in the last named class.

In a paper to follow, certain aspects of the present investigation will be considered from a point of view not adequately covered herein. The relations of vermiculites to the three layer clay minerals will also be discussed.

Summary

1. It has been shown that vermiculite has pronounced base exchange property. Its base exchange capacity is approximately 50 per cent greater than of montmorillonite. The exchangeable cation in certain samples is exclusively Mg. Samples from other localities contain exchangeable Mg and Ca ions.

2. The exchange process is reversible as between Na, Ca, Mg, and K ions, but not completely as between K, NH_4, Rb, and Cs ions. The latter behavior of the exchange process has been known as "fixation."

3. Large flakes of vermiculite undergo base exchange upon leaching with salt solutions almost as readily as fine grained samples.

4. One of the most unique properties discovered is that the kind of exchangeable ion present between the lattice layers determines: (*a*) the degree of expansion of the lattice, and (*b*) the degree of hydration and the nature of the differential thermal curves of the material.

5. When K saturated, the properties of vermiculite closely approximate those of ordinary biotite.

6. Gruner's hydrobiotite may be looked upon as ordinary biotite interleaved with vermiculite containing replaceable Mg and Ca ions. It can be converted completely into vermiculite by leaching with $MgCl_2$ solution or into biotite by leaching with KCl solution.

7. It was shown that vermiculite may be interleaved with chlorite as Hendricks et al. suggested.

8. Ordinary biotite can be converted into vermiculite by prolonged leaching with $MgCl_2$ solution.

9. It follows therefore that vermiculite is simply Mg mica with Mg ions playing the same role as K ions play in micas.

10. A new formula is proposed for vermiculite.

References

1. Barshad, I., A pedologic study of California Prairie soils: *Soil Sci.*, **61,** 423–442 (1936).
2. Gruner, J. W., The structure of vermiculites and their collapse by dehydration: *Am. Mineral.*, **19,** 557–574 (1934).
3. Gruner, J. W., Ammonium mica synthesized from vermiculite: *Am. Mineral.*, **24,** 428–433 (1939).
4. Harvey, C. O., Some notes on the calculation of molecular formulas for glauconite: *Am. Mineral.*, **28,** 541–543 (1943).
5. Hendricks, S. B., and Jefferson, M. E., Crystal structure of vermiculites and mixed vermiculite-chlorites: *Am. Mineral.*, **23,** 851–862 (1938).
6. Martin, J. C., Overstreet, R., and Hoagland, D. R., Potassium fixation in soils in replaceable and nonreplaceable forms in relation to chemical reactions in the soil: *Soil Sci. Soc. Am. Proc.*, **10,** 94–101 (1945).
7. Pauling, L., The nature of the chemical bond: *Cornell Univ. Press* (**1940**).

PROGRESS IN SILICATE STRUCTURES*

John W. Gruner,
University of Minnesota, Minneapolis, Minnesota.

Introduction

Once a year the members of each scientific society are asked to listen to an address by its retiring president. One of the favorite subjects of such an address is a review of recent work which falls within the scope of the speaker's principal interests. My address, therefore, will be a review of the work in silicate structures of the last ten years. This decade has not been as startlingly full of discoveries in this field as the previous one, largely because many investigators equipped with better apparatus and mathematical tools, invaded organic chemistry as well as other fields unfamiliar to a mineralogist.

In the time at my disposal, I will not be able to cover more than an outline of the progress in silicate studies. I will not even touch on ceramics and cement products, interesting as they are.

Classification of Structures

W. L. Bragg proposed a structural classification of the silicates in 1930 which, with a few changes, has stood the test of time. Berman (1937) followed Bragg closely with his "Constitution and Classification of the Natural Silicates." Strunz introduced a new concept in 1937 by proposing that any tetrahedra containing as cations P, As, S, B, Be, Zn, Fe, or Mg be considered structurally similar to tetrahedra of Si and Al. There is no question regarding the validity of his reasoning. This places, however, all Be silicates into other classes, the majority of them among framework structures. Boron silicates are partly affected. Willemite and hemimorphite become frameworks. The melilite group also joins the sheet structures from its former classification as finite groups, and there are other changes. Eitel (1941, page 15) in his encyclopedic work "Physikalische Chemie der Silikate," agrees with Strunz in general, though he indicates that on the basis of the infrared reflection spectrum the older classification may be better. The speaker favors the original one for the simple reason that it was designed for the silicates (including those in which Al replaces Si), regardless of the presence of other tetrahedral configurations. Our discussion will follow this older order.

* Address of the retiring President of the Crystallographic Society of America, delivered at the annual meeting of the Society at Yale University, April 1, 1948.

Isolated SiO_4 Tetrahedra

Apparently there have been no new structures discovered in this group unless those compounds are included which resemble, and are isomorphous with, phosphate structures. Ellestadite, as McConnell (1937) has shown, has the apatite structure, but contains in place of PO_4 tetrahedra, approximately equal numbers of SiO_4 and SO_4 tetrahedra. Klement (1941) has succeeded in synthesizing this mineral in the F as well as (OH) variety. Hägle and Machatschki (1939) describe the mineral britholite as a cerium silicate-apatite in which SiO_4 and PO_4 tetrahedra occur together in the ratio of 2:1.

Strunz (1942) thought that he had found another silicate with the apatite structure in the highly complex and rare earth silicate *steenstrupine*. Machatschki, in a reply in 1943, claimed that this mineral is not related to apatite but has a structure still unknown. There have been some interesting isotypic and isomorphous series described which, though only partly among the silicates, may be worthy of mention. O'Daniel and Tscheischwili (1943) found the following minerals and compounds to be isomorphous:

low-Ca orthosilicate	low-Ca_2SiO_4
glaucochroite	$(Mn, Ca)_2SiO_4$
tephroite	Mn_2SiO_4

They (1941 and 1942) were able to show with the aid of the crystal structure of sodium beryllium tetrafluoride, Na_2BeF_4, which is isotypic with low-Ca_2SiO_4, that the latter is orthorhombic and has the structure of olivine. Since Ca has a coordination of 6 in this low temperature form, they argue that the two high temperature forms which are important in slags and cements must have a lower coordination for Ca, probably of 4, which makes these silicates very reactive, a view also held earlier by Brandenberger.

O'Daniel and Tscheischwili (1942) also showed that the Ba and Sr orthosilicates, Ba_2SiO_4 and Sr_2SiO_4, are isotypic with potassium beryllium tetrafluoride, K_2BeF_4 and, therefore, with low-K_2SO_4 and a large group of other sulfates and chromates. The large cations are surrounded by 9 and 10 oxygen ions. Bredig (1945) finds that high Ca_2SiO_4 has the same structure as low K_2SO_4 and defends his view that Ca has a higher coordination in high-Ca_2SiO_4 than in low-Ca_2SiO_4, which is in opposition to the opinion of O'Daniel and Brandenberger. He also shows that merwinite, $Ca_3Mg(SiO_4)_2$, has practically the same structure as high-Ca_2SiO_4 and for this reason suggests that merwinite is not a definite compound but a high temperature isomorphous mixture of forsterite in high-Ca_2SiO_4. The forsterite component acts as a stabilizer in this instance. The dis-

cussion of these compounds of Ca_2SiO_4 and K_2SO_4 sounds confused, because Ca_2SiO_4 has four polymorphs which are named γ, β, α' and α, and K_2SO_4 has two, β and α. This is the order used from low to high temperature and, therefore, is the reverse of that customarily used for minerals.

This discussion of isolated tetrahedra structures would not be complete without mention of the isotypes of the garnet structures. Pabst (1937) described the structure of plazolite, $Ca_3Al_2(SiO_4)_2(OH)_4$, in which one of the SiO_4 groups is replaced by four hydroxyl groups. Still more unusual are the artificial hydrogarnets or garnetoids in which nearly all the tetrahedral SiO_4 positions are occupied by (OH) groups, as for example, $Ca_3Al_2(OH)_{12}$, according to Flint, McMurdie and Wells (1941).

Finite Groups

$CaSiO_3$ occurs in three modifications, pseudowollastonite, wollastonite, and parawollastonite. The structure of the latter, which is the monoclinic form, has been determined in detail by Barnick (1936). It is supposed to consist of Si_3O_9 rings which lie in planes normal to the *b* axis. The morphological and other properties of the mineral do not suggest such a structure, however.* As the triclinic wollastonite is very similar morphologically to parawollastonite, its structure may be assumed to resemble it closely. Bustamite (Peacock, 1935), vogtite, pectolite, and schizolite, which are isomorphous with wollastonite, should have comparable structures. Since some of these minerals contain an (OH) in place of an O, does this mean that the hydroxyls are tied to the Si ions? This has been thought unlikely in the past. It is of considerable interest that O'Daniel (1943) discovered that the sodium beryllium fluoride $NaBeF_3$ has the same structure as wollastonite and can be used as a model structure.

The detailed structure determination of rhodonite is still missing. Rhodonite possesses isomorphous relatives containing (OH) groups in babingtonite, and inesite, which have been investigated by Richmond (1937 and 1942).

According to Belov (1942), dioptase, $CuSiO_3 \cdot H_2O$, has a structure similar to beryl with hexagonal rings of SiO_4 tetrahedra. He assigns to catapleiite $Na_2Zr(Si_3O_9) \cdot 2H_2O$, a trigonal ring similar to that in benitoite. While these two structures had been predicted in these minerals, Belov seems to be responsible for complete determinations. Though the structure of cordierite, $Al_3Mg_2(Si_5Al)O_{18}$, had been known in a general way for over ten years, the details of it were not worked out until 1942 by Bystrom. He confirms its beryl-like structure.

* Several members of the Society, in particular Miss Gabrielle Hamburger, expressed the same opinion.

The structure of tourmaline in its main features has been determined by Gabrielle Hamburger and M. J. Buerger (1948).* It consists of hexagonal rings of SiO_4. The arrangement of the rings gives polarity to the structure. The rings are held together by the other cations including Al in octahedral coordination.

Chain Structures

Chain structures are largely limited to pyroxenes, amphiboles, and a few minerals which seem to provide the link between chain and layer structures. Though pyroxenes and amphiboles represent chemically highly complicated isomorphous mixtures, the structures themselves seem to display fewer complications than other silicates. Little work has been published on the pyroxenes in the last decade. It would be of interest to know, for example, what the maximum ratio of Al to Si ions in a single chain can be, and how this ratio compares with Al to Si tetrahedra ratios in other silicates. Such a statistical study might throw some light on the stability of pyroxene chains. Based on a study of pyroxenes by Niggli (1943) the speaker has computed a few of the highest ratios of Al to Si in the tetrahedra of the single chains. The highest value in a titanaugite from Aberdeenshire is 1:2.6. The next highest is about 1:3.

The lithium pyroxene spodumene changes to a new phase on heating to about 1000° to 1100° C. which has been called β-spodumene. This decomposition product has no chain structure but consists of a framework of tetrahedra of Si and Al similar to quartz and eucryptite, according to a still unpublished work by Gruner and Ellestad.

The amphiboles are almost the only representatives of double chain structures. Two recent papers by Hallimond (1943) and A. N. Winchell (1945) give us an excellent idea of the distribution of the ions in these complicated substitution structures. Here the maximum substitution of Al for Si tetrahedra reaches a ratio of 1 to 3 in the *Ca-bearing* amphiboles, which is probably not exceeded in any of the others.

One of the chain (or layer) structures still very imperfectly known is serpentine in its two dimorphs, antigorite and chrysotile. According to recent work by Warren (1941) and Aruja (1944) both are probably layer structures and not double chains as originally described. The layers would resemble those of kaolinite closely, but the presence of Mg in place of Al in chrysotile would cause the strained layers to grow no wider than probably 30 to 100 Å. The result would be ribbon-like fibres, according to Warren. It is very interesting that serpentine seems to change directly to forsterite without passing through the amorphous phase (except for the excess SiO_2) on heating to about 600° C. This observa-

* Described more fully in *Am. Mineral.*, **33**, 532–540 (1948).

tion, made by Gruner (1939) and Hargreaves and W. H. Taylor (1944), is particularly noteworthy, as the single chain structure of enstatite is more closely related to serpentine than is the structure of forsterite, and one might have expected enstatite for this reason. Even more surprising is the fact, first observed by Hargreaves and Taylor (1944), and confirmed and carried further by Gruner (unpublished experiments) that chrysotile fibres after decomposition above 600° C. give a fairly well defined rotation photograph, which means that forsterite now either exists as a single crystal in the fibre or as many crystals, all possessing identical orientation. These heated fibres show parallel extinction. Therefore, one of the three crystallographic axes of forsterite must be parallel to the fibres. Inspection of the rotation photograph indicates that the c axis of forsterite is parallel to the axis of the original fibre. In terms of structural bonds, this would mean that the SiO_4 tetrahedra separate on heating, but the MgO_6 octahedra retain their linkages. Held at a temperature of 1200° to 1300° C., one of the enstatite phases will appear as an additional compound in the fibres or powders as shown by the strongest lines of enstatite in the film. The enstatite is visible as minute grains but shows no orientation. Definite proof of the presence of enstatite may be had by dissolving out the forsterite with acid and x-raying the residue. The reactions in the solid state take place as follows:

$$\underset{\text{serpentine}}{Mg_6Si_4O_{10}\cdot(OH)_8} \xrightarrow[\text{and above about 1100° C. or 1200° C.}]{\text{Above 550° C. to about 1000° C.}} \underset{\text{forsterite}}{3Mg_2SiO_4} + \underset{\text{amorphous}}{SiO_2} + 4H_2O$$

$$\underset{\text{forsterite}}{3Mg_2SiO_4} + \underset{\text{amorphous}}{SiO_2} \rightarrow \underset{\text{forsterite}}{2Mg_2SiO_4} + \underset{\text{enstatite}}{2MgSiO_3}$$

Thilo (1939 and 1941) and associates made a number of experiments on the stability of talc, anthophyllite, tremolite, and enstatite. A bundle of fibres of anthophyllite after heating at 1000° C. gives a rotation photograph of enstatite fibres which shows clearly that the double chains have split lengthwise resulting in single chains. Thilo explains this division by the elimination of (OH) groups in the structure. This seems a plausible suggestion, for amphiboles with fluorine substituting for (OH) have been grown from melts, according to Scheumann and Lüdke, while (OH) amphiboles have never been synthesized.

Attapulgite, $Mg_5Si_8O_{20}(OH)_2\cdot 8H_2O$, is a clay mineral with a double chain structure related to that of the amphiboles. It has large spaces between the chains, containing H_2O molecules, according to W. F. Bradley (1940). Since sepiolite and such indefinite Mg-silicates as mountain cork give very similar x-ray powder photographs, it may be assumed that they have practically the same structures as attapulgite. The monoclinic

structure of epidote, $Ca_2O \cdot (Al, Fe)O_2OH \cdot Al \cdot Al \cdot Si_3O_9$, has been investigated recently by Ito (1947). He arrives at an unusual chain or band structure of Si and Al tetrahedra, which is parallel to the *b*-axis of the mineral. This composite band, $(Si, Al)_4O_9$, is the basic structure. The distortions of the SiO_4 tetrahedra are so extreme that one wonders whether considerable adjustments of parameters will not be necessary in a future study. Ito regards zoisite a twinned epidote (or rather a twinned clinozoisite).

Sanbornite, $Ba_2Si_4O_{10}$, notwithstanding a similar formula, is not similar in structure to gillespite, $BaFeSi_4O_{10}$. The latter has a layer structure according to Pabst (1943). Hendricks (1942) has suggested that sanbornite is made up of sets of chains of Si_3O_8 similar to those in epididymite, which may also be interpreted as sheets of Si_4O_{10}, as pointed out under layer structures.

Layer Structures

Many investigators have been busy on the members of this structure type. Though most of these structures have the same pattern of endless tetrahedral $(Si, Al)_4O_{10}$ layers, to which are attached octahedral metal oxygen layers, the possible combinations and variations of them appear to be inexhaustible. A. N. Winchell (1942) has classified the micas into hepta- and octophyllites, depending upon the total number of cations associated with their simplest chemical molecules. Considering the complexity of the chemical compositions, it is surprising that this classification holds good in the great majority of the structures as shown by Hendricks and Jefferson (1939), Stevens (1938) and others. In other words, any isomorphous mixing between heptaphyllites and octophyllites is not common. An interval exists between the octophyllites, which have most of their three octahedral positions occupied, and the heptaphyllites, which have only two or slightly more than two filled. The resulting holes in these pseudohexagonal layers give rise to different symmetry elements depending on the shifts, rotations and stackings of the hexagons. According to Hendricks and Jefferson (1939) hexagonal, monoclinic and triclinic unit cells result, many of superlattice dimensions. In addition to such complications, the layers also undergo rapid changes in composition in their planes as evidenced by the varying optical properties, especially the optic angles, as observed under the microscope in single continuous mica sheets.

The exceedingly fine-grained micas, which go under such names as sericite, illite, and hydromuscovite, are in a class by themselves. They are defect structures *principally* with regard to missing alkali cations. What takes the place of these ions? Analyses show definitely that as K

decreases H_2O increases. Does this mean that hydronium ions could perhaps substitute for K, a possibility which should be investigated in the infrared spectrum. Aruja (1944) has shown recently that the unusual fibrous mineral gümbelite has the muscovite structure. This makes it a hydromuscovite in which considerable Mg may replace a part of octahedral Al.

Glauconite, $(OH)_{6-10} \cdot K_{2-3}(Mg, Fe'', Ca)_{1-3}$ $(Fe''', Al)_{3-6}$ $(Si_{13-14}Al_{2-3})$ O_{38-40}, has a mica structure as shown by Gruner (1935) and by Hendricks (1941). Though the mineral has a composition which, while similar to the phengites, has too high a Si:Al ratio, too much ferric iron and not enough K, it does show a structure closely resembling biotite. To be sure, the ions do not fit perfectly as evidenced by the fact that the individual crystals never grow beyond microscopic size.

The preceding observation with regard to grain size could be considered a rule for the growth of silicate crystals. The greater the number of substitutions, other conditions being equal, the smaller the crystals unless they were formed at high temperature; for only heat will lend great mobility to the ions and give them an opportunity to find the most suitable neighbors and permit larger growth.

Pyrophyllite and talc, notwithstanding their relatively simple compositions, show anomalous structures which, according to Hendricks and Jefferson (1938) can be best explained with shifts of the neutral layers over one another by simple submultiples of the length of the *b*-axis. We used to think that talc rarely could accommodate more than a very few percent of ferrous iron in its structure. Recently Gruner (1944) has found a talc structure, however, which is made up of 75% of Fe and 25% of Mg with reference to the octahedral cations. This new mineral, minnesotaite, $(Fe'', Mg)_{11}$ $(Si, Al, Fe''')_{16}O_{37} \cdot (OH)_{11}$, as it is called, though occurring in enormous amounts in ancient iron formations, has all the earmarks of a metastable defect structure with omissions in the octahedral positions and with considerable (OH) substitution for O.

A still less stable and very unusual structure is the iron silicate stilpnomelane, $(K, Na, Ca)_{0-1}$ $(Fe, Mg, Al)_{7-8}$ $Si_8O_{23-24} \cdot 2\text{–}4H_2O$. Neither mica nor chlorite, though often mistaken for either, this mineral can accommodate Fe, (OH), H_2O and K between its mica layers in a manner somewhat similar to Fe and (OH) in the orthosilicate staurolite. Its *x*-ray photographs indicate a very large superlattice according to Hutton and Fannkuchen (1938). The speaker, without wishing to appear facetious, would say that a hand specimen could be called one giant superlattice, so variable is the composition from point to point in one specimen. Chloritoid $Fe(OH)_2[(OH)_2$ $(Mg, Fe, Al)_3$ $(SiAl)_4O_{10}]$ seems to have a similar structure according to Machatschki and Mussgnug (1942). If it is

correct it is the most condensed layer structure known, for notwithstanding additional Fe″ and (OH) between its mica-like layers, the spacing of the layers is closer than that in pyrophyllite.

When Pauling (1930) first suggested the structure of kaolinite, it appeared that this polar lattice would remain confined to the kaolinite group. This is not the case, for Hendricks (1939) has found that cronstedtite, $(2FeO \cdot Fe_2O_3 \cdot SiO_2 \cdot 2H_2O)$, has this structure. Iron not only replaces Al in the octahedral layers, but also a part of the Si in the tetrahedral layers. Amesite, $(Mg, Fe)_4Al_2(Si_2Al_2O_{10}) \cdot (OH)_8$, which for many years had been considered an end member of the chlorite group, also possesses a modified kaolinite structure in which a large part of the Si in the tetrahedral layer is replaced by Al. According to Gruner (1944), a few units of chlorite are interstratified with the kaolinite units in amesite leading to superstructures over a hundred Å units thick. It has already been mentioned in another place that Warren and Aruja think that the serpentines possess a kaolinite structure.

The structure of kaolinite itself was thought to have the monoclinic symmetry *m*. This has been challenged very recently by Brindley (1946) who has discovered that some of the ions have slightly different parameters than determined previously, placing the unit cell in the triclinic asymmetric class. This seems to be the first instance that an important silicate mineral has been found without symmetry.

A problem still unsolved in connection with kaolinites is the high content in Si in anauxite, $Al_2O_3 \cdot 3SiO_2 \cdot 2H_2O$, a variety of kaolinite. The ratio Al:Si instead of being 1 to 1 as in kaolinite proper, reaches 2:3 in well crystallized anauxite. To explain this excess of SiO_2, Hendricks (1942) has made a novel suggestion that neutral layers of SiO_2 are interstratified with the kaolinite sheets. Each SiO_2 layer would consist of two tetrahedral SiO_4 layers facing one another and having, therefore, all corners shared. The three dimensions of these layers correspond very closely to those of kaolinite. The speaker has for years been fascinated by such a simple hypothetical structure for SiO_2 and still wonders why it should be thermodynamically less stable than talc or pyrophyllite, for example.

It is only natural that one should ask why there is not more interstratification on a molecular layer scale of any of these structures since they all have the same pattern of very similar dimensions. Most of these structures would also be stable under the same conditions. The answer may be found more likely in the relatively stationary or only slowly changing chemical environment in a system, than in any aversion on the part of the structures to change from layer to layer. In other words, if the cation supply and composition could be changed at the same rate at which the

growths of individual layers proceeded, we could conceivably get a single crystal containing any combination or all of the different layers without any more flagrant violations of the laws of symmetry than we have encountered in other structures.

So far we have not even mentioned the complicated montmorillonite and halloysite types of structures which have received almost as much attention during the last decade as all the other layer silicates combined. As more than a score of investigators of these minerals have not been able to reach agreement on these structures, it would take us too long to present the subject fairly on this occasion.

Two other minerals will be mentioned here, though their layers are quite different from the Si_4O_{10} structures discussed. Gillespite, $BaFeSi_4O_{10}$ has been described by Pabst (1943). Its layers are built of tetragonal meshes of tetrahedra which, similar to those in apophyllite, point alternately up and down if the sheet is horizontal. Unusual is the coordination of the Fe ion in the center of a *square* of O ions. Ito, who had described the structure of orthorhombic epididymite in 1934, has found recently (1947) that the structure of its monoclinic dimorph eudidymite, $HNaBeSi_3O_8$, is very similar. The orthorhombic one may conceivably be considered an internal twin of the monoclinic modification. The layers in both structures have the composition $NaSi_3O_7$. Unusual is the sharing of faces of SiO_4 tetrahedra with faces of Na octahedra in both minerals. Sanbornite $Ba_2Si_4O_{10}$ has been mentioned as a probable layer structure by Hendricks.

Framework Structures

The most important structures in this class are the feldspars. They have received additional attention in a more quantitative way by Chao, Smare, Hargreaves, and W. H. Taylor (1939 and 1940). According to them the lamellae of microperthite consist of monoclinic K feldspar and triclinic Na feldspar. The latter, however, is somewhat different in structure from albite. A homogeneous and stable triclinic structure can be obtained by heating the lamellae to 1075° C. The stabilization is apparently brought about by some slight modification in the structure. These investigators were able to show that there are marked differences in the sizes of the Si and Al tetrahedra. Chao and W. H. Taylor (1940) have also been able to demonstrate that the plagioclase feldspars do not form a complete isomorphous series. Miscibility is found at each end of the series but does not seem to include andesine and labradorite which seem to consist of interstratified lamellae of the other members of the series if at relatively low temperatures.

The structure of nepheline based on that of tridymite has now been

worked out by M. J. Buerger, G. E. Klein, and G. Hamburger (1947). About half of the Si positions in the tridymite-similar structure are replaced by Al. Nepheline practically always contains an excess of SiO_2 which can easily be explained now on the basis of its tridymite-similar framework in which not all the Al for Si substitutions have occurred.

M. J. Buerger and Washken have discovered recently that eucryptite, $LiAlSiO_4$, has a derivative quartz structure.* The speaker wishes to add here that β-spodumene, $LiAlSi_2O_6$, has the same kind of structure from which the lithium may be removed leaving a quartz-like framework of Al and Si tetrahedra in which hydrogen probably as hydroxyl preserves electrostatic balance. This hydrogen is driven off as water (a total of about 5.5%) between 400° and 650° C. Judging from x-ray powder patterns the structure persists though the compound has lost an O from one of its positions as indicated by the equation:

$$2HAlSi_2O_6 \rightarrow (AlSi_2)_2O_{11} + H_2O.$$

This loss reminds one of the sillimanite-mullite relationship. The structure finally collapses around 850° C. to quartz and amorphous Al_2O_3 which changes to cristobalite and mullite near 1200° C. It is possible that heating for weeks instead of days would change the transformation temperatures somewhat.

Leucite, chemically the K equivalent of β-spodumene, has a structure very similar to pollucite, $CsAlSi_2O_6 \cdot nH_2O$, and, therefore, also similar to analcite, $NaAlSi_2O_6 \cdot H_2O$, as determined by Náray-Szabó (1942) in a detailed investigation. This seems to explain why leucite can be readily changed to analcite in Na-salts solutions. But why does leucite contain no water? There seems to be room for it just as there is in pollucite which has a slightly larger cell. It is interesting in this connection that Fleischer and Ksanda (1941) could dehydrate pollucite but were unable to introduce water again at room temperature. They were partially successful when they used high pressures and temperatures.

The zeolites have come in for their share of attention particularly through publications by W. H. Taylor and M. H. Hey. As most of the more recent work deals with the behavior of zeolitic water, they will not be discussed.

Conclusion

Highly fascinating and important as all these contributions have been, they have advanced us only a short distance toward one of our ultimate goals. This is the fundamental relationship of structures to phase equilibria between solids as well as between solids and solutions. Why do some

* Verbal communication.

bonds give way to others if we change the physical and chemical environment? To answer satisfactorily most questions like these may require several generations so that our present knowledge may look very insignificant to the student of the solid state of the next century.

References

Aruja, Endel (1944), An *x*-ray study on the crystal structure of gümbelite: *Mineral. Mag.*, **27,** 11–15.

——— (1944), An *x*-ray study of the crystal structure of antigorite: *Mineral. Mag.*, **27,** 65–74.

Barnick, M. (1936), Strukturuntersuchung des natürlichen Wollastonits. Dissertation, Berlin 1936. Abstract in *Strukt. Ber.*, **4,** 207.

Belov, N. V. (1942), New silicate structures: *Compt. Rend. Acad. Sci. Russ.*, **37,** 139–140.

Berman, Harry (1937), Constitution and classification of the natural silicates: *Am. Mineral.*, **22,** 341–408.

Bradley, W. F. (1940), The structural scheme of attapulgite: *Am. Mineral.*, **25,** 504–410.

Bredig, M. A. (1945), High-temperature crystal chemistry of AmBXn compounds with particular reference to calcium orthosilicate: *Jour. Phys. Chem.*, **49,** 537.

Brindley, G. W. (1946), The structure of kaolinite: *Mineral. Mag.*, **27,** 242–253.

Buerger, M. J., Klein, G. E., and Hamburger, G. (1947), The structure of nepheline: *Am. Mineral.*, **32,** 197.

Bystrom, Anders (1942), The crystal structure of cordierite: *Arkiv. Kemi. Min. Geol. Stockholm*, **15B,** No. 12.

Chao, S. H., Hargreaves, A., and Taylor, W. H. (1940), The structure of orthoclase: *Mineral. Mag.*, **25,** 498–512.

———, Smare, D. L., and Taylor, W. H. (1939), An *x*-ray examination of some potash-soda-feldspars: *Mineral. Mag.*, **25,** 338–350.

——— and Taylor, W. H. (1940), Isomorphous replacement and superlattice structures in the plagioclase feldspars: *Proc. Roy. Soc.* (A), **176,** 76–87.

Fleischer, M., and Ksanca, C. J. (1940), Dehydration of pollucite: *Am. Mineral.*, **25,** 666–672.

Flint, E. P., McMurdie, H. F., and Wells, L. S. (1941), Hydrothermal and *x*-ray studies of the garnet-hydrogarnet series and the relationship of the series to hydration products of portland cement: *Jour. of Research, Nat. Bur. Stand.*, **26,** 13–33.

Gruner, J. W. (1935), The structural relationship of glauconite and mica: *Am. Mineral.*, **20,** 699–714.

——— (1939), The behavior of serpentines between 500° and 650° C: *Am. Mineral.*, **24,** 186.

——— (1944), The structure of stilpnomelane reexamined: *Am. Mineral.*, **29,** 291–298.

——— (1944), The composition and structure of minnesotaite, a common iron silicate in iron formations: *Am. Mineral.*, **29,** 363–372.

——— (1944), The kaolinite structure of amesite, $(OH)_8(Mg, Fe)_4Al_2(Si_2Al_2)O_{10}$, and additional data on chlorites: *Am. Mineral.*, **29,** 422–430.

Hägele, G., und Machatschki, F. (1939), Der Britholith ist ein Cererden Silikatapatit: *Zent. Bl. Mineral.*, **A,** 165–167.

Halimond, A. F. (1943), On the graphical representation of the calciferous amphiboles: *Am. Mineral.*, **28,** 65–89.

Hamburger, Gabrielle, and Buerger, M. J. (1948), Preliminary report of the structure of tourmaline. Read at the meeting of the Crystallographic Society at Yale University, April 1948.

HARGREAVES, A., AND TAYLOR, W. H. (1944), An x-ray examination of decomposition products of chrysotile (asbestos) and serpentine: *Mineral. Mag.*, **27,** 204–216.

HENDRICKS, S. B., AND JEFFERSON, M. A. (1938), Crystal structure of vermiculites and vermiculite-chlorites: *Am. Mineral.*, **23,** 851.

——— AND JEFFERSON, M. E. (1939), Polymorphism of the micas: *Am. Mineral.*, **24,** 729–771.

——— AND ROSS, C. S. (1941), Chemical composition and genesis of glauconite and celadonite: *Am. Mineral.*, **26,** 683–708.

——— (1942), Lattice structure of clay minerals and some properties of clays: *Jour. Geol.*, **50,** 276–290.

——— (1944), Polymer chemistry of silicates, borates and phosphates: *J. Wash. Acad. Sci.*, **34,** 241–251.

HUTTON, C. O. (WITH I. FANNKUCHEN) (1938), The stilpnomelane group of minerals: *Mineral. Mag.*, **25,** 172–207.

ITO, T. (1947), The structure of eudidymite)$HNaBeSi_2O_8$): *Am. Mineral.*, **32,** 442–452.

KLEMENT, R., AND DIHN, P. (1941), Isomorphe Apatitarten: *Naturwiss*, **29,** 301.

MACHATSCHKI, F. (1943), Steenstrupin ist kein Silikat vom Formeltypus Apatit: *Naturwiss.*, **31,** 438.

——— AND MUSSGNUG, F. (1942), Über die Kristallstruktur des Chloritoids: *Naturwiss.*, **30,** 106.

MCCONNELL, DUNCAN (1937), The substitution of SiO_4 and SO_4 groups for PO_4 groups in the apatite structure, ellestadite, the end-member: *Am. Mineral.*, **22,** 977–986.

NÁRAY-SZABÓ, ST. V. (1938), Die Struktur des Pollucits $CsAlSi_2O_6 \cdot xH_2O$: *Zeit. Krist.*, **99,** 277–282.

——— (1942), Die Struktur des Leucits: *Zeit. Krist.*, **104,** 39–44.

NIGGLI, PAUL (1943), Gesteinschemismus und Mineralchemismus: *Schweiz. Min. und Petrog. Mitteil.*, **23,** 538–607.

O'DANIEL, H., AND TSCHEISCHWILI, L. (1942), Zur Struktur von γ-Ca_2SiO_4 and Na_2BeF_4: *Zeit. Krist.*, **104,** 124–141.

——— AND TSCHEISCHWILI, L. (1943), Strukturuntersuchungen an Tephroit Mn_2SiO_4, Glaukochroit (Mn, Ca)$_2SiO_4$ and Willemit Zn_2SiO_4 von Franklin Furnace: *Zeit. Krist.*, **105,** 273–278.

——— AND TSCHEISCHWILI, L. (1942), Zur Struktur von K_2BeF_4, Sr_2SiO_4 and Ba_2SiO_4: *Zeit. Krist.*, **104,** 348–357.

——— AND TSCHEISCHWILI, L. (1941), Zur Struktur von Na_2BeF_4: *Zeit. Krist.*, **103,** 178–185.

——— AND TSCHEISCHWILI, L. (1943), Modellsubstanzen zu Silikaten: *Naturwiss.*, **31,** 209–210.

PABST, ADOLF (1937), The crystal structure of plazolite: *Am. Mineral.*, **22,** 861–868.

——— (1943), Crystal structure of gillespite, $BaFeSi_4O_{10}$: *Am. Mineral.*, **28,** 372–390.

PEACOCK, M. A. (1935), On wollastonite and parawollastonite: *Am. Jour. Sci.*, **30,** 495–529.

RICHMOND, W. E. (1942), Inesite $Mn_7Ca_2Si_{10}O_{28}(OH)_2 \cdot 5H_2O$: *Am. Mineral.*, **27,** 563–569.

——— (1937), On babingtonite $Fe_2'''Fe_2''Ca_4Si_{10}O_{25}(OH)_2$: *Am. Mineral.*, **22,** 630–642.

STEVENS, R. E. (1938), New analyses of lepidolites and their interpretation: *Am. Mineral.*, **23,** 607–628.

STRUNZ, H. (1937), Systematik und Struktur der Silikate: *Zeit. Krist.*, **98,** 60–83.

THILO, ERICH (1939), Die Umwandlung von Tremolit in Diopsid beim Erhitzen: *Zeit. Krist.*, **101,** 345–350.

——— AND ROGGE, G. (1939), Chemische Untersuchungen von Silikaten, VIII: *Ber. d. deutsch. Chem. Gesell.*, **72,** 341-362

——— AND SCHWARZ, ULRICH (1941), Über weitere Versuche mit dem Pyrophyllit $Al_2(Si_4O_{10})(OH)_2$ und dem Vergleich seiner Reaktionen mit denen des Talks $Mg_3(SiO_{10})$-$(OH)_2$: *Ber. Deutsch. Chem. Ges.* (B) **74,** 196–204.

WARREN, B. E. (1941), The random structure of chrysotile asbestos: *Phys. Rev.*, **59,** 925.

WINCHELL, A. N. (1942), Further studies of the lepidolite system: *Am. Mineral.*, **27,** 114–130.

WINCHELL, A. N. (1945), Variations in composition and properties of calciferous amphiboles: *Am. Mineral.*, **30,** 27–50.

REEXAMINATION OF THE SOPER, OKLAHOMA METEORITE*

E. P. Henderson and Stuart H. Perry,
U. S. National Museum, Washington, D. C.

This iron meteorite was found 6 miles northwest of Hugo, Oklahoma, and was first described by E. C. Wood and C. A. Merrith.[1] It was correctly identified as belonging to the ataxite group with an unusually high schreibersite content. The U. S. National Museum acquired a 1317 gram sample of this iron from the authors shortly after the description appeared. This meteorite was restudied because the analysis first reported did not agree with the series of accepted analyses now being compiled for other low nickel ataxites.

The following table gives the only two analyses of Soper that have so far been made.

Soper, Oklahoma Meteorite

	1	2
Fe	90.89	91.71
Ni	6.21	5.66
Co	.70	.54
P	2.23	2.08
C	.02	N.D.
S	.03	none
Al	.10	none
Cl	trace	N.D.
	100.18	99.99
Sp.G.	7.387	7.644

No. 1. S. G. English, *Am. Mineral.*, **24**, 59–61 (1939).
No. 2. E. P. Henderson.

The second analysis reports a slightly lower nickel content and a higher iron value but confirms the unusually high percentage of phosphorus. The 5.66 value for nickel, brings this meteorite into consistent agreement with other analyses of nickel-poor ataxites.

A thin slice of the material to be analyzed was polished and etched to determine if the structure was the average for the entire meteorite and to make certain that no large inclusions of any accessory minerals were

* Published by permission of the Secretary of the Smithsonian Institution.

[1] *Am. Mineral.*, **24**, 59–61 (1939), The Soper, Oklahoma meteorite.

included. The slice was then dissolved in dilute hydrochloric acid and the gas liberated was passed through a solution of dilute lead acetate. Since no black precipitate of lead sulfide formed, there was no troilite in the specimen analyzed.

Schreibersite is practically insoluble in dilute hydrochloric acid and hence it remains behind as a residue. To make certain that all the kamacitic iron was removed, the hydrochloric acid solution stood in contact with the residue for 12 hours before filtering.

The schreibersite portion was then dissolved in mixed hydrochloric and nitric acid; after several repeated boilings only a very small quantity of the dark material remained as an insoluble residue and this may be the carbon reported in the first analysis. It was not determined.

Analyses of Kamacite and Schreibersite in Soper, Meteorite
E. P. Henderson, analyst

	Kamacite	ratios		Schreibersite	ratios	
Fe	95.35	1.707	21.85	68.22	1.2218	
Ni	4.11	.070	1.0	15.61	.2660	3.02
Co	.51	.008		.77	.0130	
P	none			15.38	.4958	1.0

The results give a kamacite with an unusually low percentage of nickel. The alpha iron, or kamacite, could have any nickel content from 0 up to about 5.5 percentage; the higher value seems to be the limit of solubility for nickel in alpha iron. The strange fact is that in hexahedrite meteorites, which consist entirely of alpha iron, the nickel contents of the reliable analyses are remarkably constant. The average nickel content for hexahedrites[2] was found to lie between 5.519 and 5.60. In all of the old published analyses, of less than 5 per cent nickel, which have been reinvestigated, those low values have been found to be erroneous, generally indicating that in the analytical work the nickel was not completely separated from iron. This low value of 4.11 for the kamacite is reported with confidence as it was carefully checked.

Farrington[3] lists 24 analyses of schreibersite of which all but six are higher in nickel than the Soper schreibersite. Since the phosphide particles are so uniformily dispersed in the Soper meteorite it is suggested that during the interval when this iron was reheated and modified into an ataxite, the temperature was raised high enough and retained long enough to permit some nickel to migrate from the kamacite and combine with the phosphide to form schreibersite.

[2] Henderson, E. P., Chilean hexahedrites and the composition of all hexahedrites: *Am. Mineral.*, **26,** 546–550 (1941).

[3] Meteorites, Privately published by O. C. Farrington (**1913**).

If the nickel is not taken from the alpha iron or kamacite, as suggested above, the iron must be quite low in nickel, which has been found rejected as small drops[4] in the Fe-Ni-P eutectic structures and has migrated and combined with the kamacite. Either process will result in a kamacite which is lower in its nickel content than the normal kamacite from hexahedrites.

A study is now being made of the low nickel ataxites by these authors and a general descriptive paper will soon appear.

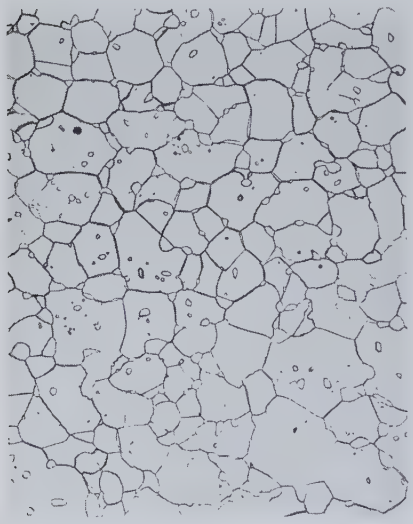

1

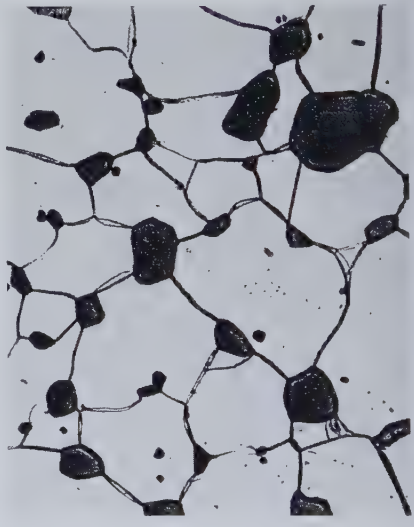

2

Explanation for illustrations.

1. The schreibersite particles are developed along the boundaries of the kamacite. Some minute particles of phosphide are found within the kamacite grains, but otherwise the kamacite is clear and structureless.

2. The phosphide bodies are shown to have a mottled structure probably indicating an Fe-P-Ni eutectic.

[4] Stuart H. Perry, The Metallography of Meteoric Iron: *U. S. National Museum., Bull.* **184.**

A MANGANESE OXIDE MINERAL FROM BUCHAN, VICTORIA

H. R. Samson* and A. D. Wadsley*

Abstract

A manganese mineral occurring as dense nodules intimately associated with hematite is found in Eastern Victoria. The mineral is of the psilomelane type and possesses a colloform texture. *X*-ray powder patterns and chemical analysis indicate a mineral species corresponding closely to an oxide prepared in the laboratory and previously named manganous manganite.

The manganese ore minerals studied were obtained from the Oxide Mine situated about 4 miles S. E. of Buchan in Eastern Victoria. The ore-body occupies what appears to be a fault in andesitic tuffs of Lower Devonian age and occurs close to the boundary of massive limestones which overlie the volcanic series. The hanging-wall of the fault consists of kaolinized pyroclastic material and the ore-body is composed of soft red earthy hematite in which the manganese ore occurs as dense nodules.

The deposit is apparently supergene in origin, derived from solutions carrying manganese and iron which were precipitated at fairly low temperatures as indicated by the colloform texture. The source of the manganese and iron was probably the overlying limestones and volcanic deposits, the kaolinized tuffs representing part of the leached host rocks. Alternatively, kaolinization may have accompanied oxidation of the previously deposited ore, the fault zone providing channels for circulating waters. There is an extensive development of ochreous iron oxides accompanied by partly weathered nodules which contain numerous pockets of goethite, and possess a distinctive colour and texture. In addition to the fresh unaltered material (specimens 1 and 2) which is a steel-grey colour, a more weathered sample (specimen 3) was examined. This is slightly bluer in colour, more friable owing to the presence of abundant soft goethite, and possesses a distinctive pisolitic texture visible even without polishing.

A polished section of an unaltered nodule is seen under the ore-microscope to consist of an apparently homogeneous mineral, which appears to correspond to the "psilomelane" type of Fleischer and Richmond (4), and is almost completely isotropic, showing pale grey-brown polarization colours. Etching with hydrofluoric acid reveals a zonal texture in massive specimens; occasionally colloform banding is visible without the acid of etch reagents (Figure 1).

* An officer, Division of Industrial Chemistry, Council for Scientific and Industrial Research, Melbourne, Australia.

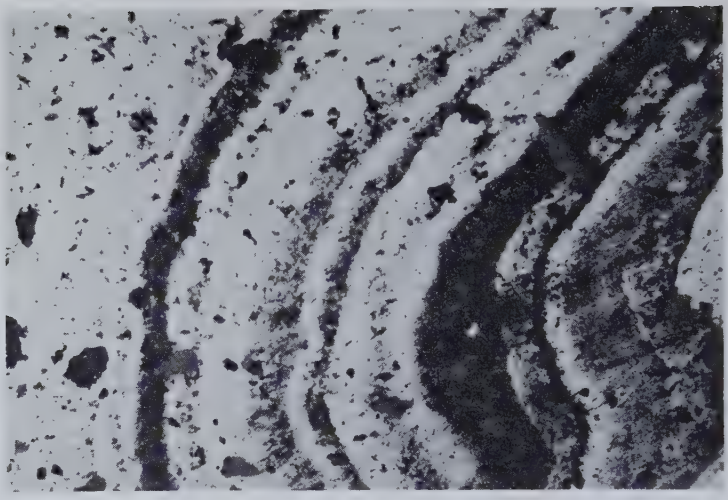

FIG. 1. Colloform texture of Buchan Minerals marked by zones of differing composition, and also by lines of inclusions. Unetched (×75).

Etching with a nitric acid-hydrogen peroxide mixture, however, reveals the presence of a very finely disseminated phase which remains unaltered after the manganiferous portion has reacted with effervescence. Figure 2 shows the unattacked mineral under oil-immersion appearing as embayed aggregates, and rod-like dendritic growths. The mineral is isotropic and may also take the form of irregular lines, following the colloform banding of the ore. Optical identification is uncertain since the material is so finely divided, but in the light of other evidence (x-ray powder photographs) there is no doubt that this mineral is hematite.

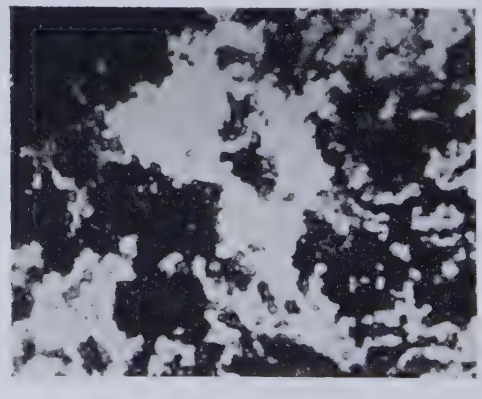

FIG. 2. Etched specimen of manganese ore, Oxide Mine, Buchan. Black = manganese mineral; white = hematite (×1000).

The intimacy with which the manganese mineral and the hematite are associated makes their separation impossible by the ordinary means. Some specimens contain narrow veinlets of a strongly pleochroic mineral, showing marked anisotropism, and more rarely, small pockets of goethite ringed by needles of the same mineral. Positive identification is uncertain owing to the minute size, but the presence of small percentages of zinc in each specimen, and the occurrence of crystalline chalcophanite associated with goethite in nearby parts of the ore body, suggest that these needles may be chalcophanite and not pyrolusite as might at first be supposed. This view is supported by the fact that specimen 3, the analysis of which shows the highest percentage of zinc, contains more of this mineral than Specimens 1 and 2, and the powder pattern contains the strongest lines of chalcophanite.

Thin sections revealed the presence also of quartz and small amounts of sericite.

The following etch reactions cannot be regarded as being strictly characteristic of the manganese mineral, because of the admixed hematite. Etch reactions of the psilomelane minerals, moreover, are never specific and vary with composition of the mineral except in the case of $SnCl_2$, H_2O_2, etc., which invariably react vigorously.

Negative: HCl, KOH, KCN, $FeCl_3$.
Positive: H_2O_2, $H_2O_2+HNO_3$, blackens with effervescence: $SnCl_2$, stains brown slowly. HNO_3 conc., darkens slowly.

Specimen 3 has undergone considerable alteration by weathering, containing less disseminated hematite and more goethite and chalcophanite. A transition is noted between the clean unaltered material and areas of extremely fine chalcophanite needles associated with fragments of brown goethite. This appears to represent a partial crystallization or transformation of the gel-like matrix.

The optical examination of the specimens indicates that they possess the properties of a typical member of the psilomelane group, being an isotropic gel mineral, colloform in texture, and with a hardness and reflecting power about equal to that of hematite.

The loosely adherent impurities were removed with a hard scrubbing brush, and each specimen was ground to approximately -60 B.S.S. mesh and then agitated violently with water in order to disperse the earthy material occasionally found in pockets inside the massive specimen. After removal of these impurities, the samples were dried at 60° C. Although physical separation of the major phases is impossible from the finely ground specimens, separation can be effected chemically, as hematite, goethite, sericite and quartz are not appreciably affected by an ice cold 5% nitric acid-hydrogen peroxide mixture by which the manganese mineral is attacked.

A blank was carried out on the earthy materials associated with each specimen, and in each case only traces of iron were dissolved, but not in sufficient quantity to affect the analytical results as expressed. Consequently a complete analysis was made of each specimen by the normal methods, and in addition analyses were made of the material insoluble in this acid mixture.

The results are reported in Table 1. The water figure is regarded as uncertain, and in the subsequent treatment of these results will not be considered since the water content of near colloidal materials is of little significance. The distribution of the alkali metals is on the basis that alumina is present in the insoluble portion as sericite.

Table 1. Manganese Ore, Oxide Mine. Chemical Analyses

Fraction		Specimen 1	Specimen 2	Specimen 3
Acid Soluble	MnO_2	60.33	56.58	60.15
	MnO	3.93	4.60	4.50
	Al_2O_3	4.02	2.56	2.48
	Fe_2O_3	1.01	0.38	0.80
	ZnO	1.25	1.08	3.27
	K_2O	1.05	1.42	0.97
	Na_2O	0.28	0.31	0.24
Acid Insoluble	SiO_2	2.70	1.52	3.98
	Al_2O_3	—	0.71	1.18
	Fe_2O_3	22.19	26.12	15.42
	K_2O	—	0.22	0.36
Indeterminate	$H_2O-120°$	1.07	0.36	1.14
	$H_2O+120°$	3.79	3.67	4.31
	Total	101.62	99.53	98.80

All samples contain spectroscopic traces of Co, Ca and Mg. Ba is absent.

The acid soluble portion of Table 1 corresponds to the manganese phase. Assuming the zinc to be present as chalcophanite, an analysis of these results gives a formula of the type

$$(Na, K)_2O \cdot xMnO_2 \cdot y(Al, Fe)_2O_3 \cdot zMnO$$

but x, y and z differ slightly from specimen to specimen, and as a result precise formulation is not contemplated.

The relatively small amounts of aluminium and iron suggest that they have replaced manganese of a corresponding valency. If this is so, then

the mineral free from these substituted ions will be of the form

$$(Na,\ K)_2O \cdot xMnO_2 \cdot yMn_2O_3 \cdot zMnO,$$

and substances of this type are usually simplified to

$$MnO_n$$

where n is the atomic ratio O:Mn.

The analytical results must further be corrected for the presence of chalcophanite in small quantities. The formula of this mineral is usually given as $ZnO \cdot 2MnO_2 \cdot 2H_2O$, and for each analysis two equivalents of MnO_2 are subtracted for each equivalent of ZnO.

Treated in this way, the results in Table 1 lead to values of n for each specimen of 1.88, 1.88 and 1.87, respectively.*

The mineral may therefore be regarded as having the formula $MnO_{1.88}$ in which the trivalent manganese has been completely replaced by the more stable ions of iron and aluminium.

A more precise formula is not proposed as it is believed that in common with many of the manganese and other metal oxide minerals, this material may exhibit radical departures from stoichiometry due to the reduction of some cations from a high to a low valency with an equivalent number of vacant anionic sites.

X-ray powder patterns were made on each specimen mounted by the wedge method using Fe Kα radiation. In each case the lines of hematite, silica and the manganese mineral were found and in addition the most prominent lines of goethite for specimens 2 and 3, and of chalcophanite for specimen 3.

The line spacings and intensities are given in Table 2 for the pattern of specimen 1, the lines of the impurities being indicated. The residual pattern which is taken as that of the manganese mineral, appears to be derived from a tetragonal cell having two possible sets of cell dimensions—

$a=6.97$ Å	$c=7.12$ Å
or $a=9.89$ Å	$c=7.12$ Å

Whilst the powder pattern possesses many lines common to that of cryptomelane, a commonly occurring manganese dioxide mineral containing essential potassium, for which the tentative formula KR_8O_{16} ($R=Mn^{iv}$, etc.) has been proposed (4), both of these possible sets of dimensions differ considerably from that proposed by Ramsdell (6) for cryptomelane.

Studies in this laboratory have shown that neither the naturally oc-

* An oxide of this composition reported by Dubois (2) was shown to be identical with γ-MnO_2 (1).

curring mineral nor synthetic cryptomelane possess patterns differing by more than experimental error from Frondel's values (4). These specimens have, however, exhibited a wide variation in composition, both in potassium content and Mn:O ratio, and the possibility that the Buchan specimens are disordered forms of cryptomelane due to lattice imperfec-

TABLE 2. *X*-RAY DIFFRACTION DATA

Manganese Ore Oxide Mine		Extra Phases	Buchan Mineral	Theoretical Pattern		Manganous Manganite	
I	*d*		*d*	*hkl*	*d* (calc.)	*I*	*d*
				(001)	7.12	MS	7.13
W	6.99		6.99	(100)	6.97		
Wd	4.91		4.91	(110)	4.93		
VW	4.24	SiO_2					
VWd	3.99		3.99	(111)	4.06		
M	3.670	Fe_2O_3		(002)	3.56	W	3.53
VWd	3.502		3.502	200)	3.48		
MW	3.326	SiO_2					
Md	3.132		3.132	(201)	3.132		
VW	2.755		2.755				
S	2.700	Fe_2O_3					
MS	2.510	Fe_2O_3					
MS	2.392		2.392	(003)	2.375	M	2.41
M	2.203	Fe_2O_3					
Md	2.152		2.152	(113)	2.140	VWd	2.14
VWd	2.086		2.086	(311)	2.107		
S	1.836	Fe_2O_3					
S	1.691	Fe_2O_3					
				(411)	1.646		
W	1.633		1.633	(330)	1.643		
				(313)	1.616		
MW	1.597	Fe_2O_3					
MWd	1.542		1.542	(214)	1.547		
M	1.482	Fe_2O_3					
MS	1.449	Fe_2O_3					
MW	1.425		1.425	(005)	1.425	VW	1.42
				(115)	1.369		
Wd	1.368		1.368	(501)	1.369		
				(510)	1.367		
Wd	1.358		1.358	(333)	1.351		
Wd	1.348		1.348	(511)	1.343		

S=strong, MS=medium strong, M=medium, MW=medium weak, W=weak, VW=very weak, d=diffuse.

tions must therefore be rejected. In addition, it is known that variations in composition usually produce slight changes in cell dimensions, whereas the possible values listed above differ very markedly from those calculated by Ramsdell.

Recently Feitknecht and Marti studying the oxidation of manganous hydroxide, reported several new structures which could be distinguished as oxidation proceeded (3). The final oxidation product which they named manganous manganite, had a characteristic powder pattern comprising five distinct lines. In Table 2 the pattern of the manganese mineral is compared with that of manganous manganite prepared by their method. The theoretical pattern obtained from the unit cell values $a = 6.97$ Å, $c = 7.12$ Å is also included.

Although the lines of manganous manganite are few, they agree fairly well with those of the theoretical pattern. By this comparison, four of the five lines in the manganous manganite pattern are seen as reflections from the (00 *l*) planes whilst the remaining line is due to the (113) plane. Although there is insufficient data to reconcile these two powder patterns, it is nevertheless very probable that they are derived from similar crystals in which the *c* axis dimensions would be identical, whilst the *a* and *b* axes are a matter of some doubt.

Feitknecht and Marti in a brief analysis of their oxide, claimed that the pattern of manganous manganite could be derived from a structure of the cadmium iodide type, consisting of layers of MnO_2 with $Mn(OH)_2$ molecules between every fourth and fifth layer giving a formula $4MnO_2 \cdot Mn(OH)_2$ which is equivalent to $MnO_{1.80}$. Whilst this lends support to the views outlined briefly above the structure of manganous manganite may actually be more complex. A manganese oxide treated with potassium pyrophosphate in neutral ammonium acetate will give a pink solution of the manganese complex if Mn^{+++} is present in the lattice (5). By means of this test, it can be shown that manganous manganite contains an appreciable percentage of Mn^{+++}. In addition, depending upon the mode of preparation, up to 6% of alkali metal (expressed as the oxide) may be retained by this oxide which cannot be removed by washing with water.

Two preparations of manganous manganite were shaken with an aqueous solution of ferric ammonium sulphate. The sodium is replaced zeolitically, and the Mn^{+++} completely, by ferric iron, and in each case the *x*-ray powder patterns were unchanged.

The analytical results, corrected for the ion exchange of Na, are given in Table 3, and are compared with recalculated data for specimen 1.

Structurally the mineral shows similarities to manganous manganite on the one hand and to cryptomelane on the other, but the evidence does

TABLE 3

	Manganous Manganite (*a*)	(*b*)	Buchan Mineral (1)
MnO_2	84.7	86.9	86.5
MnO	8.8	7.6	5.9
Fe_2O_3	6.5	5.5	1.5
Al_2O_3	—	—	6.0
n	1.86	1.88	1.88

not support the view that the mineral may be classed merely as a disordered form of cryptomelane. It is our belief that the hydrated manganese minerals, chalcophanite, lithiophorite, psilomelane, and rancieite are perhaps closely related, and the purpose of this account is to describe our specimen without assigning to it a new name at this stage. Further work to estimate its significance in a paragenetic scheme of the hydrated manganese mineral is in progress.

ACKNOWLEDGMENTS

The authors wish to express their gratitude to Dr. A. B. Edwards of the Mineragraphic Section, C.S.I.R. for his assistance in the microscopical examination; to Mr. J. M. Cowley of the Division of Industrial Chemistry, C.S.I.R. for taking the powder photographs; to Mr. A. J. Gaskin, Geology Department, Melbourne University for assistance in the collection of specimens. The work described in this paper was carried out as part of the research programme of the Division of Industrial Chemistry, Council for Scientific and Industrial Research, Australia.

REFERENCES

1. COLE, W. F., WADSLEY, A. D., AND WALKLEY, A., *Trans. Electrochem. Soc.* Preprint 92/2 (1947).
2. DUBOIS, P., *Ann. Chimie*, **5**, 411–482 (1936).
3. FEITKNECHT, W., AND MARTI, W., *Helv. Chim. Acta*, **28**, 129–148 (1945).
4. FLEISCHER, M., AND RICHMOND, W. E., *Econ. Geol.*, **38**, 269–286 (1943).
5. LEEPER, G. W., AND JONES, L. H. P., Private communication.
6. RAMSDELL, L. S., *Am. Mineral.*, **27**, 611–613 (1942).

TRANSFORMATION OF AXES

W. L. Bond,
Bell Telephone Laboratories,
Murray Hill, New Jersey.

In choosing axes for a crystal often the first selection is later found to be unsatisfactory and a new set must be chosen. For example, the first chosen cell may turn out to be larger than necessary and simplification will follow adoption of the smaller cell. In dealing with the most general crystal system—the triclinic—it becomes obvious that the crystal axes **a b c** are not the axes of immediate reference. *X*-ray measurements determine d_{001} for example, not c, and the relation between d_{001} and c is not simple. An optical goniometer measures the angle between normals to the faces (001) and (100) which is not β nor related simply to β. Both these types of measurements are related simply to a set of axes which are perpendicular to the cell faces—the so called reciprocal cell axes. We find that, in dealing with triclinic crystals we must have two systems of axes, the direct system and the reciprocal system. This dual axial system is a great convenience in computations for all crystal systems. Hence we seek ways of converting information gathered and expressed in one system into its proper expression in another system.

On a set of axes, **a, b, c** called the a basis we define a new set **a′, b′, c′** called the a' basis by means of the vector expressions:

$$\left.\begin{aligned}\mathbf{a}' &= \Phi_{11}\mathbf{a}+\Phi_{21}\mathbf{b}+\Phi_{31}\mathbf{c}\\ \mathbf{b}' &= \Phi_{12}\mathbf{a}+\Phi_{22}\mathbf{b}+\Phi_{32}\mathbf{c}\\ \mathbf{c}' &= \Phi_{13}\mathbf{a}+\Phi_{23}\mathbf{b}+\Phi_{33}\mathbf{c}\end{aligned}\right\}. \tag{1}$$

A vector **V** can be written on the a' basis as

$$(\mathbf{V})_{a'} = \mathrm{V}_1'\mathbf{a}'+\mathrm{V}_2'\mathbf{b}'+\mathrm{V}_3'\mathbf{c}'. \tag{2}$$

We can convert this back to the a basis by substituting for **a′**, **b′** and **c′** their equivalents on the a basis (eq. (1)):

$$\begin{aligned}(\mathbf{V})_a = {} & \mathrm{V}_1'(\Phi_{11}\mathbf{a}+\Phi_{21}\mathbf{b}+\Phi_{31}\mathbf{c})\\ & +\mathrm{V}_2'(\Phi_{12}\mathbf{a}+\Phi_{22}\mathbf{b}+\Phi_{32}\mathbf{c})\\ & +\mathrm{V}_3'(\Phi_{13}\mathbf{a}+\Phi_{23}\mathbf{b}+\Phi_{33}\mathbf{c})\end{aligned}$$

which can be rearranged as:

$$\begin{aligned}(\mathbf{V})_a = {} & (\Phi_{11}\mathrm{V}_1'+\Phi_{12}\mathrm{V}_2'+\Phi_{13}\mathrm{V}_3')\mathbf{a}\\ & +(\Phi_{21}\mathrm{V}_1'+\Phi_{22}\mathrm{V}_2'+\Phi_{23}\mathrm{V}_3')\mathbf{b}\\ & +(\Phi_{31}\mathrm{V}_1'+\Phi_{32}\mathrm{V}_2'+\Phi_{33}\mathrm{V}_3')\mathbf{c}\end{aligned} \tag{3}$$

Let us adopt a short hand notation. The vector $(\mathbf{V})_{a'} = V_1'\mathbf{a}'+\mathrm{V}_2'\mathbf{b}'+\mathrm{V}_3'\mathbf{c}'$ will be written

$\begin{pmatrix} V_1' \\ V_2' \\ V_3' \end{pmatrix}_{a'}$. In this notation $(\mathbf{V})_a = \begin{pmatrix} V_1 \\ V_2 \\ V_3 \end{pmatrix}_a$. But by eq. (3) this is

$$\begin{pmatrix} \Phi_{11}V_1' + \Phi_{12}V_2' + \Phi_{13}B_3' \\ \Phi_{21}V_1' + \Phi_{22}V_2' + \Phi_{23}V_3' \\ \Phi_{31}V_1' + \Phi_{32}V_2' + \Phi_{33}V_3' \end{pmatrix}_a .$$

The last array can be obtained by a purely mechanical manipulation of the arrays $\Phi = \begin{pmatrix} \Phi_{11}\Phi_{12}\Phi_{13} \\ \Phi_{21}\Phi_{22}\Phi_{23} \\ \Phi_{31}\Phi_{32}\Phi_{33} \end{pmatrix}$ and $(\mathbf{V})_{a'} = \begin{pmatrix} V_1' \\ V_2' \\ V_3' \end{pmatrix}_{a'}$. We write

$$(\mathbf{V})_a = \Phi(\mathbf{V})_{a'} \tag{4}$$

which is equivalent to:

$$\begin{pmatrix} V_1 \\ V_2 \\ V_3 \end{pmatrix}_a = \begin{pmatrix} \Phi_{11}\Phi_{12}\Phi_{13} \\ \Phi_{21}\Phi_{22}\Phi_{23} \\ \Phi_{31}\Phi_{32}\Phi_{33} \end{pmatrix} \begin{pmatrix} V_1' \\ V_2' \\ V_3' \end{pmatrix}_{a'} = \begin{pmatrix} \Phi_{11}V_1' + \Phi_{12}V_2' + \Phi_{13}V_3' \\ \Phi_{21}V_1' + \Phi_{22}V_2' + \Phi_{23}V_3' \\ \Phi_{31}V_1' + \Phi_{32}V_2' + \Phi_{33}V_3' \end{pmatrix}_a . \tag{4'}$$

The first term of the resultant vector is formed by the first row of the prefactor (Φ in this case) and the first column of the post factor ($\mathbf{V}'$, which has but one column, in this case). This first term of the resultant vector is the sum of the products taken in order. Likewise the second term of the resultant is formed from the second row of the prefactor and the first column of the post factor, similarly for the third term of the resultant, as can be seen by studying eq. (4′). If the post factor had more than one column we could consider each column as a separate vector, and get a resultant with the same number of columns as has the post factor. This manipulation is "matrix multiplication." It is merely a mechanical method of handling equations.

As an example we take:

$$\mathbf{a}' = \begin{pmatrix} 1 \\ 0 \\ 0 \end{pmatrix}_a , \mathbf{b}' = \begin{pmatrix} 0 \\ 1/2 \\ 1/2 \end{pmatrix}_a , \mathbf{c}' = \begin{pmatrix} 0 \\ -1/2 \\ 1/2 \end{pmatrix}_a$$

what does a vector $\begin{pmatrix} 1 \\ 2 \\ 3 \end{pmatrix}_{a'}$ become on the a basis? By eq. (4)

$$(\mathbf{V})_a = \begin{pmatrix} 1 & 0 & 0 \\ 0 & 1/2 & -1/2 \\ 0 & 1/2 & 1/2 \end{pmatrix} \begin{pmatrix} 1 \\ 2 \\ 3 \end{pmatrix}_{a'} = \begin{pmatrix} 1 \\ -1/2 \\ 5/2 \end{pmatrix}_a .$$

We now examine the converse case, that is, convert a given $(\mathbf{V})_a$ to the a' basis. We imagine a matrix Φ^{-1} such that multiplying equation (4) through by Φ^{-1} as a prefactor we get $\Phi^{-1}(\mathbf{V})_a = \Phi^{-1}\Phi(\mathbf{V})_{a'} = (\mathbf{V})_{a'}$. Our problem now is to find such a matrix. We can solve eq. (1) by determinants and find $\mathbf{a}, \mathbf{b}, \mathbf{c},$ in terms of $\mathbf{a}', \mathbf{b}',$ and $\mathbf{c}'$. In terms of the new functions of the Φ_{ij}'s we could now go through the previous analysis and

reach the answer. The actions necessary to solve this problem by determinants can be made into a mechanical manipulation.

By the determinant of a square matrix Φ we mean the same array of values but considered as a determinant instead of as a matrix, it is commonly written $|\Phi|$; when we mean the value of the determinant rather than the array we will use Δ, By the (ij) minor of the determinant we mean the determinant left after striking out the ith row and jth column. For example the (21) minor of $|\Phi|$ is:

$$\Delta_{ij}=\begin{vmatrix}\Phi_{12} & \Phi_{13}\\ \Phi_{32} & \Phi_{33}\end{vmatrix}.$$

A determinant of but four terms can be immediately evaluated as the major diagonal product less the other diagonal product:

$$\Delta_{21}=\begin{vmatrix}\Phi_{12} & \Phi_{13}\\ \Phi_{32} & \Phi_{33}\end{vmatrix}=\Phi_{12}\Phi_{33}-\Phi_{32}\Phi_{13}.$$

The 9 term determinant can be evaluated in terms of the minors of any row or column. For example to develop the determinant of Φ in terms of the minors of the first row:

$$\Delta=\Phi_{11}\Delta_{11}-\Phi_{12}\Delta_{12}+\Phi_{13}\Delta_{13}.$$

The expression for development in terms of any other row or column is obvious, except for the matter of signs. The signs must be taken from the scheme $\begin{vmatrix}+&-&+\\ -&+&-\\ +&-&+\end{vmatrix}$ which gives to each ij minor the sign $(-1)^{i+j}$.

We define the "transposed" matrix $\bar{\Phi}$ which is merely Φ with columns written as rows and rows as columns.*

$$\bar{\Phi}=\begin{pmatrix}\Phi_{11}\Phi_{21}\Phi_{31}\\ \Phi_{12}\Phi_{22}\Phi_{32}\\ \Phi_{13}\Phi_{23}\Phi_{33}\end{pmatrix}. \tag{5}$$

If Δ is the value of the determinant of Φ in these terms we have:

$$\overline{(\Phi^{-1})}=\frac{1}{\Delta}\begin{pmatrix}\Delta_{11}(-1)^{1+1} & \Delta_{12}(-1)^{1+2} & \Delta_{13}(-1)^{1+1}\\ \Delta_{21}(-1)^{1+2} & \Delta_{22}(-1)^{2+2} & \Delta_{23}(-1)^{2+2}\\ \Delta_{31}(-1)^{1+3} & \Delta_{32}(-1)^{3+2} & \Delta_{33}(-1)^{3+3}\end{pmatrix}.$$

Since $(\overline{\Phi^{-1}})=(\bar{\Phi})^{-1}$ we can omit the parentheses and immediately write Φ^{-1} from (5). As an example, for $\Phi=\begin{pmatrix}1 & 0 & 0\\ 0 & 1/2 & -1/2\\ 0 & 1/2 & 1/2\end{pmatrix}$. $\Delta=1/2$ (Δ is the relative cell size. If Δ is negative one system is right handed, the other left handed.)

* This transposed matrix is identical to Barker's matrix:

$$uvw/u'v'w'/u''v''w''=\begin{pmatrix}u & v & w\\ u' & v' & w'\\ u'' & v'' & w''\end{pmatrix}$$

$$\bar{\Phi}^{-1}=2\begin{pmatrix}1/2 & 0 & 0\\ 0 & 1/2 & -1/2\\ 0 & 1/2 & 1/2\end{pmatrix}=\begin{pmatrix}1 & 0 & 0\\ 0 & 1 & -1\\ 0 & 1 & 1\end{pmatrix} \text{ or } \Phi^{-1}=\begin{pmatrix}1 & 0 & 0\\ 0 & 1 & 1\\ 0 & -1 & 1\end{pmatrix}.$$

In terms of our new matrix Φ^{-1} we now write

$$(\mathbf{V})_{a'}=\Phi^{-1}(\mathbf{V})_a. \tag{6}$$

Now Φ^{-1} is so related to Φ that $\Phi\Phi^{-1}=\Phi^{-1}\Phi=I$, where I is a matrix with ones on the major diagonal and zeros everywhere else:

$$I=\begin{pmatrix}1 & 0 & 0\\ 0 & 1 & 0\\ 0 & 0 & 1\end{pmatrix}.$$

In multiplying one square matrix by another we can consider the second one as three single column matrices (vectors) and multiply them out to give three vectors (single column matrices) which are written side by side in proper order. This array is then considered to be the resultant matrix. Trial proves that $VI=IV=V$ hence we can consider eq. (6) as derived from eq. (4) by multiplying eq. (4) through by the prefactor Φ^{-1}.

It is a fact that only square matrices have reciprocals and that not every square matrix has a reciprocal.

As an example of the use of a reciprocal matrix we solve for the components of $\begin{pmatrix}1\\ -1/2\\ 5/2\end{pmatrix}_a$ when written on the a' basis. By eq. (6);

$$(\mathbf{V})_{a'}=\Phi^{-1}(\mathbf{V})_a=\begin{pmatrix}1 & 0 & 0\\ 0 & 1 & 1\\ 0 & -1 & 1\end{pmatrix}\begin{pmatrix}1\\ -1/2\\ 5/2\end{pmatrix}_a=\begin{pmatrix}1\\ 2\\ 3\end{pmatrix}_{a'}.$$

We notice in this equation that the three columns of Φ^{-1} are the components of **a, b,** and **c** respectively on the a' basis. If we call $(\mathbf{V})_a$ the "combined vector," since it is multiplied by the matrix prefactor Φ^{-1}, and $(\mathbf{V})_{a'}$ the "uncombined vector," since it is multiplied by no matrix prefactor; we can write this observation in the form of the following transformation theorem which is a useful memory aid for vector transformation equations.

Transformation Theorem.

In a vector transformation equation the three columns of the matrix prefactor are the components of the three base vectors of the "combined vector" on the reference system of the "uncombined vector."

Applying this memory aid to Eq. (4), that is to the converse relation $(\mathbf{V})_a=\Phi(\mathbf{V})_{a'}$ we would say that the three columns of Φ are the three components of the a' base vectors on the a basis. This is actually the case.

Vector Products: By definition the vector product of two vectors **r** and **s** is a vector, perpendicular to both **r** and **s** and of length rs sin (**rs**). It is

apparent that it is the area of a parallelogram defined by $\mathbf{r}$ and $\mathbf{s}$, hence its vector nature. It is an absolute quantity, independent of the basis on which it is expressed. From its definition we see that $\mathbf{r}\times\mathbf{s}=-\mathbf{s}\times\mathbf{r}$ and that $\mathbf{r}\times\mathbf{r}=0$. The cross $\times$ earmarks this product as a vector product to distinguish it from other kinds of products.

If we express both $\mathbf{r}$ and $\mathbf{s}$ on the a basis, then write the vector product, $\mathbf{r}\times\mathbf{s}$ we have:

$$\mathbf{s}=s_1\mathbf{a}+s_2\mathbf{b}+s_3\mathbf{c}$$
$$\mathbf{r}=r_1\mathbf{a}+r_2\mathbf{b}+r_3\mathbf{c}$$
$$\mathbf{r}\times\mathbf{s}=(r_2s_3-r_3s_2)\mathbf{b}\times\mathbf{c}+(r_3s_1-r_1s_3)\mathbf{c}\times\mathbf{a}+(r_1s_2-r_2s_1)\mathbf{a}\times\mathbf{b}.$$

This is in terms of three new vectors, each of which is perpendicular to a pair of the original set. We define these new ones as $u\mathbf{A}=\mathbf{b}\times\mathbf{c}$, $u\mathbf{B}=\mathbf{c}\times\mathbf{a}$, $u\mathbf{C}=\mathbf{a}\times\mathbf{b}$. We call this new set the A basis and say that it is a set reciprocal to the set a.

In terms of these new base vectors we may write a vector product mechanically by writing each vector twice in one column, striking out the top and bottom member and "cross multiplying" as:

$$(\mathbf{r})_a\times(\mathbf{s})_a=\begin{array}{c} r_1 \quad s_1 \\ \hline r_2 \quad s_2 \\ r_3 \quad s_3 \\ r_1 \quad s_1 \\ r_2 \quad s_2 \\ \hline r_3 \quad s_3 \end{array} =u\begin{bmatrix} r_2s_3-r_3s_2 \\ r_3s_1-r_1s_3 \\ r_1s_2-r_2s_1 \end{bmatrix}_A. \tag{7}$$

Since A is perpendicular to $\mathbf{b}$ and $\mathbf{c}$, and $\mathbf{B}$ is perpendicular to $\mathbf{c}$ and $\mathbf{a}$, then $\mathbf{c}$ is perpendicular to $\mathbf{A}$ and $\mathbf{B}$. Similarly $\mathbf{a}$ is perpendicular to $\mathbf{B}$ and $\mathbf{C}$, and $\mathbf{b}$ to $\mathbf{C}$ and $\mathbf{A}$. Hence, if the $\mathbf{A}$ basis is reciprocal to the a basis, then the a basis can be made reciprocal to the A basis and the reciprocity is mutual. We can hence form vector products of two vectors written on the A basis and get an answer written on the a basis but involving an as yet undetermined scalar constant U'.

Plane Normals: A plane (hkl) has axial intercepts $\mathbf{a}/h$, $\mathbf{b}/k$, $\mathbf{c}/l$. A vector $(-\mathbf{a}/h+\mathbf{b}/k)\times(-\mathbf{a}/h+\mathbf{c}/l)$ is perpendicular to this plane. Expanding the cross product we have:

$$\mathbf{N}_{hkl}=\frac{\mathbf{b}\times\mathbf{c}}{kl}+\frac{\mathbf{c}\times\mathbf{a}}{lh}+\frac{\mathbf{a}\times\mathbf{b}}{hk}.$$

If we multiply through by the scalar hkl/u and substitute $\mathbf{A}$ for $l/u\mathbf{b}\times\mathbf{c}$, $\mathbf{B}$ for $l/u\mathbf{c}\times\mathbf{a}$, $\mathbf{C}$ for $l/u\mathbf{a}\times\mathbf{b}$ we have, as a normal to the plane (hkl)

$$\mathbf{N}_{hkl}=\begin{pmatrix} h \\ k \\ l \end{pmatrix}_A. \tag{8}$$

That is, a line from the origin to the point $\begin{pmatrix} h \\ k \\ l \end{pmatrix}_A$ is perpendicular to the plane (*hkl*).

Scalar Products: By definition, the scalar product $\mathbf{r} \cdot \mathbf{s}$ of two vectors **r** and **s** is a scalar of magnitude $rs \cos(\mathbf{rs})$. It is an absolute quantity, independent of the basis on which it is written. It is the length of one of the vectors multiplied by the component of the other vector on the first. It is earmarked by the dot to distinguish it from the vector product.

The Scalar Triple Product: Combining the definition of vector product and scalar product we have the scalar triple product of three vector **r, s,** and **t** as $\mathbf{r} \times \mathbf{s} \cdot \mathbf{t}$. (The cross product is to be taken first.) It is easily seen to be the volume of the parallelepiped defined by **r, s** and **t**. It is also an absolute quantity, independent of the basis on which it is written.

The scalar product can be formed rather simply by mixing the bases, since **A** is perpendicular to **b** and **c** it has no component on them similarly for **B** and **C**, hence we find:

$$\begin{gathered} \mathbf{r} = r_1\mathbf{a} + r_2\mathbf{b} + r_3\mathbf{c} \\ \mathbf{S} = S_1\mathbf{A} + S_2\mathbf{B} + S_3\mathbf{C} \\ \hline \mathbf{r} \cdot \mathbf{S} = r_1S_1\mathbf{a} \cdot \mathbf{A} + r_2S_2\mathbf{b} \cdot \mathbf{B} + r_3S_3\mathbf{c} \cdot \mathbf{C} \end{gathered}$$

substituting $\frac{\mathbf{b} \times \mathbf{c}}{u}$ for **A**, $\frac{\mathbf{c} \times \mathbf{a}}{u}$ for **B** and $\frac{\mathbf{a} \times \mathbf{b}}{u}$ for **C** we have:

$$\mathbf{r} \cdot \mathbf{S} = (r_1S_1 + r_2S_2 + r_3S_3) \frac{\mathbf{a} \cdot \mathbf{b} \times \mathbf{c}}{u}.$$

Hence if we take u equal to the volume of the unit cell:

$$u = \mathbf{a} \times \mathbf{b} \cdot \mathbf{c} \cdots \tag{9}$$

We can simplify the expression of the scalar product to any one of the following:

$$\begin{aligned} (\mathbf{r})_a \cdot (\mathbf{S})_A &= (\mathbf{R})_A \cdot (\mathbf{s})_a = r_1S_1 + r_2S_2 + r_3S_3, \text{ a scalar} \\ &= R_1s_1 + R_2s_2 + R_3s_3 \\ &= (\bar{\mathbf{R}})_A(\mathbf{s})_a = (\bar{\mathbf{s}})_a(\mathbf{R})_A = (\bar{\mathbf{r}})_a(\mathbf{S})_A = (\bar{\mathbf{S}})_A(\mathbf{r})_a. \end{aligned} \tag{10}$$

If the *a* basis has a reciprocal basis A, the *a'* basis must have a reciprocal basis A'. The scalar product of two vectors is an absolute quantity, independent of the basis of expression. Hence $(\bar{\mathbf{S}})_A(\mathbf{r})_a - (\bar{\mathbf{S}})_A\Phi(\mathbf{r})_{a'}$ since $(\mathbf{V})_a = \Phi(\mathbf{V})_{a'}$.

Here $(\bar{\mathbf{S}})_A\Phi$ must equal $(\bar{\mathbf{S}})_{A'}$ whence

$$(\mathbf{V})_{A'} = \bar{\Phi}(\mathbf{V})_A. \tag{11}$$

Conversely

$$(\mathbf{V})_A = \bar{\Phi}^{-1}(\mathbf{V})_{A'}. \tag{11'}$$

We see then that the columns of Φ are the A base vectors expressed on the A' basis and that the columns of Φ^{-1} are the A' base vectors expressed on the A basis.

Transformation of Plane Indices: By eq. 8, a plane of indices (hkl) has a normal $\begin{pmatrix} h \\ k \\ l \end{pmatrix}_A$ and conversely, a line $\begin{pmatrix} h \\ k \\ l \end{pmatrix}_A$ defines a plane (hkl). Hence by eq. (11) a transformation from the basis a to the basis a' by means of $(\mathbf{V})_a = \Phi(\mathbf{V})_{a'}$ implies a transformation from indices (hkl) to $(h'k'l')$ where

$$(h'k'l') = (hkl)\Phi. \tag{12}$$

For example, using the previous value of Φ, a plane $(111)_a$ becomes, on the a' basis:

$$(hkl)_{a'} = (111)_a \begin{pmatrix} 1 & 0 & 0 \\ 0 & 1/2 & -1/2 \\ 0 & 1/2 & 1/2 \end{pmatrix} = (110)_{a'} .$$

Zonal Relations: Since the plane (hkl) has a normal $\mathbf{N} = \begin{pmatrix} h \\ k \\ l \end{pmatrix}_A$ and the plane $(h'k'l')$ has a normal $\mathbf{N}' = \begin{pmatrix} h' \\ k' \\ l' \end{pmatrix}_A$ the line that is common to both planes is perpendicular to both normals. It is given by the vector product $\mathbf{N} \times \mathbf{N}'$. Since cross multipying of two vectors in the reciprocal system gives the resultant vector in the direct system, we see that the vector $\mathbf{Z} = \begin{pmatrix} kl' - k'l \\ lh' - l'h \\ hk' - h'k \end{pmatrix}_a$ lies in both planes and is hence their intersection. $\mathbf{Z}$ is called the zone axis. It is generally given as a *zone symbol* $[uvw]$ in square brackets and if u, v, w have a common factor it is divided out. It is emphasized that the zone symbol gives the components on the a basis of a line parallel to all planes belonging to that zone.

Any plane $(h''k''l'')$ belonging to the zone Z has its normal perpendicular to the vector Z. Hence the scalar product must vanish, and by eq. (10) we have the zonal equation:

$$(uvw)_a \begin{pmatrix} h \\ k \\ l \end{pmatrix}_A = uh + vk + wl = 0 . \tag{13}$$

Rectangular Axes: We now introduce a special set of rectangular axes, **xyz**. They are of unit length, mutually perpendicular and chosen so that **z** lies along **c** and **x** lies in the plane of **a** and **c**. We have a transformation which changes vectors from one basis to the other as:

$$(\mathbf{V})_x = \mathrm{m}(\mathbf{V})_a \tag{14}$$

and conversely

$$(\mathbf{V})_a = \mathrm{m}^{-1}(\mathbf{V})_x \tag{14'}$$

where by the transformation theorem:

$$\mathrm{m}=\begin{vmatrix} a\sin\beta & v_1 b & 0 \\ 0 & v_2 b & 0 \\ a\cos\beta & b\cos\alpha & c \end{vmatrix}, \qquad \mathrm{m}^{-1}=\begin{vmatrix} \dfrac{1}{a\sin\beta} & \dfrac{-v_1}{a v_2 \sin\beta} & 0 \\ 0 & 1/(v_2 b) & 0 \\ \dfrac{-1}{c\tan\beta} & \dfrac{v_1\cot\beta-\cos\alpha}{v_2 c} & 1/c \end{vmatrix}.$$

Here we do not assume that b is necessarily unity. If we are interested in x-ray problems we use the true translations a_0, b_0, c_0 as in eq. (18″). If we are interested only in interfacial angles, etc., we can use the axial ratio values with $b=1$ in which case m becomes M. Since **x**, **y** and **z** are mutually perpendicular and of unit length the volume of this cell is unity and the x basis is self reciprocal. Since the columns of m are the components of **a**, **b** and **c** on the x basis, we can write the scalar product of **a** and **b** as: $\mathbf{a}\cdot\mathbf{b}=ab\cos\gamma=ab\,v_1\sin\beta+ab\cos\alpha\cos\beta$

whence

$$v_1=\frac{\cos\gamma-\cos\alpha\cos\beta}{\sin\beta}$$

as $v_1^2b^2+v_2^2b^2+b^2\cos^2\alpha=b^2$ we find that:

$$v_2=\frac{\sqrt{1+2\cos\alpha\cos\beta\cos\gamma-(\cos^2\alpha+\cos^2\beta+\cos^2\gamma)}}{\sin\beta}. \tag{15}$$

As

$$\begin{aligned} &(\mathbf{V})_{a'}=\Phi^{-1}(\mathbf{V})_a \quad \text{and} \quad (\mathbf{V})_a=\mathrm{m}^{-1}(\mathbf{V})_x \quad \text{then} \\ &(\mathbf{V})_{a'}=\Phi^{-1}\mathrm{m}^{-1}(\mathbf{V})_x \quad \text{and conversely} \\ &(\mathbf{V})_x=\mathrm{m}\Phi(\mathbf{V})_{a'}. \end{aligned} \tag{16}$$

Derivation of New Crystallographic Data: On the a' basis, $\mathbf{a}'=\begin{pmatrix}1\\0\\0\end{pmatrix}_{a'}$, whence we can compute its components on the x basis by (16). Its true length is the square root of the sum of the squares of its components on the x basis. Similarly we compute $\mathbf{b}'$ and $\mathbf{c}'$ and can then find a new axial ratio $a':b':c'$.

Having computed $(\mathbf{a}')_x$ and $(\mathbf{b}')_x$ we normalize* them and take their scalar product. This is $\cos\gamma'$. Similarly for α' and β'.

As an example we consider a monoclinic crystal for which $a:b:c=1.6:1:1.5$, $\beta=95°$. This was found to be body centered when indexed on this cell. A transformation $\phi=\begin{pmatrix}1&0&0\\0&1&0\\-1&0&1\end{pmatrix}$ is used to give a base centered cell. We wish to find the new $a:b:c$ ratio and the new β angle. Since

* Normalizing is reducing a vector to unit length by dividing each component by the true length of the vector.

$$M=\begin{pmatrix} 1.5939 & 0 & 0 \\ 0 & 1 & 0 \\ -.1395 & 0 & 1.5 \end{pmatrix}, (\mathbf{a}')_x=M\Phi\begin{pmatrix}1\\0\\0\end{pmatrix}=\begin{pmatrix}1.5939\\0\\-1.6395\end{pmatrix}_x,$$

$$(\mathbf{b}')_x=m\Phi\begin{pmatrix}0\\1\\0\end{pmatrix}=\begin{pmatrix}0\\1\\0\end{pmatrix}_x, (\mathbf{c}')_x=m\Phi\begin{pmatrix}0\\0\\1\end{pmatrix}=\begin{pmatrix}0\\0\\1.5\end{pmatrix}.$$

This new a axis has a length $a'=\sqrt{1.5939^2+1.6395^2}=2.2866$, while $b'=1.00$ and $c'=1.500$. Hence $a:b:c=2.2866:1:1.500$. Also since $(a')_x$ and $(c')_x$ normalize to

$$\begin{pmatrix}.69706\\0\\-.71700\end{pmatrix}_x \text{ and } \begin{pmatrix}0\\0\\1\end{pmatrix} \text{ respectively } \mathbf{a}\cdot\mathbf{c}=-.717, =\cos\beta', \text{ whence } \beta'=135°49'.$$

Just as the transformation from the a basis to the a' basis by means of $(\mathbf{V})_{a'}=\Phi^{-1}(\mathbf{V})_a$ leads to the transformation from the A basis to the A' basis by means of $(\mathbf{V})_{A'}=\bar{\Phi}(\mathbf{V})_A$ so the transformation from the a basis to the x basis by means of $(\mathbf{V})_x=m(\mathbf{V})_a$ leads to the transformation from the A basis to the x basis by means of:

$$(\mathbf{V})_x=\bar{m}^{-1}(\mathbf{V})_A \tag{17}$$

(because the x basis is self reciprocal). We can now write an equation relating the A basis directly to the a basis by combining (14) and (17):

$$(\mathbf{V})_a=m^{-1}\bar{m}^{-1}(\mathbf{V})_A \tag{18}$$

and conversely:

$$(\mathbf{V})_A=\bar{m}m(\mathbf{V})_a. \tag{18'}$$

On expanding (18') we find:

$$(\mathbf{V})_{A0}=\begin{pmatrix} a_0^2 & a_0b_0\cos\gamma & a_0c_0\cos\beta \\ a_0b_0\cos\gamma & b_0^2 & b_0c_0\cos\alpha \\ a_0c_0\cos\beta & b_0c_0\cos\alpha & c_0^2 \end{pmatrix}(\mathbf{V})_a. \tag{18''}$$

Here we have used the true translation vectors $\mathbf{a}_0$, $\mathbf{b}_0$, $\mathbf{c}_0$ in order to derive the standard equations (21) and (22). The subscript zero of A_0 indicates the fact that this basis is reciprocal to the a_0 basis instead of the a basis. Actually just as $\mathbf{a}_0$ is $\mathbf{b}_0$ times as long as is $\mathbf{a}$ so A_0 is $1/b_0$ times as long as is $\mathbf{A}$. If the axial angles of the reciprocal system are α^*, β^* and γ^* an expression similar to eq. (18') must hold.

$$(\mathbf{V})_a=\begin{pmatrix} A_0^2 & A_0B_0\cos\gamma^* & A_0C_0\cos\beta^* \\ A_0B_0\cos\gamma^* & B_0^2 & B_0C_0\cos\alpha^* \\ A_0C_0\cos\beta^* & B_0C_0\cos\alpha^* & C_0^2 \end{pmatrix}(\mathbf{V})_A. \tag{19}$$

Hence the 3×3 matrix in equation (18'') must be identical to the reciprocal of the 3×3 matrix in eq. (19). This reciprocal is:

$$u=\frac{1}{V_2^2\sin^2\gamma^*}\begin{vmatrix} \frac{1}{A_0^2}\sin^2\alpha^* & \frac{1}{A_0B_0}(\cos\alpha^*\cos\beta^*-\cos\gamma^*) & \frac{1}{A_0C_0}(\cos\gamma^*\cos\alpha^*-\cos\beta^*) \\ \frac{1}{A_0B_0}(\cos\alpha^*\cos\beta^*-\cos\gamma^*) & \frac{1}{B_0^2}\sin^2\beta^* & \frac{1}{B_0C_0}(\cos\beta^*\cos\gamma^*-\cos\alpha^*) \\ \frac{1}{A_0C_0}(\cos\gamma^*\cos\alpha^*-\cos\beta^*) & \frac{1}{B_0C_0}(\cos\beta^*\cos\gamma^*-\cos\alpha^*) & \frac{1}{C_0^2}\sin^2\gamma^* \end{vmatrix}$$

where $$V_2=\frac{\sqrt{1+2\cos\alpha^*\cos\beta^*\cos\gamma^*-(\cos^2\alpha^*+\cos^2\beta^*+\cos^2\gamma^*)}}{\sin\gamma^*}. \tag{20}$$

Equating corresponding major diagonal terms of (18″) and u:

$$\left.\begin{aligned} a_0^2&=\frac{\sin^2\alpha^*}{V_2^2A_0^2} \\ b_0^2&=\frac{\sin^2\beta^*}{V_2^2B_0^2} \\ c_0^2&=\frac{\sin^2\gamma^*}{V_2^2C_0^2}. \end{aligned}\right\} \tag{21}$$

Equating the other corresponding terms and making use of eqs. (21) we obtain

$$\left.\begin{aligned} \cos\alpha&=\frac{\cos\beta^*\cos\gamma^*-\cos\alpha^*}{\sin\beta^*\sin\gamma^*} \\ \cos\beta&=\frac{\cos\gamma^*\cos\alpha^*-\cos\beta^*}{\sin\gamma^*\sin\alpha^*} \\ \cos\gamma&=\frac{\cos\alpha^*\cos\beta^*-\cos\gamma^*}{\sin\alpha^*\sin\beta^*} \end{aligned}\right\}. \tag{22}$$

If the unstarred terms become starred and the starred terms lose their stars the resulting equations are also true.

The Reciprocal Lattice: The volume of the tetrahedron defined by the vectors $\mathbf{a}/h$, $\mathbf{b}/k$, $\mathbf{c}/l$ is alternatively;

$$\text{Vol}=\frac{1}{6}\,\frac{\mathbf{a}}{h}\times\frac{\mathbf{b}}{k}\cdot\frac{\mathbf{c}}{l} \quad \text{and} \quad \text{Vol}=\frac{1}{6}\,d_{hkl}\times\left(\frac{\mathbf{a}}{h}-\frac{\mathbf{b}}{k}\right)\cdot\left(\frac{\mathbf{a}}{h}-\frac{\mathbf{c}}{l}\right)$$

where $\mathbf{d}_{hkl}$ is the perpendicular from the origin to the plane (hkl). Equating these values of the volume and simplifying we have:

$$\mathbf{d}_{hkl}\cdot\begin{pmatrix}\mathrm{h}\\ \mathrm{k}\\ \mathrm{l}\end{pmatrix}_{A_0}=1. \tag{23}$$

Since d_{hkl} and $\begin{pmatrix}h\\ k\\ l\end{pmatrix}_{A_0}$ are both perpendicular to the plane (hkl) we may write their absolute values:

$$\left|\frac{1}{d_{hkl}}\right|=\left|\begin{pmatrix}h\\ k\\ l\end{pmatrix}_{A_0}\right|. \tag{24}$$

Hence we see that the space lattice formed from the base vectors $\mathbf{A}_0$, $\mathbf{B}_0$ and $\mathbf{C}_0$ by giving h, k and l all integral values is not only a three dimensional plot of the normals of all planes (hkl) but is also a three dimensional plot of the reciprocals of distances between atomic planes. It is called a reciprocal lattice.

Since the absolute value of $\mathrm{m}=\begin{pmatrix}h\\k\\l\end{pmatrix}_{A_0}$ is the square root of the sum of the squares of its components on the x basis and this, by Eq. (17) is: $\bar{\mathrm{m}}^{-1}\begin{pmatrix}h\\k\\l\end{pmatrix}$ we can use the $\bar{\mathrm{m}}^{-1}$ matrix as a means of computing interplanar spacings. This is especially convenient for triclinic crystals.

Formally.
$$\frac{1}{d_{hkl}}=\sqrt{\mathrm{D}_1^2+\mathrm{D}_2^2+\mathrm{D}_3^2} \tag{25}$$

where

$$\begin{pmatrix}\mathrm{D}_1\\\mathrm{D}_2\\\mathrm{D}_3\end{pmatrix}=\bar{\mathrm{m}}^{-1}\begin{pmatrix}h\\k\\l\end{pmatrix}. \tag{26}$$

By means of the transformation theorem we can set up the $\bar{\mathrm{m}}^{-1}$ matrix in terms of reciprocal cell constants. By Eq. (17), the columns of m^{-1} must be the vectors $\mathbf{A}_0$, $\mathbf{B}_0$, $\mathbf{C}_0$, on the x basis. Hence

$$\mathrm{m}^{-1}=\begin{pmatrix}\mathrm{A}_0\sin\gamma^* & 0 & \mathrm{C}_0\mathrm{V}_1\\ \mathrm{A}_0\cos\gamma^* & \mathrm{B}_0 & \mathrm{C}_0\cos\alpha^*\\ 0 & 0 & \mathrm{C}_0\mathrm{V}_2\end{pmatrix} \tag{27}$$

where

$$\mathrm{V}_1=\frac{\cos\beta^*-\cos\alpha^*\cos\gamma^*}{\sin\gamma^*} \tag{28}$$

and V_2 is given by Eq. (20).
Applying the above we see that, indeed

$$\mathrm{A}_0=\frac{1}{d_{100}},\qquad \mathrm{B}_0=\frac{1}{d_{010}},\qquad \mathrm{C}_0=\frac{1}{d_{001}}.$$

Hence we can evaluate the constants of (27) by x-ray measurements alone since:

$$\cos\alpha^*=\frac{d_{010}d_{001}}{2}\left(\frac{1}{d_{011}^2}-\frac{1}{d_{010}^2}-\frac{1}{d_{001}^2}\right)=\frac{-d_{010}d_{001}}{2}\left(\frac{1}{d_{01\bar{1}}^2}-\frac{1}{d_{010}^2}-\frac{1}{d_{001}^2}\right),$$

$$\cos\beta^*=\frac{d_{001}d_{100}}{2}\left(\frac{1}{d_{101}^2}-\frac{1}{d_{100}^2}-\frac{1}{d_{001}^2}\right)=\frac{-d_{001}d_{100}}{2}\left(\frac{1}{d_{10\bar{1}}^2}-\frac{1}{d_{100}^2}-\frac{1}{d_{001}^2}\right)$$

and finally

$$\cos\gamma^*=\frac{d_{100}d_{010}}{2}\left(\frac{1}{d_{110}^2}-\frac{1}{d_{100}^2}-\frac{1}{d_{010}^2}\right)=\frac{-d_{100}d_{010}}{2}\left(\frac{1}{d_{1\bar{1}0}^2}-\frac{1}{d_{100}^2}-\frac{1}{d_{010}^2}\right). \tag{29}$$

As an example let us assume that

$$d_{110}=5.000, \qquad d_{010}=6.667, \qquad d_{001}=4.000$$

$$d_{011}=3.091, \qquad d_{101}=2.889, \qquad d_{110}=4.178.$$

From this data, Eqs. (29) give $\alpha^*=74°49'$, $\beta^*=80°2'$, $\gamma^*=85°1'$. Also $V_1=0.1510$, $V_2=0.9532$. So that:

$$\bar{\mathfrak{m}}^{-1}=\begin{pmatrix} .1992 & 0 & .0378 \\ .0174 & .1500 & .0655 \\ 0 & 0 & .2383 \end{pmatrix}.$$

From this matrix we can compute the d spacing and vector normal of any plane. Let us do this for the plane $(12\bar{3})$.

Here
$$D=\bar{\mathfrak{m}}^{-1}\begin{pmatrix} 1 \\ 2 \\ -3 \end{pmatrix}=\begin{pmatrix} .0858 \\ .1209 \\ -.7149 \end{pmatrix}.$$

So that

$$\frac{1}{d_{12\bar{3}}}=\sqrt{.0858^2+.1209^2+.7149^2}=.7301$$

whence $d_{123}=1.370$. Finally the unit normal of the plane $(12\bar{3})$ is

$$1.370\begin{pmatrix} .0858 \\ .1209 \\ -.7149 \end{pmatrix}=\begin{pmatrix} .1175 \\ .1655 \\ -.9792 \end{pmatrix},$$

that is, the factor that normalizes the vector perpendicular of the face (hkl) on the x basis is d_{hkl}.

Summary

1. $(\mathbf{V})_a=\Phi(\mathbf{V})_{a'}$ transforms vectors $(\mathbf{V})_{a'}$ on the a' basis to the proper expression on the a basis. Here the columns of Φ are the a' base vectors expressed on the a basis.

2. $(\mathbf{V})_{a'}=\Phi^{-1}(\mathbf{V})_a$ transforms $\mathbf{V}$ from the a basis to the a' basis, the columns of Φ^{-1} are the a base vectors written on the a' basis.

3. The vector product of two vectors $\mathbf{r}$ and $\mathbf{s}$ written in the same system is expressed on the reciprocal system as

$$u\begin{pmatrix} r_2s_3-r_3s_2 \\ r_3s_1-r_1s_3 \\ r_1s_2-r_2s_1 \end{pmatrix}_A$$

where u is the volume of the direct space unit cell.

4. The scalar product of two vectors $\mathbf{r}$ and $\mathbf{s}$ one of which is expressed on the direct system, the other on the reciprocal system is: $r_1s_1+r_2s_2+r_3s_3$.

5. A plane (hkl) has a normal $\begin{pmatrix} h \\ k \\ l \end{pmatrix}_A$ and this vector is of length $\frac{1}{d_{hkl}}$ where d_{hkl} is the distance of this plane from the origin. Hence it is the distance between such planes.

6. The vector product of the normals of two planes (hkl) and $(h'k'l')$ is a vector parallel to the line of intersection of the two planes. It is called the zone axis. The vector, written in transposed form is the zone symbol.

7. The vector product of two vectors formed from zone symbols is a vector in reciprocal space and hence represents a plane in direct space.

THE IDENTITY OF FALKMANITE AND YENERITE WITH BOULANGERITE

S. C. Robinson,
Queen's University, Kingston, Ontario, Canada.

Abstract

Two recently named lead sulphantimonite minerals, falkmanite and yenerite, are re-examined. *X*-ray powder patterns are indistinguishable from that of boulangerite. Structural lattice dimensions, deduced from *x*-ray rotation and Weissenberg photographs, agree with those of boulangerite within limits of accuracy of measurement. Other properties supposed to distinguish the three minerals are critically reviewed.

Introduction

Nearly twenty mineral names have been proposed for minerals belonging to the Pb-Sb-S system. The two most recent of these, falkmanite ($12PbS \cdot 4Sb_2S_3$) described by Hiller (1939) and by Ramdohr and Ödman (1940), and yenerite ($11PbS \cdot 4Sb_2S_3$) described by Bayramgil (1945), appear to differ very little from boulangerite ($10PbS \cdot 4Sb_2S_3$) as described by Berry (1940) and Palache and Berman (1942). In the course of an investigation of the Pb-Sb-S system (Robinson 1948) the writer was unable to confirm either of these new species; it was felt, therefore, that further examination of natural type material was warranted.

A type specimen of yenerite from Isikdag, Turkey, collected and described by Bayramgil (1945) was obtained through the kindness of Professor Reinhard, Basel. For specimens of falkmanite from the Bayerland Mine, Bavaria, and from Boliden, Sweden, the writer is indebted both to Professor Ramdohr, Berlin, and jointly to Professor Quensel and Dr. Ödman, Stockholm. Unfortunately the specimens of falkmanite from Minas Geraeson which Hiller carried out his *x*-ray investigation were destroyed during the war. Professor Berry, under whose supervision this work was carried out, was also kind enough to make available his original *x*-ray photographs of boulangerite. For purposes of comparison, specimens of boulangerite from the Sullivan Mine, British Columbia, supplied by courtesy of the Consolidated Mining and Smelting Co., were used. These clean acicular crystals were analyzed by J. R. Williams & Son, Vancouver, B. C. (Warren & Thompson 1944, p. 82).

Examination of yenerite and falkmanite was restricted to determination of such data as may be evaluated from *x*-ray powder, rotation, and Weissenberg photographs. For this purpose filtered Cu*K* radiation was employed in powder photographs and unfiltered Cu*K* radiation for rotation and Weissenberg photographs. Camera radius in all cases is 90π mm. (1 mm. on film $= 1^\circ\theta$).[1] In *x*-ray powder photographs of minerals

[1] Each camera was calibrated by measurement of *x*-ray photographs of calcite.

such as boulangerite, which are markedly acicular in habit, the effect of preferred orientation of many individual particles in the powder specimen frequently gives rise to divergences in the proper intensity of diffractions from planes in the zone parallel to the direction of elongation of the mineral, relative to those from other planes. Particular care was taken in preparation of powder "spindles" both to reduce this phenomenon to a minimum and also to attain approximately equal thickness of powder specimens.

Since the *x*-ray powder pattern of falkmanite is described by Hiller (1939) as being identical with that of boulangerite, and that of yenerite is said to differ only slightly (Bayramgil 1945), rotation and Weissenberg photographs of each were also taken. These were both measured and compared directly by superposition on a screen with the corresponding photographs of boulangerite.

Description of Specimens

Yenerite, in the one specimen available, occurs as a mass of loose felted hair-like crystals in a vug with euhedral quartz crystals. It is found also as needles in quartz associated with subhedral pyrite, euhedral arsenopyrite, and massive sphalerite, in a rather friable quartz and calcite gangue.

Falkmanite forms the bulk of the specimens both from Bayerland and Boliden. Typically it appears in sub-parallel bundles of fibres, such bundles commonly being so oriented as to yield a mosaic appearance. In polished section its association with chalcopyrite, pyrite, galena, and bournonite has been well illustrated in photographs of polished sections in the paper by Ramdohr and Ödman (1940). The bournonite veins chalcopyrite, these veins extending into fractures in the falkmanite caused by flexing of the parallel bundles; in both cases replacement by bournonite is indicated. Galena appears commonly as rounded "remnants" in falkmanite and as irregular rounded or elongated inclusions down to sizes barely resolved under magnification of 50 diameters. This distribution of galena is common in varying amounts to all available specimens of falkmanite, both from Bayerland and Boliden.

X-ray Analysis of Boulangerite, Falkmanite and Yenerite

X-ray powder patterns of yenerite, falkmanite, and boulangerite are identical except for barely discernible differences in intensity due to preferred orientation of particles in the specimen. Similar variations in intensity have been demonstrated in two powder "spindles" made up from identical material. *X*-ray powder photographs of the three minerals are reproduced in Figures 1, 2, 3, 4. Identity is best established by direct

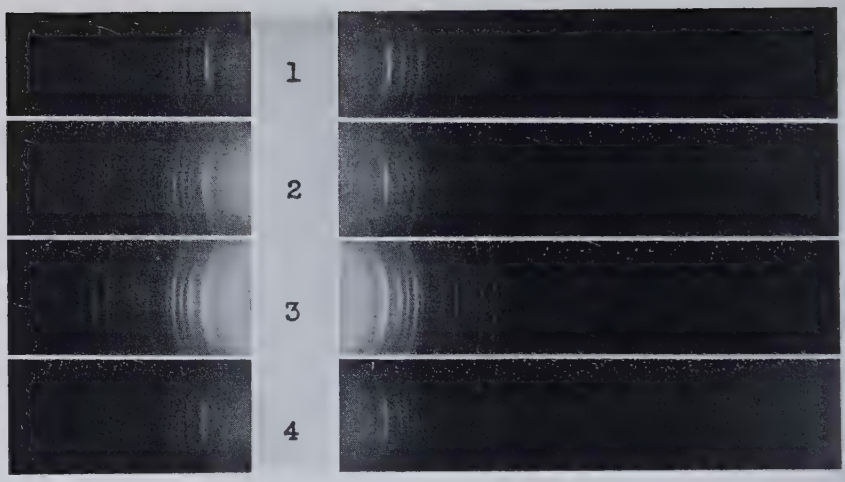

FIG. 1–4. *X*-ray powder photographs with Cu radiation (Ni filter); camera radius $90/\pi$ mm. (1 mm. on film $= 1°\theta$); full size reproductions of contact prints.

FIG. 1. Boulangerite, Sullivan Mine, Kimberley, B.C.
FIG. 2. Yenerite, Isikdag, Turkey.
FIG. 3. Falkmanite, Bayerland Mine, Bavaria, Germany.
FIG. 4. Falkmanite, Boliden, Sweden.

comparison using a screen with a cursor; the differences in spacing of lines in Table 1 are, in fact, due to the limited accuracy of measurement.

Spacings for the different planes corresponding to these diffractions, calculated from measured dimensions of the unit cell of boulangerite have already been published (Berry 1940, Table 2, pp. 14–15). Several lines in addition to those listed by Berry are included in the above table; each of these was found in more than one *x*-ray powder photograph.

The possibility exists that two minerals which are chemically and structurally similar, may yield *x*-ray powder photographs in which differences are so slight as to be barely discernible,[2] particularly when such differences may be attributable either to preferred orientation or to diffractions from minor impurities. In such cases it is necessary to employ *x*-ray rotation photographs and Weissenberg resolutions of the various layers. Such photographs can be indexed and diffractions due to extraneous causes are then readily recognized.

Rotation and Weissenberg photographs of the zero, first, and second layers were made and indexed for boulangerite and yenerite. In the case

[2] Such a case is well illustrated by similarity in *x*-ray powder photographs of andorite, ramdohrite and fizelyite (Nuffield 1945).

TABLE 1. *X*-RAY POWDER PHOTOGRAPHS

Diffractions having glancing angles θ (Cu) less than 38.45 only

1		2		3		4			5		6	
$I\phi$	θ(Cu)	$I\phi$	θ(Cu)	$I\phi$	θ(Cu)	$I\phi$	θ(Cu)	d(meas.)	$I\phi$	θ(Cu)	$I\phi$	θ(Cu)
—	—	1/2	6.6°	—	—	1/2	6.55°	6.74 kX				
—	—	1	7.3	—	—	1	7.2	6.13	—	—	—	—
—	—	—	—	—	—	1/2	8.5	5.20	—	—		—
—	—	—	—	—	—	1/2	9.1	4.86	—	—		—
—	—	—	—	—	—	1/2	9.6	4.61	—	—	—	—
1/2	10.2°	1	10.15	1/2	10.51°	1	10.15	4.36	—	—	—	—
—	—	—	—	—	—	—	—	—	—	—	vvw	10.8°
2	11.4	2	11.4	2	11.4	2	11.4	3.89	vw	11.3°	vw	11.4
10	11.95	10	11.95	10	11.95	10	11.95	3.71	vvs	11.9	s	12.0
1	12.95	1	12.95	1	12.95	1	12.95	3.43	vvw	12.9	—	—
3	13.4	3	13.4	3	13.45	3	13.4	3.32	vw	13.4	—	—
5	13.85	5	13.85	4	13.9	5	13.85	3.21	m	13.8	—	—
4	14.7	4	14.75	3	14.8	4	14.75	3.02	m	14.8	m	14.9
8	15.85	8	15.85	8	15.85	8	15.85	2.815	vvs	15.85	s	15.9
3	16.6	3	16.55	2	16.65	3	16.6	2.691	w	16.8	m	16.7
1	17.35	1	17.35	1	17.35	1	17.35	2.578	vvw	17.3	vw	17.3
1/2	17.85	—	—	1/2	17.85	1/2	17.8	2.515	—	—	—	—
1/2	18.35	1/2	18.45	1/2	18.45	1	18.4	2.435	—	—	—	—
—	—	—	—	—	—	—	—	—	vvw	19.0	—	—
6	19.2	6	19.15	6	19.25	5	19.2	2.337	vw	19.3	m	19.2
6	19.45	—	—	—	—	1/2	19.5	2.303	—	—	—	—
1/2	20.15	1/2	20.15	1/2	20.25	1/2	20.2	2.226	—	—	m	20.2
5	20.95	4	21.0	5	21.05	4	21.0	2.145	w	21.1	m	21.1
—	—	1/2	21.45	—	—	—	—	—	—	—	—	—
1	21.95	2	22.05	2	22.0	2	21.95	2.056	w	22.1	s	22.1
1	22.95	1/2	23.0	1	23.1	1	23.0	1.967	vvw	23.1	vw	23.2
3	23.6	2	23.65	3	23.65	2	23.6	1.920	m	23.6	m	23.7
7	24.35	7	24.45	7	24.45	7	24.4	1.861	vvs	24.3	vs	24.5
—	—	1/2	24.95	—	—	1/2	24.85	1.829	—	—	vw	25.0
7	25.95	6	25.95	6	26.0	6	25.95	1.757	s	26.0	s	26.0
2	26.45	1	26.45	1	26.45	2	26.45	1.726	m	26.4	—	—
2	27.55	2	27.55	—	—	1	27.45	1.668	—		—	—
—	—	—	—	2	27.65	2	27.65	1.657	—	—	vvw	27.6
1	29.05	1/2	29.0	1/2	29.0	1/2	28.95	1.588	—	—	vvw	29.1
—	—		—	1/2	30.1	1/2	30.0	1.537	—	—	vvw	30.3
—	—	—	—	—	—	1	30.75	1.504	—	—	—	—
2	31.6	1	31.75	1	31.75	1	31.65	1.465	w	31.4	m	31.6
—	—	—	—	—	—	—	—	—	—	—	vw	32.5
3	33.05	2	33.1	3	33.1	2	33.1	1.408	s	33.0	s	33.2
1	33.8	1/2	33.95	1	33.95	1	33.9	1.378	—	—	vw	33.9
—	—	—	—	—	—	—	—	—	—	—	vw	35.4
1	36.1	1	36.05	1	36.25	1/2	36.15	1.303	m	36.1	m	36.4
1	38.3	1	38.4	1	38.45	1	38.35	1.239	m	38.1	s	38.4

1. Falkmanite, Bayerland Mine, Bavaria.
2. Falkmanite, Boliden, Sweden.
3. Yenerite, Isikdag, Turkey.
4. Boulangerite, Sullivan Mine, Br. Columbia.
5. Boulangerite, Mullan Idaho (Berry 1940).
6. Boulangerite, Hiller (Berry 1940).

$I\phi$—Intensity estimated visually.

θ(Cu)—Glancing angle corrected for divergence in camera radius from $90/\pi$ mm. and for film shrinkage.

d(meas.)—Planar spacing (Å).

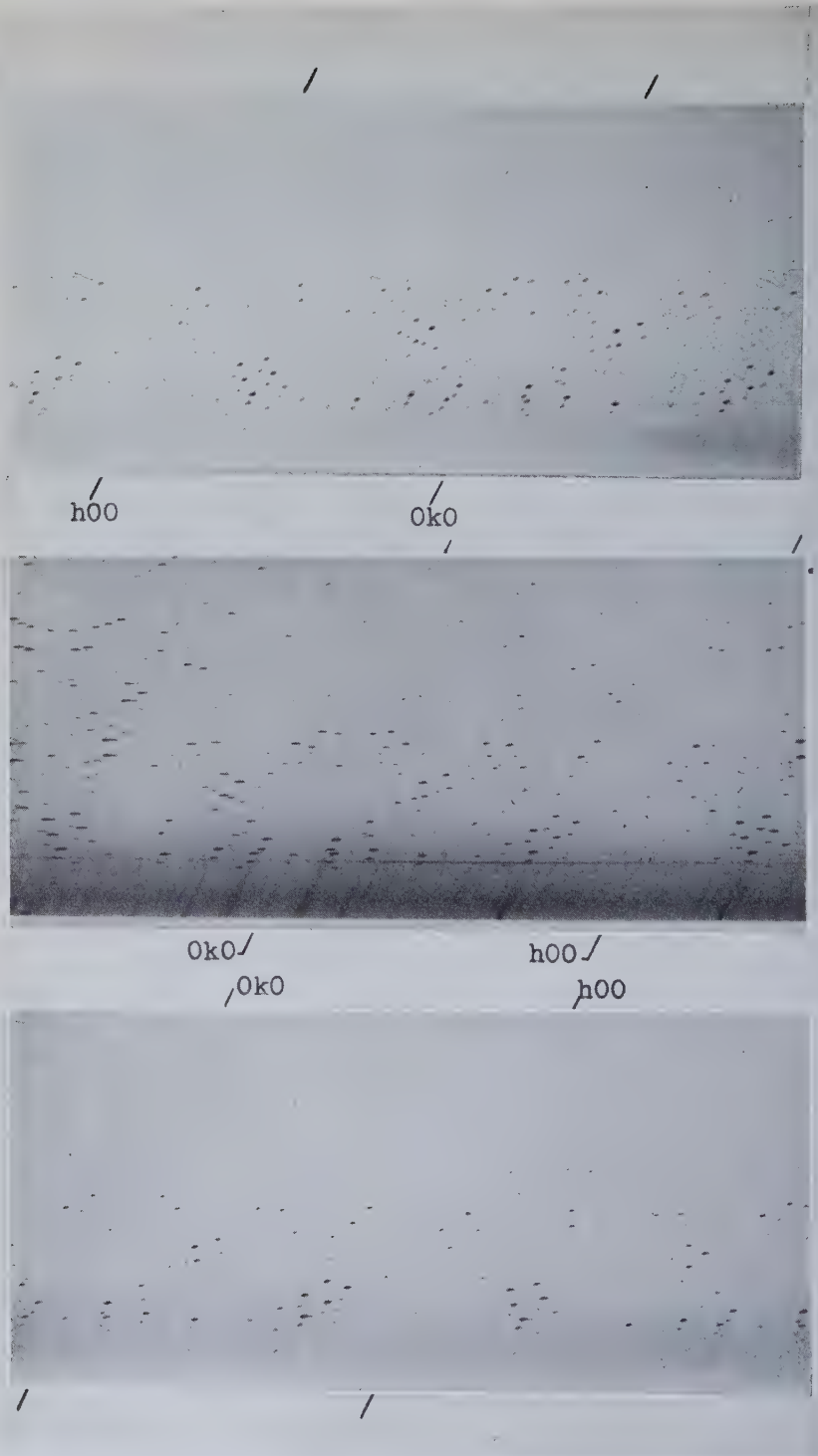

FIGS. 5–7. Weissenberg resolutions of the zero-layer-line about the needle-axis [001]; Cu radiation unfiltered; full size reproduction of contact prints.

FIG. 5. Yenerite, Isikdag, Turkey.

FIG. 6. Boulangerite, Mullan, Idaho.

FIG. 7. Falkmanite, Bayerland Mine, Bavaria, Germany.

of falkmanite, rotation and zero-layer photographs only were made. These single crystal photographs of the zero-layer with rotation about the axis of elongation (c-axis) for crystals of boulangerite and yenerite and for a crystal fragment of falkmanite are illustrated in Figures 5, 6, 7. In all cases the relative photographs of all three are identical both in relative intensity and in spacing. This fact is best established by superposing one photograph upon the other; differences in the following table of elements of the unit cell are entirely due to limitations in accuracy of measurement of the photographs.

Table 2. Cell Dimensions of Boulangerite, Falkmanite, and Yenerite

Specimen	a	b	c	β
Boulangerite (Sullivan)	21.46 kX	23.49 kX	8.07 kX	100° 50′
Boulangerite (Berry 1940)	21.52	23.46	8.07	100 48
Falkmanite (Bayerland)	21.53	23.49	8.08	100 49
Falkmanite (Bayerland)	21.49	23.46	8.07	100 49
Yenerite (Isikdag)	21.47	23.44	8.08	100 51

Indexed reciprocal lattice projections of Weissenberg resolutions of the zero, first and second layer lines of boulangerite and yenerite show that systematically missing reflections conform to the conditions: hOl present only with h even; $0k0$ present only with k even. These conditions coincide with those determined by Berry (1940) for boulangerite from Mullan, Idaho, and are characteristic for the space group: $C_{2h}^5 - P2_1/a$.

Review of Some of the Criteria Advanced for Distinction Between Boulangerite, Yenerite and Falkmanite

A review of Hiller's x-ray work on falkmanite shows that while he found the x-ray powder patterns of falkmanite and boulangerite to be identical, he obtained monoclinic elements for falkmanite as compared with his earlier and incorrect orthorhombic elements for boulangerite. His falkmanite elements roughly correspond in two dimensions and the β angle with the true elements for boulangerite, although his setting differs. In view of his erroneous results on boulangerite and other minerals (Berry 1943 footnote, p. 19), it seems possible that his values for falkmanite are equally in error.

X-ray analysis of yenerite in the original paper rests entirely on minor differences between its powder pattern and that of boulangerite. These differences may be due to preferred orientation or to impurities in one specimen or the other. Neither in falkmanite nor in yenerite was any attempt made to verify the powder pattern by calculation of spacings based on elements of the unit cell.

Although this investigation has been limited to such properties as may be obtained from x-ray analysis, some comment may be advisable also regarding other criteria on which determination of falkmanite and yenerite rests.

In both cases chemical analysis indicates higher lead content than is required for boulangerite, but in both cases the material analyzed contained minerals other than falkmanite and yenerite, respectively. In both cases, too, galena is closely associated with the sulpho-salt; in eight polished sections of type falkmanite from Boliden and Bavaria no single area was found to be free from interstitial galena. While Ramdohr and Ödman (1940) do note the presence of galena, apparently they did not make any correction for it in recasting their analysis.

Bayramgil (1945) considers that his determination of specific gravity corroborates a lead-content in yenerite greater than that of boulangerite and proposes the use of specific gravity determination as an indication of composition for the lead sulphantimonites. In his graph illustrating this suggestion, Bayramgil shows specific gravities of boulangerite 5.79, falkmanite (Hiller) 6.23 and yenerite 6.05. Ramdohr and Ödman (1940) record 6.195 and 6.20 as the specific gravity of falkmanite. Most recent determinations of specific gravity of boulangerite (Palache, Berman and Frondel 1944 p. 421) are 6.23 and 5.98 (measured) and 6.21 (calculated). Thus the measured specific gravity of both falkmanite and yenerite falls in the range of recent determinations for boulangerite.

The writer considers that the data presented above adequately establish the mutual identity of boulangerite, falkmanite, and yenerite. Since the name boulangerite has precedence in the literature it is suggested that it be retained and that the names falkmanite and yenerite be discarded.

References

Bayramgil, O. (1945), Mineralogische Untersuchung der Erzlagerstätte von Isikdag (Türkei): *Schweiz. Min. u. Pet. Mitt.*, **25,** 23–114.

Berry, L. G. (1940), Studies of mineral sulpho-salts: III—Boulangerite and "epi-boulangerite": *Univ. Toronto Studies, Geol. Ser.*, No. **44,** 5–20.

——— (1943), Studies of mineral sulpho-salts: VII—A systematic arrangement on the basis of cell dimensions: *Univ. Toronto Studies, Geol. Ser.*, No. **48,** 9–27.

Hiller, J. E. (1939), Über den Falkmanit: *Zeit. Krist.*, **102,** 138–142.

Nuffield, E. W. (1945), Studies of mineral sulpho-salts: X—Andorite, ramdohrite, fizelyite: *Trans. Roy. Soc. Can.*, **39,** Sec. 4, 41–50.

Palache, C., and Berman, H. (1942), Boulangerite: *Am. Mineral.*, **27,** 552–562.

Palache, C., Berman, H., and Frondel, C. (1944), *The System of Mineralogy of J. D Dana and E. S. Dana*, 7th Ed., Vol. **1** (New York).

Ramdohr, P., and Ödman, O. (1940), Falkmanit, ein neues Bleispiessglanzerz, und sein Vorkommen, besonders in Boliden und Grube Bayerland: *Neues Jahrb. Min., Abt. A*, Beil. Bd. **75,** 315–350.

ROBINSON, S. C. (1948), Studies of mineral sulpho-salts: XIV—Artificial sulphantimonites of lead: *Univ. Toronto Studies, Geol. Ser.*, No. **52** 54–70.

WARREN, H. V., AND THOMPSON, R. M. (1944), Antimony minerals from British Columbia and Yukon Territory: Boulangerite, chalcostibite, jamesonite, zinkenite: *Univ. Toronto Studies, Geol. Ser.*, No. **49**, 78–84.

USEFUL ASPECTS OF THE FLUORESCENCE OF ACCESSORY-MINERAL-ZIRCON*

WILFRID R. FOSTER,

Champion Spark Plug Company, Ceramic Division, Detroit, Michigan.

ABSTRACT

The mineral zircon has long been known to exhibit fluorescence when exposed to ultraviolet radiation. Hitherto little practical use appears to have been made of this phenomenon. Its application is here recommended in the inspection of commercial concentrates of zircon and of other minerals containing zircon as an impurity. Comparison of the fluorescent behavior of grains of zircon from igneous rocks of different ages, and from igneous as compared to sedimentary sources, reveals certain contrasts. The possible usefulness of such contrasts in the solution of a number of petrological problems is discussed. Reference is also made to the fluorescence of accessory-mineral apatite, and of certain other minerals found in association with zircon.

INTRODUCTION

Mineral fluorescence is generally regarded as little more than an interesting and spectacular phenomenon, and of but little practical value to the mineralogist or petrologist. A number of exceptions to this generalization might be enumerated however. Its usefulness in the control of grade of concentrates of New Jersey zinc ores (8) (12), and in the location and evaluation of tungsten ores (2) (22) (24), is well known. It also facilitates the sorting of a wide variety of other non-metallic minerals (1) (20) (23) (26). Other applications include the study of the occurrence and distribution of sodalite in alkaline igneous rocks (7) (10) (11) (16), and the localization of ore minerals in polished sections (27).

The fluorescence of zircon, although known for many years, does not seem to have received much attention. Zircon is frequently omitted from tabulations of the fluorescent minerals, and is said to be the most frequently overlooked of such minerals (26). Statements that zircon does not usually fluoresce (3), or that it fluoresces only under the shorter ultraviolet wave lengths (19), are at variance with the experience of the writer. Examination of hundreds of samples of fine-grained accessory-mineral zircon has demonstrated that, for this type at least, fluorescence is the rule rather than the exception, and may be exhibited under either short or long radiation or both.

Fluorescence in minerals depends upon the presence of elements in solid solution in certain optimum concentrations to function as activators, and the absence of appreciable amounts of other elements in solid solution which might poison or inhibit the activators (15). The precise

* Contribution from the Research Laboratories of the Ceramic Division of the Champion Spark Plug Company.

agent or agents responsible for fluorescence in zircon have not in all cases been determined, although it is probable that they are included among the elements of the rare earth and radioactive groups. The yellowish fluorescence of many zircons is perhaps suggestive of uranium, which with thorium is known to occur in zircon, even if only in the minutest traces. The red fluorescence of zircon has been ascribed to samarium and terbium, and the green fluorescence to dysprosium (9). Hafnium in zircon has been shown to vary from 0.2 to 16 per cent and to average three per cent (5), and the suggestion has been made that this element may be an activator of the fluorescence (4).

This paper is not concerned with the causal agents nor mechanism of zircon fluorescence. The sole purpose is to arouse an interest in its application to evaluate commercial concentrates and in its possible diagnostic value in heavy-mineral correlation studies. The results here presented are largely preliminary in character, yet they appear to indicate that further work is warranted. It is hoped that this initial study may prepare the way for more thorough studies by other workers.

Sources of Ultraviolet Radiation

The first requirement for such fluorescence studies is an adequate source of ultraviolet light for irradiating the specimens. It has been shown that the hue, intensity, and even existence of fluorescence in a particular mineral specimen depends on the wave length of the incident radiation (14). The ideal unit would be one capable of yielding essentially monochromatic radiations of high and uniform intensity over the wavelength band from about 2500 to 4000 angstrom units (A.U.). Such characteristics are not embodied in any commercial unit. Most currently available sources provide either a predominantly short-wave (2537 A.U.) or a predominantly long-wave (3650 A.U.) radiation. Unfortunately there is considerable variation in the intensity and degree of monochromaticity of different units. Accordingly, one should always specify the particular type of unit employed, in order to permit correlation with the work of other investigators. The possibility of any such correlation has been questioned on the grounds that not only are the lamps of a given manufacturer too variable in behavior, but a single lamp may display considerable change in output in service.* Such an extreme view should not be allowed to discourage fluorescence studies and comparisons, and it appears in no way to invalidate the general conclusions arrived at in this study.

Facilities for an exhaustive comparison of the effect of a wide variety of ultraviolet sources on the fluorescence of ziron were not available, nor

* Hugh S. Spence, personal communication.

did such a comparison appear necessary, for this preliminary investigation. Attention was confined to several units which happened to be at hand. These included a Magnaflux ZB22 Blacklight, a General Electric B-H-4 bulb, and an R & M unit. The two former are classed among the so-called long or near ultraviolet sources, and give their predominant emission at 3650 A.U. The third is a representative of the short or far ultraviolet sources, its radiation being concentrated at a wave length of 2537 A.U. Of the two long-wave sources the Magnaflux unit was found to give much the more intense radiation, and was used almost exclusively when 3650 A.U. radiation was required. The R & M lamp did not furnish as intense a radiation as might be desired. Another lamp of the same type, the Mineralight, apparently has a much higher radiation intensity, but unfortunately it was not available. Undoubtedly other sources superior to even the best of the above-mentioned lamps will before long be obtainable, particularly if studies such as the present one demonstrate a need for them.

Method of Study

No fixed method of sample preparation was followed for these studies. In most cases the condition of the sample as examined was that in which it was received, and included highly concentrated, partially concentrated, and unconcentrated conditions.

Highly Concentrated Samples: Commercial zircon samples are already highly concentrated. The manner in which they are evaluated for industrial use is described in a later section. These concentrates furnished excellent material for studying the variety of fluorescent responses displayed by zircon. A high degree of concentration is particularly desirable for critical comparison of the responses of zircons of various rock types and ages. Fortunately, some of the samples lent to the writer were received in this condition.

Partially Concentrated Samples: Some samples were received in the form of heavy-mineral concentrates in which the often minor zircon is accompanied by the usual accessory mineral associates. In order to protect these borrowed samples from depletion, contamination, or change in mineral proportions they were studied without any attempt at further concentration. Permanent grain mounts, if embedded in Canada balsam or any of the other customary media, are not amenable to direct study, since the fluorescence of the mounting medium masks that of the zircon. It has been suggested to the writer that the mounting medium can be readily dissolved with acetone, if desired.†

Unconcentrated Samples: Although some degree of concentration is

† S. A. Tyler, personal communication.

desirable, it is by no means mandatory. Considerable information can be obtained from rock chips, despite the minuteness of the grain size and the quantity of zircon in its host rock. A number of rock chips presenting reasonably smooth though not necessarily plane or polished surfaces should be available for such direct examination. Such a step is a worthwhile preliminary to the study of any suite of rocks for which zircon concentrates are not already available. Background fluorescence due to the enclosing rock is seldom so pronounced as to obscure the response of the zircon grains, especially if the rock is fresh. A single rock thin section generally presents too restricted an area to reveal the characteristic response of the zircon. Thin sections, too, suffer from the same disadvantage as permanent grain mounts on account of the fluorescence of the mounting medium.

The examination procedure is extremely simple, and observations can be rapidly made. The sample is merely exposed directly to the radiation from the ultraviolet source. The visible light thereupon emitted by the sample can usually be detected with the unaided eye, and in some cases direct examination is satisfactory. In most cases, however, it is preferable to make the observations under the low magnification (10× or thereabouts) of a binocular microscope. For sparse granular samples, it is well to use a black non-fluorescing background. In general, where glass or plastic-capsule containers are used the samples must be removed therefrom. Glass, although transmitting the longer ultraviolet wave lengths, cuts out the shorter radiation, whereas plastic capsules are themselves fluorescent. A general rule to be followed in the comparison of a series of samples is that the conditions of observation and of the samples be the same throughout.

General Observations

The pronounced variation in fluorescent response exhibited by zircon is strikingly evident if one examines but a single sample of commercial granular zircon under the binoculars with ultraviolet illumination. Close examination of many such samples has given rise to the descriptive classification presented in Table 1. Admittedly, it is very qualitative and leaves much to be desired if one is interested in a rigorous approach to the problem of fluorescence in zircon. Yet it is quite satisfactory for present purposes, where one is interested primarily in general trends in behavior among the zircons from different sources.

As regards the hue of fluorescence quite a few types can be recognized under the same lamp. The more intense Magnaflux lamp reveals sharper distinctions in hue than do the weaker R & M and General Electric B-H-4 lamps. Intensity of fluorescence under a given lamp shows all

Table 1. Fluorescence—Characteristics of Zircon

HUE OF FLUORESCENCE					
1. Red	2. Yellow	3. Orange	4. Green	5. Orange-Yellow	6. Greenish Yellow
INTENSITY OF FLUORESCENCE					
1. Imperceptible		2. Faint	3. Distinct	4. Bright	5. Intense
CHANGE IN FLUORESCENCE INTENSITY WITH CHANGE IN WAVE LENGTH					
1. Increase		2. Decrease		3. Essentially Unchanged	
UNIFORMITY OF BULK FLUORESCENCE					
1. Uniform		2. Somewhat Nonuniform		3. Very Nonuniform	
EFFECT OF CHEMICAL TREATMENT ON FLUORESCENCE INTENSITY					
1. Increase		2. Decrease(?)		3. Essentially Unchanged	

possibilities from imperceptible to intense. Where the response is faint, it is difficult if not impossible to assign to it any definite hue. It is significant that the weaker R & M short-wave unit reveals intensities every bit as great (although not necessarily in the same zircon grains) as does the stronger Magnaflux long-wave source.

The change in fluorescence intensity of a given zircon grain with change from the short-wave to the long-wave source may follow one of three general patterns. Thus, cases have been noted in which fluorescence was enhanced, diminished, or remained essentially unchanged in changing from a short to a long-wave source. As demonstrated in a later section, these patterns may prove very useful and significant in distinguishing zircons from rocks of different ages. Some zircons actually show a stronger response under the weaker R & M unit than under the strong Magnaflux lamp. This is mentioned to emphasize the fact that, although inherently a poorer representative of the short-wave units than is the Magnaflux lamp of the long-wave class, the R & M unit nevertheless is not without merit in revealing varying types of fluorescent response.

Another feature which is considered highly significant in the petrological applications is the uniformity or lack of uniformity of bulk fluorescence. Thus, igneous zircon concentrates tend to be very similar in response from grain to grain, giving a uniform bulk response, whereas sedimentary zircon concentrates tend to be very non-uniform. Further reference will be made to this feature in a later section.

In the decoloration of zircon by chemical means iron is said to be one of the elements removed (25). Since iron is reputed to be a poison or inhibitor of fluorescence in certain minerals, it was decided to determine if

chemical treatment of zircon would perceptibly influence its fluorescence. Accordingly, samples in the form either of granular concentrates or rock chips were subjected to overnight heating on a steam bath with 20% oxalic acid solution. In the few such tests carried out, not only was the color removed but also the fluorescence was increased, in some cases pronouncedly. Treatment by oxalic acid, or other chemical reagents, would thus appear to be a promising preliminary step in the study of samples which give little or no response if untreated.

Some Fluorescent Associates of Zircon

It is necessary to keep in mind that certain common associates of zircon, in both igneous and sedimentary modes of occurrence, may be expected to fluoresce. No difficulty need be experienced, however, because of similarity of response to that of zircon. Apatite is almost universally present in granitic rocks, and many rock chips show fluorescent grains of this mineral. The grains are commonly larger and less regular than those of zircon, and the fluorescence is usually dingy greenish-yellow (sometimes brown or whitish) of only moderate intensity. Sodalite often exhibits an intense orange-red emission somewhat similar to that of certain zircons, but is more prone to occur within the light-colored constituents of the rock, and as less regular grains. Calcite sometimes displays an intense yellowish fluorescence. Oil-coated quartz grains and one type of corundum also give a yellow response easily mistaken for that of zircon. All of these minerals are readily distinguished from zircon microscopically.

Fluorite rarely if ever resembles zircon in fluorescence. Corundum, spinel, and kyanite, minerals which often accompany zircon in sediments, frequently emit a pink or red fluorescence not easily to be mistaken for that of zircon. Monazite and xenotime, the minerals most easily confused with zircon petrographically, do not appear to resemble it in fluorescent behavior. Tests on monazite from India and Brazil were negative, and it has recently been reported that xenotime from New Zealand gave no response to ultraviolet excitation (6). The foregoing enumeration is believed to include most of the fluorescent minerals which might cause confusion in zircon studies. It is always well to confirm the identity of any fluorescent grains presumed to be zircon, particularly in the case of rock chips, in which apatite is so often also present. With a little care a fluorescent grain can readily be pried loose with an oil-dipped needle and mounted for microscopic check.

Evaluation of Commercial Concentrates

Of recent years zircon has become an important raw material in the ceramic industry (12) (21). It is because of such desirable properties as

chemical stability, high refractoriness and mechanical strength, good electrical insulating characteristics, low thermal expansion, and good resistance to thermal shock that the demand for zircon for enamels, refractories, spark plug insulators and special porcelains has steadily increased. Zircon is also the source material for zirconia, another ceramic raw material, and for zirconium. It is because of these demands that the microscopic grains of zircon which constitute but a fraction of a per cent of both solid and unconsolidated rocks can be economically concentrated. It may come as a surprize to many mineralogists to learn that zircon, obtained largely by the beneficiation of beach sands already considerably concentrated by tidal action, may be purchased in carload lots of practically 100 per cent in purity.

Commercial grades of zircon vary considerably in the nature and extent of the impurities, of which the chief are rutile, tourmaline, and quartz. The dark color of the first two renders them easily visible. Samples containing quartz as the sole or chief impurity, however, give a false impression of high purity because the colorless quartz is indistinguishable from the zircon. A test based on the fluorescence of zircon and the non-fluorescence of quartz furnishes a simple and rapid means for evaluating such samples. As practiced in the writer's laboratory, the average sample obtained from each shipment is placed in an eight ounce bottle so as to fill the latter no more than about three-fourths, and turned over and over under the Magnaflux Blacklight. Such action causes the quartz to segregate into dark purple swirling strands, which contrast sharply with the yellowish background of the fluorescing zircon. The sensitivity of this test is high: as little as one tenth of one per cent of quartz can be readily detected. With practice in the use of prepared standards for comparison, it is possible to estimate the quartz content to the nearest one-half per cent, at least up to a five per cent limit, which is rarely exceeded by commercial samples.

There appears to be no reason why the above technique could not be used with profit in following the course of beneficiation of zircon-bearing sands, and as a prospecting method for the location of beach deposits of workable grade. Examination in ultraviolet light is also useful in revealing the extent to which granular concentrates of other minerals are contaminated by zircon. Thus commercial grades of rutile, ilmenite, chromite sillimanite, monazite, and glass sand may be profitably studied by this method. In these instances the scattered grains of zircon, even though their fluorescent response is faint, show up quite clearly against the non-fluorescing background of the predominant mineral. At the same time the presence of corundum, spinel, or kyanite may be revealed by the red fluorescence sometimes shown by these minerals.

Petrogenetic Significance

Of recent years, too, zircon has assumed an important role in the solution of a variety of petrological problems. Numerous workers, after careful study of accessory-mineral suites, have singled out zircon as a mineral of particular promise in this regard. In view of the extent to which the other varietal features of zircon have been critically studied, it is somewhat surprizing that its fluorescence has been completely neglected by heavy-mineral workers. Even the limited observations of the present study suggest that this property may possess a diagnostic value equal to, or greater than, that of the other varietal characteristics so far studied.

There appears to be a distinct tendency on the part of zircon from igneous rocks to display a uniform bulk fluorescence, whereas zircon from sedimentary sources is as a rule variable in response from grain to grain. This tendency is doubtless to be attributed on the one hand to the uniform physico-chemical environment in which zircon forms in a given igneous rock, and on the other to the heterogeneous origin of the material contributing to a given sedimentary occurrence. The above generalization is not without exceptions, and the latter may perhaps be accounted for as follows. Sedimentary zircon derived from the weathering of a single igneous intrusive would tend to be uniform. Furthermore, an igneous rock may contain several generations of zircon, or may acquire zircon present in the intruded rocks in addition to its own primary zircon.

The fact that zircon from a given igneous rock tends to be very uniform in fluorescence is believed to be highly significant in correlation studies. Thus, preliminary studies on a limited number of rock specimens from the Sawatch Range in Colorado give promise of success. The two Precambrian granites and one Tertiary batholith recognized in this area (17) (18) appeared to offer a means of testing the technique. Concentrates were not available, so the isolated zircon grains in rock chips, presenting about twelve square inches of surface, were carefully studied. Although the conditions of observation and comparison were thus not the best obtainable, yet a distinctive fluorescent response could be discerned for each of the three ages of intrusives. The older of the two Precambrian intrusives (the Pikes Peak granite) reveals no fluorescent zircon in either long or short ultraviolet light. Occasional grains of dingy greenish-yellow fluorescent apatite are observed. Under long ultraviolet the younger Pre-cambrian instrusive (the Silver Plume granite) displays numerous bright orange zircon grains, which become imperceptible to faint under short wave length. Many grains of dingy yellow apatite are also visible. In sharp contrast to both of these are the rock chips of the

Tertiary Mt. Princeton batholith. No fluorescent apatite is seen, while the zircon not only displays a bright orange response in the long-ultraviolet but shows an even brighter yellow at the shorter wave length.

The above observations on the contrast in the zircons of the three Sawatch Range intrusives are summarized in Table 2, as are also additional results on some igneous rocks from several other areas. Some excellent samples in the form of concentrates were available for the Valverde tonalite and the Rubidoux Mountain granite of the Southern California batholith. Three samples were at hand for each of the two rock types, and for each rock the behavior of the three samples was identical. Thus the Valverde tonalite samples displayed a very uniform bulk fluorescence of a bright to intense yellow under both long and short radiation. In contrast the Rubidoux Mountain granite samples showed a rather non-uniform bulk response, faint under the short-wave source and faint to bright under the long-wave source, and of a decidedly orange rather than yellow hue. Careful examination of slices of granite of Killarnean age from Killarney Bay, Ontario, revealed no visibly fluores-

Table 2. Contrasts in Fluorescence of Zircon from Selected Sources

Source-Rock and Locality	Age	Sample Type	Fluorescence	
			Short (2537 A.U.)	Long (3650 A.U.)
Pikes Peak Granite Sawatch Range, Colo.	Earlier Precambrian	Rock Chip	imperceptible	imperceptible
Silver Plume Granite Sawatch Range, Colo.	Later Precambrian	Rock Chip	faint	bright orange
Princeton Batholith Sawatch Range, Colo.	Tertiary	Rock Chip	bright yellow	bright orange
Valverde Tonalite Southern Calif.	Cretaceous	Concentrate	bright yellow	bright yellow
Rubidoux Mt. Granite Southern Calif.	Cretaceous	Concentrate	faint	faint to bright orange
Killarney Granite Killarney Bay, Ont.	Killarnean	Rock Chip	imperceptible	imperceptible
Nepheline Syenite French River, Ont.	Killarnean (?)	Rock Chip	bright orange-yellow	bright orange-yellow

cent zircon. Nepheline syenite from French River, Ontario, thought by Quirke* to belong also to the Killarnean, revealed bright-orange zircon under both long and short wave. This contrast in behavior suggests the possible need for reconsideration of the age of the syenite, which Quirke admitted was not too definitely established.

The above examples illustrate the manner in which zircon fluorescence studies may possibly aid in the correlation of igneous rocks. Although no work has been done in this direction, the method may possibly be of service in distinguishing meta-igneous from meta-sedimentary rocks, through the contrast in uniformity of bulk fluorescence of the two groups. Interesting information as to the igneous source rocks of sedimentary beds may also be forthcoming. In certain cases ore deposits, particularly such non-metallic "ore" deposits as the sillimanite minerals (andalusite, kyanite, sillimanite, dumortierite, topaz) and others, may possibly be tied in with the parent igneous intrusives. For example, a distinct yellow to orange-yellow fluorescence is shown by the zircon from both the andalusite deposits of White Mountain, California, and from the dumortierite deposits of Oreana, Nevada. It does not appear to be venturing too far into the realm of conjecture to suggest that each of these hydrothermal deposits might be correlated with its proper igneous intrusive.

A further comment might not be amiss regarding the reproducibility of results by different workers using different ultraviolet units. If the sole purpose of their studies is to characterize the fluorescence exactly as to hue and intensity, they might not agree in their descriptions of the responses observed. On the other hand, if the purpose is simply to classify the fluorescence according to general behavior patterns, different workers should be able to obtain essentially the same contrasts. Assuming each uses similar types of units (even although not from the same manufacturer) the broad conclusions as to uniformity or non-uniformity of the fluorescence, its strength or weakness, and the nature of the intensity change (increase, decrease, or no change) with change in wavelengths, should be quite similar.

Summary and Conclusions

Accessory-mineral zircon, such as occurs as tiny crystals and grains in igneous and sedimentary rocks, has been found to exhibit fluorescence to a considerably greater extent than one would conclude from the few literature references to the phenomenon.† A rather wide variety of fluorescent responses can be detected, even with the ordinary com-

* T. T. Quirke, personal communication.

† Whether this applies also to gem and pegmatitic zircons was not investigated.

mercially available ultraviolet units. A crude classification of response-patterns has been presented, and a simple procedure for study has been outlined. Associated minerals which also fluoresce have been discussed. A rapid but very sensitive test for the detection of quartz in commercial zircon concentrates has been outlined.

Interesting possibilities of the successful use of zircon fluorescence in the solution of a number of petrological problems have been suggested. The preliminary nature of the study from this standpoint has been emphasized. No sweeping claims for the method in such problems can be made, and any real appreciation of its value must await more careful application to specific problems. The probable utility of the method in any given case can be evaluated with a minimum of time and effort. The technique as outlined can doubtless be greatly improved upon. Rejection of the method on the ground that presently available ultraviolet units are unsatisfactory appears unwarranted.

Acknowledgments

The writer wishes to express his gratitude for the kind loan of specimens to Professors F. F. Grout, E. S. Larsen, R. W. Marsden, the late T. T. Quirke, J. T. Stark, Carl Tolman, and S. A. Tyler. The helpful suggestions and criticism of Professor Larsen and of Dr. Hugh S. Spence are also gratefully acknowledged.

References

1. Arrance, F. C. (1947), Black light, fluorescence, and ceramics: *Jour. Am. Ceramic Soc.*, **30,** 250–255.
2. Cannon, R. S., and Murata, K. J. (1944), Estimating Mo content of scheelite or $CaWO_4$ by visual color of its fluorescence. U. S. Patent No. 2,346,661.
3. Dake, H. C., and DeMent, J. (1941), Fluorescent Light and Its Application (Chemical Publishing Co., Inc., Brooklyn, N. Y.), p. 155.
4. DeMent, J. (1945), Fluorochemistry (Chemical Publishing Co., Inc., Brooklyn, N. Y.), p. 485.
5. Hevesy, G., and Jantzen, V. T. (1923), The hafnium content of zirconium ores: *Jour. Chem. Soc.* (London), **123,** 3218–3223.
6. Hutton, C. O. (1947), Determination of xenotime: *Am. Mineral.*, **32,** 141–145.
7. Miser, H. D., and Glass, J. J. (1941), Fluorescent sodalite and hackmanite from Magnet Cove, Arkansas: *Am. Mineral.*, **26,** 437–445.
8. Palache, C. (1928), The phosphorescence and fluorescence of Franklin minerals: *Am., Mineral.*, **13,** 330–333.
9. Pringsheim, P., and Vogel, M. (1943), Luminescence of Liquids and Solids (Inter-Science Publishers, Inc., New York, N. Y.), p. 97.
10. Quinn, A. (1935), A petrographic use of fluorescence: *Am. Mineral.*, **20,** 466–468.
11. Quinn, A. (1937), Petrology of the alkaline rocks at Red Hill, New Hampshire: *Bull. Geol. Soc. Am.*, **48,** 373–402 (1937).
12. Ralston, O. C., and Stern, G. (1944), Fluorescent minerals used in lighting and elsewhere: *U. S. Bureau of Mines I. C.* **7276,** 18 pp.

13. Russell, R., and Mohr, W. T. (1947), Characteristics of zircon porcelain: *Jour. Am. Ceramic Soc.*, **30,** 32–35 (1947).
14. Smith, E. S. C., and Parsons, W. H. (1938), Studies in mineral fluorescence: *Am. Mineral.*, **23,** 513–521.
15. Smith, F. G. (1945), Fluorescence as related to minerals: *Univ. Toronto Stud., Geol. Series*, No. **49,** 41–54.
16. Smith, L. L. (1937), Fluorescent sodalite: *Am. Mineral.*, **23,** 304–306.
17. Stark, J. T. (1934), Heavy minerals in the Tertiary intrusives of Central Colorado: *Am. Mineral.*, **19,** 586–592.
18. Stark, J. T., and Barnes, F. F. (1935), The correlation of Pre-cambrian granites by means of heavy mineral analyses: *Geol. Mag.*, **72,** 341–350.
19. Symons, H. H. (1944), Fluorescent minerals in the exhibit of the State Division of Mines: *California Jour. Mines & Geol.*, **40,** 361–368.
20. Taggart, A. F. (1944), Handbook of Mineral Dressing (John Wiley & Sons, Inc., New York, N. Y.), Section 19, pp. 93–94.
21. Thielke, N. R., and Jamison, H. W. (1945), Development of zircon as a versatile ceramic material: *Jour. Am. Ceramic Soc.*, **24,** 452–456.
22. Vanderburg, W. O. (1936), A note on the use of ultraviolet lamps in mines for rapid determination of scheelite in ores by fluorescence: *U. S. Bureau of Mines I. C.* **6873,** 3 pp.
23. Vanderwilt, J. W. (1946), A review of fluorescence as applied to minerals with special reference to scheelite: *Mining Technology*, **10,** T.P. 1967, 14 pp.
24. Van Horn, F. R. (1930), Replacement of wolframite by scheelite with observations on the fluorescence of certain tungsten minerals: *Am. Mineral.*, **15,** 461–469.
25. Venable, F. P. (1922), Zirconium and its Compounds (Chemical Catalog Co., Inc., New York, N. Y.), p. 101.
26. Warren, T. S. (1944), Ultraviolet light: *Colo. School of Mines Mag.*, **34,** 278–279, 282–284, 290.
27. Yagoda, H. (1946), Luminescent phenomena as aides in the localization of minerals in polished sections: *Econ. Geol.*, **41,** 813–819.

ON IRON-WOLLASTONITES IN CONTACT SKARNS: AN EXAMPLE FROM SKYE

C. E. Tilley,
University of Cambridge, England.

The ore skarn zones in the dolomite invaded by the Beinn an Dubhaich granite, Skye, often contain residual chert nodules ("sponge forms") immediately encased by wollastonite not infrequently associated with clinopyroxene. Study of the optical properties of the wollastonites of this encasing zone shows that their composition varies according to the nature of the associated clinopyroxene. Wollastonites associated with strongly coloured clinopyroxene show the optical characters of the artificial iron wollastonites, whereas the wollastonite associated with a colourless diopsidic pyroxene possesses the normal, chemical and optical properties of this mineral. The coloured clinopyroxenes found in the skarn zone are hedenbergite rich solid solutions with green to yellow green pleochroism (γ = yellow green, α = green) more or less strongly marked. The wollastonite (white) is intergrown with these or may form a separate band between two seams of the pyroxene. The remaining mineral found in close association particularly with the pyroxene is a coloured grossular-andradite. From such a skarn the wollastonite and pyroxene have been separated for analysis in order to reveal more precise data of the paragenesis. The separated wollastonite fraction yielded a product of varying specific gravity, the bulk of the material having a value of 3.09. This material provided homogeneous crystals, colourless in transmitted light, with the following optical properties: $\alpha = 1.640$, $\gamma = 1.653$, $2V_\alpha 60° \pm 3°$, $\alpha' \wedge c = 44°$ in section perpendicular to the zone of cleavages. Sections perpendicular to the acute bisectrix gave extinction angles of 5°–6° from the zone of cleavages. Simple twins on {100} (old monoclinic orientation). Analysis of such material gave the results set out in the accompanying table. In the separation a small amount of a heavier fraction (Sp. Gr. > 3.10) showed a maximum value of $\gamma = 1.660$, pointing to still higher contents of iron in solid solution in some of the material. A partial analysis of the associated hedenbergitic pyroxene (Sp. Gr. 3.55) which contained a small quantity of impurity including some fine garnet, gave SiO_2 46.62, Al_2O_3 0.59, Fe_2O_3 1.99, FeO 16.81, MnO 1.04, CaO 24.46, MgO 5.63. If alumina and ferric oxide are removed as grossular-andradite, this pyroxene analysis recalculated gives SiO_2 50.7, FeO 18.5, MnO 1.1, CaO 23.5, MgO 6.2, yielding an approximate composition $Di_{33}Hd_{67}$ ($Diopside_{33}$ $Hedenbergite_{67}$). This is a bulk composition of somewhat variable material. The maximum value of γ re-

	1	mols	metals to 6 Oxygens
SiO_2	50.00	8326	1.99
TiO_2	tr.		
Al_2O_3	—		
Fe_2O_3	nil		
FeO	9.29	1293	0.309
MnO	1.22	172	0.041 2.01
CaO	38.86	6929	1.660
MgO	nil		
H_2O	nil		$CaSiO_3$ 80.6%
Insoluble in HCl	0.45		$FeSiO_3$ 17.1
			$MnSiO_3$ 2.3
	99.82		

1. Iron wollastonite in hedenbergite skarn (with some grossular-andradite) Camas Malag, Skye. Analyst H. C. G. Vincent.

corded is 1.742 equivalent to Hd_{76}, the pyroxene as with the wollastonite showing a range of composition around the average of Hd_{67}.

The refractive indices of the analysed wollastonite solid solution accord with the data on artificial iron wollastonites of comparable composition prepared by Bowen and Schairer (1). Material of approximately this composition (20% $FeSiO_3$) could, according to experimental data, be in equilibrium with pure hedenbergite at 500°–600° C. The occurrence of such iron wollastonites in nature serves thus in a measure as a geological thermometer and the preservation of such material at ordinary temperatures may be taken as indicative of the virtual cessation of unmixing at lower temperatures. In the system $CaSiO_3$—diopside, while magnesium wollastonite solid solutions occur at high temperatures, Schairer and Bowen (2) have shown that the form of the unmixing curve is such that below 1000° C. the extent of solid solution is negligible. (See also Osborn (3). The occurrence of *normal* wollastonite* in these skarns where the associated pyroxene is colourless diopside is therefore in harmony with the experimental data. The natural occurrence of iron wollastonite has previously been reported by the writer from the endogenous zone of the dolerite of Scawt Hill (4) and more recently it has been observed in an alkali gabbro from Muck (5). Its development in a granite contact skarn (exogenous) gives reason to believe that solid solutions of this type may be not uncommon in association with hedenbergite in metasomatic contact rocks formed in higher temperature ranges. This same contact zone in Skye shows indeed that it is not limited to the environment now described.

* Analysis confirms the absence of magnesia.

References

1. Bowen, N. L., and Schairer, J. F., *Am. Jour. Sci.*, **26**, 258 (1933).
2. Schairer, J. F., and Bowen, N. J., *Am. Jour. Sci.*, **240**, 735 (1942).
3. Osborn, E. F., *Am. Jour. Sci.*, **240**, 757 (1942).
4. Tilley, C. E., *Mineralog. Mag.*, **24**, 569 (1937).
5. Tilley, C. E., *Bull. Comm. Geol. Finland*, **140**, 103 (1947).

A NEW TWO-CIRCLE GONIOMETER

C. W. Wolfe, *Boston University, Boston, Massachusetts.*

With the rapid growth of crystallography as a science a pronounced need for an adequate two-circle goniometer has been strongly felt in the United States. This need has been met in part by two new commercial sources, the principal difficulty with these sources being their high cost. Most university funds are limited to such a degree that the purchase of two-circle goniometers costing $1500–$2000 is prohibited. This high cost problem was first met by Dr. Cutler West and Mr. A. S. Makas (*Am. Mineral.*, **32,** 692, 1947) of Polaroid Corporation by making a model similar to that of Goldschmidt, using a Spencer spectroscope with its horizontal graduated circle as a base instrument.

The adaptation proved quite satisfactory, and the author decided to follow their suggested course of action. A two-circle goniometer was constructed according to my specifications by Laboratory Associates, 60 White Street, Belmont, Massachusetts. The original intention was that the work was to be restricted to the one instrument, but when it was discovered that the price of the instrument was notably less than other models available, it was decided that Laboratory Associates would make the model available at the standard price of $1,000.00. Since the instrument carries several innovations over the Goldschmidt goniometer, it was decided that colleagues in the field of crystallography might like to have similar instruments constructed or would like to purchase the goniometer from Laboratory Associates. A description of the instrument is given herewith.

Microscope-Telescope Unit. One outstanding feature of the goniometer is the character of the microscope-telescope tube. In the following discussion the numbers in parenthesis will refer to correlative numbers on the accompanying figure. The telescope tube (1) with eyepiece (2) is a regular part of the base spectroscope instrument. The magnification of the eyepiece is about 10×. The telescope, with which the reflected signal from the crystal is seen, is converted into a microscope for actually viewing the crystal by rotating the objective holder or nosepiece (3) into axial conjunction with the telescope. An adjustment in the vertical plane is provided by a screw (4). The objectives (5) are simple 48 mm., 32 mm., and 16 mm. microscope objectives. They are provided with adapters (6) for the varying focal length of the lenses, cutting the necessary amount of focusing to a minimum. When focusing is necessary, it is obtained by turning the ring-screw device (7) on the nose-piece. The 16 mm. objective with a magnification of 10X is best used on very small crystals, since the

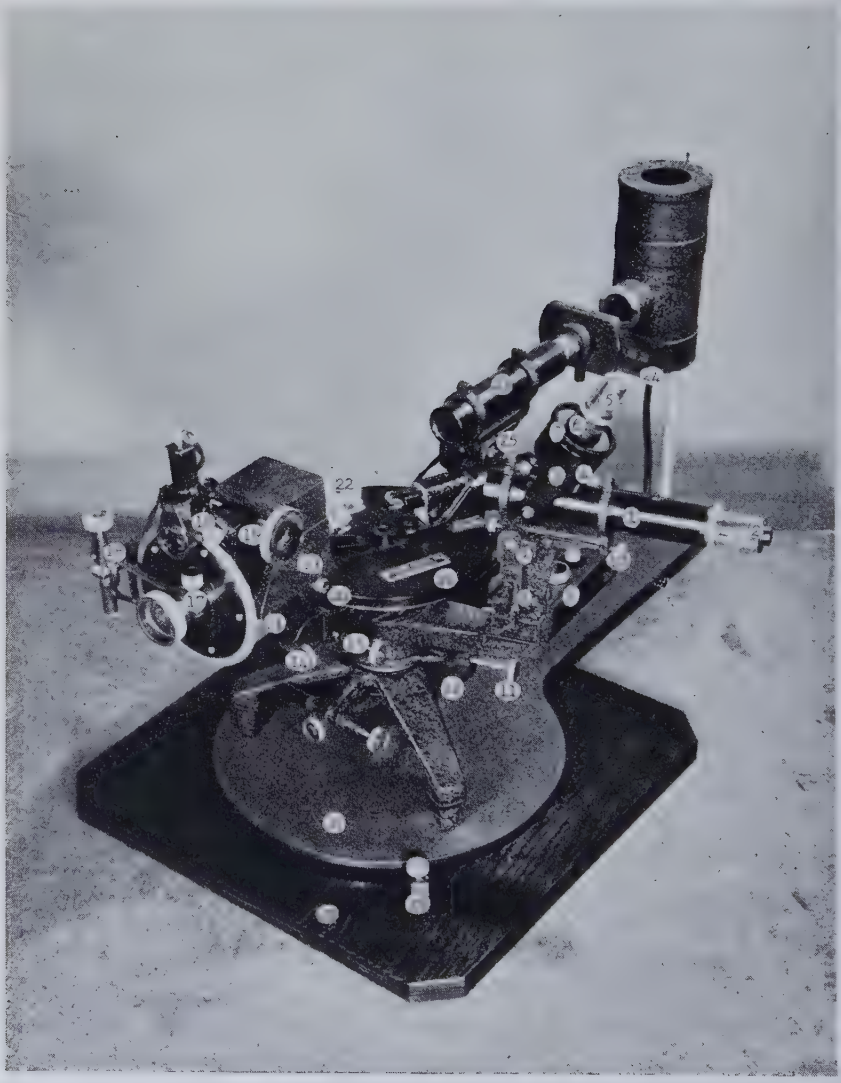

total magnification with this objective and eyepiece combination is about 100X.

Such a high magnification has been unknown in goniometers up to the present time. The goniometric study of crystals under this magnification provides much needed information concerning etch figures and growth accessories, and their reproduction on photographs will be a simple matter. Orientation of very small crystals for x-ray analysis is also facilitated. One difficulty with the high magnification, however, is the closeness of the objective to the crystal. This is best obviated by mounting the crystal on a slender glass rod which will not strike the objective when high polar angular values are being obtained or by using a special crystal mounting rod which has been developed for the purpose. This rod is the usual type of brass rod into which a small hole is bored in one end. Into this hole a phonograph needle is inserted by the blunt end, and the crystal is mounted on a minute quantity of wax at the point of the needle. Wax is generally more satisfactory than collodion or Duco, since it not only is completely adequate for holding very small crystals, but it also permits the manipulation of the crystal after mounting. Laboratory Associates will supply the bored brass pins in any length which is desired. There is no interference between crystal and objective when signals and angles are being observed, for the nosepiece is lifted and out of the way.

The microscope-telescope tube is mounted on an upright post (8) with horizontal adjusting screws (9) and with a tilting screw (10) to bring the tube into alignment. The entire unit may be rotated around the vertical central axis of the instrument, and a lock screw (11) with fine adjustment (12) is provided. When the instrument is to be used only as a two circle goniometer, the fine adjustment screw should be removed after the proper position of the unit has been fixed; this precaution precludes any inadvertent change in the chosen position of the unit. The provision for rotation around the vertical axis is desirable in case the instrument should get out of adjustment or in case minimum deviation work, with liquids in hollow prisms mounted on the goniometer head, is desired. The author has already made an adapter for this purpose, and it saves the purchase of a one-circle goniometer.

Vertical Circle Unit. The vertical circle unit is mounted in a chuck (13) which is directly tied in with the horizontal circle, the movement being controlled by a lock screw (14) and a fine adjustment screw (15). The vertical circle is engraved by C. L. Berger and reads clockwise and counter clockwise. The vernier (16) is very easily read at a distance of six inches from the circle, due to the presence of a suitable lens and adequate lighting. The vertical circle is equipped with lock screw (17) and fine adjustment screw (18) and is mounted on a simple microscope tube

(19) with rack and pinion back and forward movement of about $1\frac{1}{2}$ inches. The tube is also equipped with horizontal adjustment screws (20) and tilting screw (21) for alignment. The goniometer head (22) which is not an official part of the goniometer is detachable. If desired it may be supplied by Laboratory Associates or may be procured separately from Otto von der Heyde or Charles Supper who supply such heads with their Weissenberg equipment.

Signal Unit. The collimating tube (23) is that of the Spencer spectroscope with the slit unit omitted. In place of the old spectroscope slit a five signal target (24) has been introduced. The target is made photographically; the individual signals are obtained by sliding the target horizontally, the construction of the slide being such that each signal is centered automatically. The five signals are: the large maltese cross, the small maltese cross, the vertical bar, the horizontal bar, and the pin point. The entire collimating tube may be aligned with horizontal screws (25) and with a tilting screw. The light source is a 100 watt lamp of the narrow, vertical four helical filament type. There is a condensing lens inside the light housing which focuses the incandescent filaments on the front lens of the collimator, giving maximum illumination.

Horizontal Circle. The horizontal circle (26) is that of the Spencer spectrometer. The present spectrometer scale reads backward for goniometric purposes, making impossible the direct determination of polar angular values, but it is hoped that this may be corrected through special specifications to the American Optical Company. The reading of the horizontal scale, although reversed at present, is extremely easy, as it is well illuminated, and the focal length of the reading lens is about six inches.

The entire instrument is mounted on a metal base (27) which may be rotated upon a wooden base board (28), with a lock screw (29) to hold it in any particular position. Rotation of the entire instrument enables the ready reading of the vertical circle scale when the polar angular readings are small.

The advantages of the instrument, then, are: high magnification, intense light source, flexibility of adjustment of all parts, ready reading of the scales, simplicity of manipulation, and comparatively low cost. Angular readings are to one minute, and the over-all accuracy of the instrument leaves nothing to be desired. One disadvantage, as compared with the Goldschmidt instrument, is that there is no provision for the blacking out of reflections from different parts of the reflecting face. This may be corrected in later models.

The author wishes to acknowledge his debt to many others in the planning and building of this instrument. Of course the basic plan is that

of Goldschmidt. The use of the Spencer spectroscope was conceived by Dr. West, and several other features of the instrument were developed in principle by West and Makas. The optics were largely developed by Mr. Kenyon Zaph of the Optical Research Laboratory of Boston University, and the actual engineering and designing has been the work of Mr. Harry Gewertz of Laboratory Associates. The specifications for construction and a critical examination of the utility and engineering of the various parts have been the author's principal contributions.

NOTES AND NEWS

THE STRUCTURAL NATURE OF THE MINERALIZER ACTION OF FLUORINE AND HYDROXYL

M. J. Buerger,
Massachusetts Institute of Technology, Cambridge, Mass.

Introduction

Students of pegmatites and ore deposits have been impressed with the importance of certain elements, notably H, F, Cl, C, and S, whose presence has apparently aided the formation of the minerals in the suite. Such elements are known as *mineralizers*. Mineralizers aid in the formation of minerals in two ways. In the first place, they enter into the compositions of certain of the minerals of the suite and thus are the cause of the appearance of certain minerals uncommon to the igneous rocks. It is chiefly in this way that the mineralizers reveal their presence during mineral deposition. But their presence is also attended by an increase in the sizes of the crystals deposited. From this it is deduced that the presence of mineralizers increases the fluidity of the mineralizing solutions. Fluidity is often correlated with the volatility of the mineralizers, since the common occurrence of the elements H, F, Cl, C, and S under ordinary conditions is as the gasses H_2O, F_2, Cl_2, CO_2, and SO_2. The reduction of viscosity by mineralizers may be regarded as well established by field evidence. What is the explanation of the action?

In this note it is pointed out that the mineralizing action of hydrogen and the halogens can be explained, and even put on a semi-quantitative basis.

The Nature of Viscosity in Silicate Melts

Consider a siliceous magma. Each silicon atom is surrounded by four oxygen atoms. According to the electrostatic valency principle,[1] each silicon extends a bond of strength 1 to these oxygens; each oxygen should also receive bonds totaling its valence, namely 2. If the silicon: oxygen ratio of the melt is high, many oxygen atoms may satisfy their charge of -2 by receiving bonds of strength 1 from each of two silicon atoms. Whenever this sharing of oxygen atoms occurs, it causes the silicon and oxygen atoms to become part of an irregular but extended space network in the melt.

Now, the viscosity of a liquid pervaded by these network fragments is directly related to the average number of these Si-O-Si bridges per silicon atom. In pure melted SiO_2, there is an average of 2 bridges per Si

[1] Pauling, Linus, The principles determining the structure of complex ionic crystals: *Jour. Am. Chem. Soc.*, **51**, 1010–1026, especially 1017–1018 (1929).

atom; in melted $MgSiO_3$ there is an average of 1 bridge per Si atom; while in melted Mg_2SiO_4 there are no bridges per silicon atom. (In the magnesium silicates, the Mg-O bridges make an inferior contribution to the viscosity.) It is for this reason that increasingly siliceous "dry" magmas are increasingly viscous. In pure molten SiO_2, the viscosity of the glass is crudely comparable with the viscosity of a cristobalite crystal, which it resembles in structure, particularly with regards to nearest neighbors and number of bridges per Si atom.

This bridge relation can easily be generalized and put into quantitative form. Let,

O = the total number of oxygen atoms in the magma;
Si = the total number of silicon atoms in the magma;
S = the total number of shared oxygen atoms in the magma;
b = the total number of bridges in the magma.

Then, the total number of oxygen atoms per silicon atom is equal to the maximum 4, reduced by the number of half-oxygens belonging to other silicon atoms due to sharing, or

$$\frac{O}{Si}=4-\frac{\frac{1}{2}S}{Si}. \tag{1}$$

Therefore,

$$\frac{\frac{1}{2}S}{Si}=4-\frac{O}{Si}. \tag{2}$$

Now, where a bridge occurs, it is shared between two silicon atoms, so the bridge-per-silicon ratio is

$$\frac{b}{Si}=\frac{S}{2Si}. \tag{3}$$

Comparing this with (2), it is evident that

$$\frac{b}{Si}=4-\frac{O}{Si}. \tag{4}$$

In other words, the bridge density, per silicon, is 4 reduced by the oxygen: silicon ratio.

The Rôle of Fluorine and Hydroxyl

In case an OH^- or an F^- (or other halogen) ion is substituted for an oxygen atom at the corner of a silicon tetrahedron, the substitution removes a possible network bridge. This is because the sum of electrostatic valence bonds which can be received by a univalent ion is limited to 1. Thus, a single silicon atom saturates an OH^- or F^- ion. Of course, each oxygen bridge must be replaced by two OH^- or F^- ions in order to satisfy the two silicons on opposite ends of the substituted bridge.

The effect of hydroxyl or fluorine can be incorporated into (4), thus expressing the effect quantitatively. Let F be the total number of F^-

ions, and let OH be the total number of OH^- ions in the magma. Then since each one of these ions reduces the number of sharable oxygen atoms, the quantity $(4-F/Si-OH/Si)$ must be substituted for 4, and $(O+OH+F)$ must be substituted for O in (1), (2) and (4). Taking account of these substitutions, there results,

$$\frac{b}{Si}=\left(4-\frac{F}{Si}-\frac{OH}{Si}\right)-\frac{(O+OH+F)}{Si} \tag{5}$$

or

$$\frac{b}{Si}=4-\frac{O}{Si}-\frac{2OH}{Si}-\frac{2F}{Si}. \tag{6}$$

We are now in a position to appreciate the "fluxing" nature of fluorine and hydroxyl. When these fluxes are missing, the transition from magma to crystals is essentially that of the freezing of a silicate melt. The crystallization process is slowed down by the structural requirement of relatively slow migration of the atoms enmeshed in the silicated space net to the growing crystal nuclei. Crystallization under these conditions is equivalent to a kind of devitrification of a glass at somewhat elevated temperatures. The introduction of enough of the fluxes OH and F, however, transforms the glass structure into a liquid structure by eliminating oxygen bridges. This action effectively breaks down the continuous silicate network into an aggregate of tiny silicate islands of molecular dimensions.

Both OH and F (as well as other halogens) are independently highly effective in doing this, as can be seen from (6). In this relation, it should be observed that *not* the weight fractions of OH/Si and F/Si are involved, but rather the atomic fractions. Since both OH and F have quite small atomic weights, a small weight percentage of either of these is very effective in eliminating oxygen bridges. Furthermore, the introduction of either of these ions is twice as effective as the corresponding introduction of an additional oxygen into the melt, since the terms OH/Si and F/Si are modified by a coefficient 2 in (6).

Of course, when OH is present in the melt, it may function not only as a terminator of a silicon bond, as outlined above, but, under favorable conditions, it may also contribute to the formation of liquid water. Such conditions occur when the temperature is sufficiently low so that there is a substantial association of OH^- and H^+ to form H_2O. These functions of OH can occur simultaneously and in this way OH can contribute in a dual rôle to the transition of the magma from a glassy melt structure to a liquid structure in which crystallization occurs readily.

Conclusion

This note can be appropriately terminated by stating the conclusion that the univalent negative ions behave as mineralizers chiefly because

their presence is instrumental in causing a magma to undergo a transition from a glassy state to a liquid state.

(Arguments along somewhat similar lines can be advanced for the mineralizing action of C, P, and S, but the arguments are not so straightforward as those given above for the action of the univalent negative ions.)

THE HYDRATES OF SODIUM TETRABORATE

A. O. McIntosh and F. W. Matthews,
Central Research Laboratory, Canadian Industries Limited, McMasterville, Quebec.

During an attempt to prepare the *x*-ray diffraction powder patterns of the products formed during the dehydration of borax, several features were noted which we do not believe have been reported previously.

Samples of borax ($Na_2B_4O_7 \cdot 10H_2O$) were heated to constant weight at atmospheric pressure at temperatures of 80° C., 100° C. and 200 °C. Another portion of borax was dehydrated at room temperature (approximately 25° C.) over calcium chloride desiccant. After five weeks this last sample had not reached constant weight Table 1. The products were examined by the *x*-ray diffraction powder technique.

The powder data obtained were in good agreement with the published patterns for the deca and penta hydrates (1). The composition of these hydrates was confirmed by chemical analyses of samples prepared under controlled conditions.

Table 1. Dehydration of $Na_2B_4O_7 \cdot 10H_2O$

Temperature	Loss as Moles of Water	Structure
25° C.	5.5	$Na_2B_4O_7 \cdot 10H_2O$
80° C.	6.6	$Na_2B_4O_7 \cdot 5H_2O$
100° C.	8.2	Not crystalline
200° C.	8.9	$Na_2B_4O_7 \cdot 5H_2O$

The loss of water from the decahydrate and pentahydrate of sodium tetraborate without noticeable change in the *x*-ray diffraction pattern is evidence of the presence of water loosely held in the structure. Similar behaviour is reported in the case of calcium sulphate hemihydrate (2, 5, 7) and the zeolites (3). The fact that no *x*-ray diffraction pattern was given by the product from heating at 100° C. has an important bearing on the *x*-ray identification of sodium tetraborate in commercial products.

Sodium tetraborate tetrahydrate is found in nature as the mineral kernite. It has also been synthesized (4, 6). This synthesis was repeated, borax in a sealed tube being permitted to cool slowly from 130° C. to 65° C. The *x*-ray diffraction pattern of the product was the same as that

of a sample of kernite from Kern County, California. The identity of the natural material was confirmed by optical measurements and by chemical analysis. Since to our knowledge the x-ray powder pattern of kernite has not been published, we are reporting it here (Table 2).

TABLE 2. X-RAY DIFFRACTION POWDER PATTERN OF KERNITE†

dÅ	Relative Intensity	dÅ	Relative Intensity
	I/I_1		I/I_1
7.4	1.0	2.55	0.2
6.6	0.9	2.50	0.1
6.0	0.4	2.46	0.3
4.65	0.1	2.37	0.2
4.26	0.2	2.29	0.3
3.87	0.5	2.13	0.2
3.68	0.4	2.07	0.4
3.50	0.4	1.99	0.2
3.24	0.8	1.95	0.1
3.12	0.8	1.90	0.7
2.86	0.8	1.87	0.1
2.76	0.2	1.82	0.3
2.66	0.1	1.78	0.1
2.58	0.2	1.74	0.1

† The spacings of the x-ray pattern of kernite are in Angstrom units, the weighted mean value of the copper Kα doublet being 1.5418Å (*Jour. Sci. Instruments*, **24**, 27, 1947).

The pattern was made with Ni filtered Cu Kα radiation using a camera of effective diameter of 14.32 cm. The camera will not record spacings greater than 16.5 Å when using copper radiation.

REFERENCES

1. American Society for Testing Materials card file of x-ray diffraction date.
2. FAIVRE, RENE, CHAUDRON, GEORGES, Zeolitic nature of the water in calcium sulphate hemihydrate and the effect of its removal upon the transformation of soluble anhydrite into insoluble anydrite: *Compt. rend.*, **219**, 29–30 (1944).
3. LENGYEL, B., Röntgenographic investigation of the crystal water in zeolites: *Zeit. Phys.*, **77**, 133–138 (1932).
4. MENZEL, HEINRICH, AND SCHULZ, HANS, Der Kernit (Rasorit) $Na_2B_1O_7 \cdot 4H_2O$: *Zeit. anorg. allgem. Chem.*, **245**, 157–220 (1940).
5. ONORATO, E., Calcium sulphate hemihydrate and soluble anhydrite: *Periodico Mineral.*, **4**, 1–42 (1933).
6. SCHALLER, WALDEMAR, T., Borate minerals from the Kramer district Mohave Desert, California: *U. S. Geol. Survey, Prof. Paper* **158**, 146–163 (1930).
7. WEISER, H. B., MILLIGAN, W. O., EPHOLM, W. C., The mechanism of the dehydration of calcium sulphate hemihydrate: *Jour. Am. Chem. Soc.*, **58**, 1261–1265 (1936).

PROCEEDINGS OF SOCIETIES

THE CRYSTALLOGRAPHIC SOCIETY OF AMERICA

(JOINT MEETING WITH AMERICAN SOCIETY FOR X-RAY AND ELECTRON DIFFRACTION)

WILLIAM PARRISH, *Secretary-Treasurer,*
c/o Philips Laboratories, Inc., Irvington-on-Hudson, New York.

The third annual Spring meeting was held jointly with American Society of *X*-ray and Electron Diffraction at Yale University, New Haven, Conn., March 31–April 3, 1948. The meeting was attended by 205 people, 81 being members of C.S.A.

The officers for 1948 are:

President: Professor A. Pabst, University of California.
Vice-President: Professor J. D. H. Donnay, The Johns Hopkins University.
Secretary-Treasurer: Dr. William Parrish, Philips Laboratories, Inc.
Councilors: Professor N. W. Buerger, Postgraduate School, U. S. Naval Academy.
Professor I. Fankuchen, Polytechnic Institute of Brooklyn.

The Society now has 242 members, 25 residing outside U.S.A. Membership blanks may be obtained from the Secretary, c/o Philips Laboratories, Inc., Irvington-on-Hudson, N. Y. Abstracts of papers presented at the third annual meeting are given below.

A NEW MODIFICATION OF SODIUM

C. S. BARRETT, *University of Chicago.*

Employing techniques previously used on lithium,[1] samples of sodium (C.P. grade) were investigated at low temperatures in a Norelco spectrometer. After cold working at −253° C. the diffraction pattern at −195° C. showed a small diffraction peak in addition to the body-centered cubic pattern. Warming slightly caused the peak to disappear. If this peak is analogous to the similar one in cold-worked lithium it is the strongest line, (111), of the pattern of a face-centered cubic form of sodium. The face-centered cubic unit cell has a lattice constant equal to 5.339 Å at −195° C.

That the proposed structure is reasonable is indicated by the atomic radius computed from this lattice constant, 1.880 angstroms, which may be compared with the value 1.874 Å computed from Pauling's radii for sodium in coordination 12, corrected to this temperature. The volume change is negligible, as in lithium: the calculated values for density are 1.012 for face-centered cubic sodium and 1.014 for body-centered cubic at −195° C. Only about 1/10 of the sample has the new structure under the treatment employed.

[1] Barrett, C. S., *Phys. Rev.*, **72,** 245 (1947); Barrett, C. S., and Trautz, O. R., *A.I.M.E* Preprint, T.P. 2346, Metals Technology (**1948**).

THE NATURE OF THE ORDER OF LARGE SIZE EXHIBITED by COLLAGEN FIBRILS

RICHARD S. BEAR AND ORVIL E. A. BOLDUAN, *Massachusetts Institute of Technology.*

In order to explain the predominant small-angle diffraction effects obtained from dry tendon fibers, it is necessary to assume for the typical constituent fibril a model which has the following characteristics: while the fibril is approximately a smooth cylinder of finite width (diameter ca. 1000 Å) possessing predominantly longitudinal periodic structure, it is composed of smaller subfibrillar filaments (diameter ca. 100 Å) whose longitudinal structures are in approximate register, sufficient for diffraction in phase to low orders. Random small longitudinal displacements of the filaments progressively cause their diffractions to

fall out of phase, until at higher orders the diffraction effects are essentially those of individual filaments. Variations in effective radii of material diffracting to the higher orders indicate that the filaments themselves are not smooth but possess a periodically varying diameter.

STRUCTURAL CRYSTALLOGRAPHY OF LAZULITE, SCORZALITE AND VESZELYITE

L. G. Berry, *Queen's University.*

The following new structural data for lazulite, scorzalite and veszelyite were obtained from single crystal photographs using the Weissenberg and Precession methods and copper radiation:

Lazulite and scorzalite: monoclinic—$P2_1/n$; the unit cell with $a=7.12$, $b=7.24$, $c=7.10$ Å, $\beta=118°55'$ (lazulite, Werfen, Salzburg). $a=7.14$, $b=7.27$, $c=7.16$ Å, $\beta=119°18'$ (lazulite, Graves Mt., Georgia). $a=7.16$, $b=7.25$, $c=7.14$ Å, $\beta=118°47'$ (lazulite, Churchill, Manitoba). $a=7.15$, $b=7.32$, $c=7.14$ Å, $\beta=119°00'$ (scorzalite, Minas Geraes, Brazil), contains 2 $[(Mg, Fe'')Al_2(PO_4)_2(OH)_2]$. Specific gravity, lazulite (Mg predominant) 3.06 to 3.12 (measured, various authors), 3.14 calculated for mineral with all Mg; scorzalite (Fe'' predominant) 3.33 (Pecora, 1947), 3.39 calculated for mineral with all Fe''. Cleavage $(\bar{1}01)$ and (110) difficult. The morphological lattice (Dana 1892), is monoclinic $B2_1/a$ and pseudo-orthohexagonal.

Veszelyite: monoclinic—$P2_1/a$, the unit cell with $a=9.84$, $b=10.17$, $c=7.48$ Å, $\beta=103°25'$, $a:b:c=0.9675:1:0.7355$, contains $4[(Cu, Zn)_3PO_4(OH)_3 \cdot 2H_2O]$. Specific gravity 3.34 (Zsivny), 3.531 (Schrauf), 3.42 calculated for Cu:Zn=7:5. Cleavage (001). These data were obtained on a crystal fragment from Morawitza, Hungary. A chemical analysis of this material (Schrauf 1880) shows As substituting for P(P:As=3:2). Later analyses of materials from other localities show no arsenic. *X*-ray powder photographs indicate structural identity of veszelyite from Morawitza and Vaskő, Hungary; and 'kipushite' from Kipushi, Belgian Congo.

ON THE CRYSTAL STRUCTURE OF $AlPO_4$

R. Brill and A. deBretteville, Jr.,
Signal Corps Engineering Laboratories, Fort Monmouth, N. J.

$AlPO_4$ according to Huttenlocher[1] has a lattice similar to that of quartz. The lattice is hexagonal and has nearly the same a-axis (4.97_5 against 4.90_3 Å for quartz). The c-period is doubled (10.84 against $1/2\times10.78$ Å for quartz). The doubling of the c-spacings shows that Al and P layers alternate in planes parallel to the basal plane. In the possible space groups (see Huttenlocher) the different kinds of atoms have the following positions: Al: $3(a)$; P: $3(b)$; $O^{I}6(c)$; $O^{II}6(c)$. Under the assumption that the oxygen positions are the same as in quartz we get: $F_{003}=3(A_1-f_P)$ independent of the values of the different parameters. An absolute measurement of F_{003} should give some insight on the kind of chemical bond in $AlPO_4$, because $|f_{Al}-f_P|$ would be greater for neutral atoms (pure covalent bond-type) than for ions. Absolute intensity measurements were made of the basal plane reflections of $AlPO_4$. The crystals used were grown and prepared for our investigation by Mr. J. M. Stanley and Mrs. B. Korr of Squier Signal Laboratory. It can be shown that $1/3\times F_{003}$ is about 8. This value is so high that it cannot be explained by a difference of the scattering power of even neutral Al and P-atoms. Therefore the positions of the two kinds of oxygen atoms cannot be equal. Preliminary measurements of the intensities of 006 and 009 show that the P-O distance is smaller than the Al-O distance. Therefore, a large amount of ionic bond may be present in $AlPO_4$.

[1] Huttenlocher, H. F., *Zeit. Krist.*, (A) **90**, 508–516 (1935).

CHEMICAL BOND OF MAGNESIUM OXIDE

R. Brill,
Signal Corps Engineering Laboratories, Fort Monmouth, N. J.

The oxides of the third row of the periodic system of elements show on the left side nearly pure ionic bond (Na_2O), and on the right side covalent bond (Cl_2O_7). In the middle of that row (SiO_2), we have nearly 50% ionic and 50% covalent bond.

Investigation of magnesium oxide was made using the Fourier synthesis method to see whether a certain amount of covalent bond may be found in magnesium oxide. Investigation shows that the electron background in the whole lattice is greater than in all investigated alkaline halides. Three dimensional Fourier synthesis showed that the electron density does not decrease below 0.15 electrons per A^3 at any point of the lattice. In sodium chloride the lowest electron density was 0.006 electrons A^3. The difference cannot be caused by a higher thermal movement in MgO. Furthermore, the intensity measurements showed that the atomic scattering factor of magnesium ion at low angles is smaller than the theoretical values. Also that for oxygen ion is slightly larger than the theoretical values. This means that the magnesium ions are little more expanded and the oxygen ions slightly more contracted. All these results show that there is a certain amount of covalent bond in magnesium oxide. The investigation was carried out together with Dr. Herman and Dr. Peters.

CRYSTALS BASED ON THE SILICA STRUCTURES

M. J. Buerger,
Massachusetts Institute of Technology.

Some 15 compounds are known to occur in crystals whose structures are derivatives[1] of quartz, tridymite, or cristobalite. These can be placed in two different categories: (1) half-breed derivatives, and (2) stuffed derivatives.

In the half-breed type, half the silicon positions are occupied by trivalent atoms, half by pentavalent atoms. If these atoms are ionic, then the electrostatic valence rule requires that the proxy atoms alternate in the structure in order that the sum of the valence bonds to the shared oxygen atoms be 2. Half-breed derivatives of the silica structures are known for BPO_4, $AlPO_4$, $FePO_4$, $BAsO_4$, and $AlAsO_4$. Quartz-, tridymite-, and cristobalite-like structures are known for various members of this group. All three types are known for $AlPO_4$.

In the stuffed type, one or more of the silicon atoms is replaced by an atom of lower valence, the valence balance being supplied by an alkali atom or atoms in interstitial spaces of the structure. Only in $LiAlSiO_4$ is the alkali atom small enough to be accommodated in the small interstitial spaces of a quartz-like structure. All other compounds have a tridymite-like or cristobalite-like structure because the larger voids of these structures are required to house the alkalis Na and K. Stuffed structures are known for $LiAlSiO_4$, $NaAlSiO_4$, $KAlSiO_4$, $BaAl_2O_4$; $Na_2Al_2O_4$, $K_2Al_2O_4$, $K_2Fe_2O_4$; Na_2CaSiO_4; also for minerals with more complex but related formulae: $KNa_3Al_4Si_4O_{16}$ (natural nepheline), $NaCaAl_3Si_{15}O_{36}$ (natural tridymite).

All these structures are derivative structures[1] and therefore have a lesser symmetry content per unit volume than the corresponding silica structures. This requires either multiple cells or lowered non-translational symmetry. This last feature is frequently accompanied by twinning which increases the apparent symmetry. Twinning of this sort occurs in $LiAlSiO_4$, $NaAlSiO_4$, and $KAlSiO_4$. The potassium salt has been supposed to be hexagonal, but diffraction data suggest that the apparently single crystals have orthorhombic or lower symmetry.

[1] Buerger, M. J., Derivative crystal structures: *J. Chem. Phys.*, **15**, 1–16 (1947).

New data are presented for $LiAlSiO_4$. Powder patterns and rotation photographs about both a and c indicate that this is a derivative of the quartz structure, but the failure of the 0001 extinction which occurs in quartz shows that its symmetry is less than hexagonal and that the apparently single crystals must be twins. The apparent cell edges derived from rotation and precession photographs are:

$$a = 10.55 = 2 \times 5.275 \text{ true Å.}$$
$$c = 11.22 = 2 \times 5.61 \text{ true Å.}$$

The apparent cell has both edges about double those of the quartz cell. The crystals of $LiAlSiO_4$, whose cell characteristics are reported above, were grown by the Washken Laboratories of Cambridge, Mass., under a development contract with the Squier Signal Laboratory, U. S. Army Signal Corps, Fort Monmouth, New Jersey.

PHASE DETERMINATION WITH THE AID OF IMPLICATION THEORY

M. J. Buerger,
Massachusetts Institute of Technology.

Since the implication diagram provides the locations of atoms in crystals, there must be a close similarity between a Fourier representation of the implication diagram and the Fourier representation of the projection of electron density of the crystal on the same plane. The relation between the coefficients of the two series can be ascertained in several ways. A straightforward way which is not difficult in cases of low symmetry is to expand $FF^*(hkl)$ and then separate $F(h'k'l')$ from the rest of the expansion. For symmetries other than $\bar{1}$ it is then possible to eliminate most (if not all) of the unsymmetrical components. This is illustrated for symmetry 2 parallel to c, as follows: By a simple manipulation, the expansion of $FF^*(hkl)$ can be arranged in the following form:

$$F^2_{hkl} = \underset{(a)}{Q} + \underset{(b)}{F_{hkl}(P_0)} + \underset{(c)}{F_{hkl}(P_z)} + \underset{(d)}{Rf_{2h,2k,0}} + \underset{(e)}{\sum_j (R_j - R_j) F^1_{2h,2k,0}} \qquad (1)$$

where

$$Q = \sum_j N_j f_j, \quad N = \text{rank of equipoint}$$

and

$$R = \frac{f^2_{hkl}}{f_{2h,2k,0}}.$$

The expansion consists of five parts, which can be described in terms of the contribution of this term to the Patterson synthesis. (a) is a contribution to the origin peak, (b) represents the contribution on the Harker level to a non-Harker peak, and (c) represents a contribution on a non-Harker level to a general Patterson peak.

Term (c), which represents a very large part of the expansion, can be eliminated by the following manipulation: All terms are summed over l from $l = -L$ to $+L$, and each side of the equation is multiplied by $\cos 2\pi(kx+hy)$. The left side of (1) then represents the hk contribution to a Harker synthesis on level zero, and the parts of the right side of (1) represent the hk contributions to Fourier syntheses of quasi-electron density representations. In the complete syntheses, (c) vanishes because it represents a section on level zero, where there is no "density." The only way for this to occur is for each term, $\sum_l F(P_z)$ to vanish independently. This eliminates the term $\sum_{ll} F_{hkl}(P_z) \cos 2\pi(hx+ky)$. All terms are now divided by $\cos 2\pi(hx+ky)$. There remains

$$\sum_l F_{hkl}^2 = \underset{(a)}{\sum_l Q} + \underset{(b)}{\sum_l F_{hkl}(P_0)} + \underset{(d)}{\sum_l RF_{2h,2k,0}} + \underset{(e)}{\sum_l \sum_j (R_1 - R_j) F_{2h,2k,0}}. \qquad (2)$$

When non-Harker peaks can be recognized on the implication map, for example, by the non-appearance of satellites in certain symmetries, term (*b*) can be allowed for. Relation (2) then provides the relation of F's to F^2's for two-fold symmetry. The last term is a correction term which arises due to the fact that all atoms do not scatter with the same power. When all atoms have about the same scattering power, as in many organic compounds and in many silicates, this term vanishes. In other cases, it can be evaluated from special position information, or more generally, from the locations of certain atoms provided by the implication diagram. Where these do not apply, then this term can be evaluated for its maximum value, in which case it sets determinable limits on the part of (2) which cannot be directly computed. Since the absolute values of the F's are known, it should not be difficult in most cases to decide on phases of the F's with the aid of (2).

Equalities of a similar nature exist for each Harker level of each symmetry. It should be noted that the phases of only a fraction of the coefficients of the electron density series can be determined in this way. The fraction is $\frac{1}{4}$, $\frac{1}{3}$, $\frac{1}{2}$, or 1, corresponding, respectively to the implication ambiguity of 4, 3, 2, and 1. Therefore, if an electron density map is computed using the terms whose coefficients are determined in this manner, n possible positions appear for each atom in the crystal structure, where n is the ambiguity coefficient of the implication. The wrong positions can only be removed by supplying the electron density series with the missing terms.

VIBRATIONS OF CRYSTALS*

NICHOLAS CHAKO,
Alabama Polytechnic Institute.

In recent years extensive theoretical and experimental studies have been made of the vibrational properties of crystals, with particular reference to quartz, tourmaline and rochelle salt.[1] Recently, extensive theoretical investigations have been carried out on quartz plates and the calculated vibrations have been found in agreement with experiment.[2,3] However, because of the complexity of the problem, only the simplest types of crystals have been considered, and the treatment has been limited to certain cuts and to the simplest geometrical figures. Calculations of the vibration characteristics have been carried out for rectangular and circular plates, both of quartz[2,3,4,5] and rochelle salt.[5]

For circular plates one applies Love's theory for the calculation of extensional vibrations. It is found that the contribution of the piezoelectric terms in the calculation of characteristic frequencies are negligible for the case of quartz (less than a fraction of one per cent) whereas for rochelle salt they amount to a significant fraction of the purely elastic frequency. There exist pure shear frequencies when the direction of the electric field makes small angle ($<5°$) from the Z axis of the crystal, and these have about the same frequencies as the elastic frequencies. For larger angles there exist no pure shears, and the vibrations

* This investigation carried out in part under contract with Signal Corps Engineering Laboratories.

[1] Cady, W. G., Piezoelectricity (**1946**); Heising, R. A., Quartz Crystals, (**1946**).
[2] Bechmann, H., *Zeit. Physik*, **117,** 180 (1940); **118,** 515 (1941); **120,** 107 (1942).
[3] Mason, Sykes, Bond, in Bell Telephone Technical Journal (See Heising, l.c.)
[4] Ekstein, H., *Phys. Rev.*, **66,** 105 (1944); **68,** 11 (1945); **70,** 76 (1946).
[5] Chako, N., *Phys. Rev.*, **71,** 470 (1947).

are no longer of a simple harmonic type. In case of rochelle salt, one finds that the vibrations are not a pure harmonic type, and only for large values of the characteristic number do they become of an harmonic character. The thickness vibration of the latter are found to be non-degenerate.

THE BEHAVIOR OF PUNCH FIGURES IN THALLIUM HALIDE CRYSTALS

J. W. Davisson and B. Henvis,
Naval Research Laboratory.

The penetration of a pointed instrument such as a scriber into a thallium halide crystal results in surface dislocations called punch figures and also in preferential volume displacements. It will be shown that both the surface and volume effects are due to slip in the [100] directions.

When a [100] direction lies close to the surface, slight penetration of the scriber will produce surface dislocations extending about an inch in the [100] directions. The surface dislocations diminish in length in proportion to the degree of dip of the [100] directions. This behavior results in an extreme sensitivity of the punch figure in the neighborhood of a [100] pole. Thus it is possible to locate the [100] poles and the [100] directions on hemispherical surfaces of these crystals with precision.

Slight penetration of a (100) section $\frac{1}{4}''$ thick by means of a lead pencil produces a small pip or protuberance on the opposite surface. Similarly penetration of a $\frac{1}{4}''$ (110) section results in two pips corresponding to the two 45° [100] directions. The pips formed in the (110) sections are diamond based pyramids with well defined steps. These structures are formed by gliding of (110) planes in the [100] directions.

Contrary to the general rule established for metals, slip in the body-centered thallium halide crystals does not take place in the direction of greatest linear atomic density, but along rows of similar ions.

PERMANENT POLARIZATION OF A SINGLE CRYSTAL OF BARIUM TITANATE

A. deBretteville, S. Benedict Levin, and H. Estelle,
Signal Corps Engineering Laboratories.

A very small barium titanate crystal was silvered on two edges, mounted on a microscope slide, fitted with snug-fitting aluminum foil electrodes and a close iron-constantan thermocouple, and set in a micro-oven for continuous observation in polarized light. By a combination of heating and cooling in a strong DC field the crystal was detwinned and rendered optically homogeneous, having apparent biaxial negative character and acute bisectrix *c* coincident with the axis of dielectric polarization.

By connecting the crystal into an oscillograph circuit, the ferro-electric hysteresis loop of the crystal was observed at 15 volts 60 cycle AC, with and without an additional positive DC bias. By raising the crystal above 65° C, and cooling in a field of 2000 volts/cm. for 5 minutes and then removing the field, the crystal retained a charge which apparently is a volume polarization. This is exhibited as a distortion of the hysteresis loop. The polarity of the charge is the same as that of the formerly applied field.

The minimum temperature for which a charge will be retained, using the above fields and times is 65° C. A charge has been retained for over 80 hours, though diminished, by cooling from above the transition point with 2,500 volts/cm. initial field. Cherry[1] and Adler have obtained a somewhat similar effect for poly-crystalline barium titanate.

[1] Cherry, W. L., Jr., Adler, Robert, *Phys. Rev.*, **72**, 981–982 (1947).

ATACAMITE TWINNING RE-EXAMINED

J. D. H. Donnay,
The Johns Hopkins University.

Ford's twin law (*Am. J. Sci.*, **30,** 16, 1910) may be defined in several ways. Results of calculations made from the Zepharovitich-Klein fundamental angles (in Dana) confirm those of Friedel (*Bull. Soc. fr. Min.*, **35,** 45, 1912), who used Ungemach's axial ratios (*ibid.*, **34,** 148, 1911). The space group and unit-cell dimensions, predicted from morphology and checked by Weissenberg photographs, agree with previous x-ray results (Thoreau and Verhulst, *Ac. Roy. Belgique, Bull.*, **24,** 716, 1938). It is not necessary to use Ford's irrational definition. Using –[950]– as 3-fold twin axis, the obliquity is zero (within limits of accuracy), but the index is 61. Using –[544]– as 2-fold twin axis, the obliquity is 3°46′ and the index is 81. Such values for the twin index are abnormally high. The case is not closed!

GROPING STAGES IN SOME ORGANIC CRYSTAL STRUCTURE DETERMINATIONS

J. D. H. Donnay and C. P. Fenimore,
The Johns Hopkins University.

If an organic compound has a molecular crystal structure and if its molecules are fairly rigid, then the groping stages consist in finding the approximate position and orientation of these molecules in the unit cell. Among the many ways of attacking the problem, departures from the generalized law of Bravais, optical data, a knowledge of which planes reflect most intensely, as well as purely metrical considerations, may locate the molecules so closely that the structure can then be completed by Fourier methods. Even in the absence of heavy atoms, Patterson and Patterson-Harker syntheses may be useful checks for proposed arrangements.

Examples. The structure of orthorhombic dibiphenylene ethylene has been solved by such methods. It is shown approximately to possess a layer structure (001) by its large negative birefringence and acute bisectrix perpendicular to (001). A rough measure of the crystal pleochroism suggests that if the molecule is planar, the molecular planes are inclined $40° \pm 5°$ to (001). The crystal violates the generalized law of Bravais inasmuch as the observed $\{hk0\}$ forms are $\{130\}$ dominant and $\{200\}$ narrow; while $\{020\}$ and $\{110\}$, which should precede these in importance, are absent. A pseudo thirding of the b-axis allows an arrangement of molecular centers which accounts for the morphological anomalies, is compatible with the optical data, and is in agreement with Patterson and Patterson-Harker syntheses. A consideration of the most intensely reflecting planes of high indices leads to the orientation of the molecules in the xy and yz planes, essentially solving the structure.

Use of metrical considerations is illustrated by triclinic dipentaerythritol. The eminent cleavage (010) and biaxial negative character with acute bisectrix perpendicular to (100) point to a layer structure, as is known pentaerythritol. The ether molecular model looks promising. Such molecules can be arranged in centrosymmetrical pairs, then in chains and layers by repetition of the process. The period of the chain (in A.U.) is $2.6 \times 4 = 10.4$ (observed $a_0 = 10.4$). The distance between chains is $2.6 \times 5 = 13.0$ (observed $c_0 \sin \beta = 13.4 \times 0.968 = 13.0$). The β angle would be arctan $5 = 78°41'$ (observed, $75\frac{1}{2}°$). Hydrogen bonds will strengthen the layers. Two layers will easily fit in $d(010) = 9.6$, accounting for the structural halving observed ($0k0$, k even only).

THE CALCULATION OF STRUCTURE FACTORS BY A PUNCHED CARD METHOD

JERRY DONOHUE AND VERNER SCHOMAKER,
California Institute of Technology.

A method for the rapid calculation on punched cards of the structure factors of x-ray crystal structure analysis has been developed. It makes use of the following IBM equipment: automatic reproducing punch (type 513), automatic multiplying punch (type 601), alphabetical accounting machine (type 405), and sorter (type 11).

The general expression for the structure factor:

$$F_{hkl}=\sum_j f_j e^{2\pi i(hx_j+ky_j+lz_j)} \quad \text{(summation over the } j \text{ atoms in the unit cell)}$$

can by suitable manipulation be expressed in the following way:
$F_{hkl}=A_{hkl}+iB_{hkl}$ where A_{hkl} and B_{hkl} are of the form:

$$n\sum_j f_j \begin{Bmatrix}\cos \\ \text{or} \\ \sin\end{Bmatrix} 2\pi hx_j \begin{Bmatrix}\cos \\ \text{or} \\ \sin\end{Bmatrix} 2\pi ky_j \begin{Bmatrix}\cos \\ \text{or} \\ \sin\end{Bmatrix} 2\pi lz_j .$$

These forms of course depend on the space group under consideration. The scheme of calculation is sufficiently flexible however to enable it to be applied to any space group.

The following packs of cards must be prepared on a hand punch before starting a calculation:

1. X-cos 2πX-sin 2πX. On this pack is punched values of X together with those of cos 2πX and sin 2πX and their signs. The argument X runs from 0.000 to 0.999 in intervals of 0.001. This pack is used in all calculations.

2. Form factors. This pack contains one card for every reflection being calculated, together with the values of the corresponding form factors of each kind of atom in the cell. This pack is used in all calculations for a given crystal.

3. Parameters. These packs contain one card for each atom for each h, k, and l observed together with the values of hx, ky, and lz for the atoms, where x, y, and z are the trial parameters. This pack is used only in a particular calculation.

The scheme of the calculation consists of punching a set of atom reflection cards—one card for each (non-equivalent) atom for each (hkl)—which contain the following pertinent information: crystal, trial, atom, h, k, l, f_{atom}, hx, ky, lz, cos $2\pi hx$, cos $2\pi ky$, cos $2\pi lz$, sin $2\pi hx$, sin $2\pi ky$, and sin $2\pi lz$. (The particular trigonometric functions punched depends on the expressions for A_{hkl} and B_{hkl}.) The foregoing is accomplished by the appropriate reproducing, sorting, and gang punching operations. The products are next obtained on the multiplying punch. Each card then contains the individual atomic contributions to A_{hkl} and B_{hkl}. The cards are then sorted and the values of A_{hkl} and B_{hkl} are printed with the tabulator. If desired, the atom reflection cards may also be listed on the tabulator so that the contributions of each atom to each reflection are quickly available for reference.

The above scheme has been used to calculate a set of about 600 (hkl) reflections for a crystal with space group $P2_12_12_1$, eight non-equivalent atoms in the general positions of the cell. The time required for the actual calculation is about 24 hours, approximately one-tenth of that required for doing the calculation with a hand operated calculator. The time-saving factor will in general vary with the number of reflections being calculated, the scheme being used, and the complexity of the crystal under investigation.

STATISTICAL FLUCTUATION OF INTENSITY IN DEBYE-SCHERRER LINES DUE TO RANDOM ORIENTATION OF CRYSTAL GRAINS

HANS EKSTEIN,
Armour Research Foundation.

In the Debye-Scherrer diagram of a stationary polycrystalline sample, the intensity distribution in the line is erratic because of statistical irregularities of the crystal grain orientation. If the only causes of line breadth are the natural spectral width of the primary radiation and the small size of the crystal grains (i.e., pure Fraunhofer diffraction), the statistics of the intensity distribution can be described analytically. The "experimental" line center can be defined as the center of gravity of the intensity curve. The mean deviation of the experimental line center and, thereby, the mean deviation of the measured lattice parameter are found to be proportional to $1/\sqrt{N}$ if N is the number of crystal grains. If the irradiated area rather than the number of grains is a given constant, the mean error of the measurement becomes a function of the grain diameter. For a typical case; i.e., 1 sq. mm. irradiated area of iron with CoKα (radiation and particles of 2×10^{-4} cm. in length, the relative error $\Delta d/d$ is found to be about 2×10^{-6}; i.e., about ten times smaller than that reported in precision measurements. This indicates that the crystal statistics is not the limiting factor for precision measurements.

In the limiting case of negligible statistical fluctuation, the intensity distribution is smooth and can be approximated by a resonance curve whose width

$$B = B_{\text{spectral}} + B_{\text{size}}$$

is the sum of two terms, one due only to the spectral width of the primary beam, the other term being the usual breadth due to the grain size alone.

ACHROMATIZATION OF DIFFRACTION LINES

HANS EKSTEIN AND STANLEY SIEGEL,
Armour Research Foundation.

Large diffracting angles are necessary for the precision determination of lattice parameters. The line will be wide at these angles because of the spectral impurity of the incident characteristic radiation, and this width will limit the accuracy with which the line center can be determined. The line can be narrowed as follows:

A diverging polychromatic beam is allowed to fall on the plane surface of a single crystal. The beam diffracted by this crystal will diverge and will contain a bundle of rays whose wave length range corresponds to the finite spectral width of the characteristic radiation. The polycrystalline sample is mounted normal to the ray of wave length λ_o. If a point source is used, the rays diffracted by the sample will converge to a focus.

The condition for achromatization can be shown to be:

$$V = F\left(1+2\,\frac{\tan\theta}{\tan\theta_m}\right)\left(-\frac{1}{\cos 2\theta}\right)+l\cdot\frac{\cos(\theta_m+\alpha)}{\cos(\theta_m-\alpha)}$$

where α is the angle between the normal to the diffracting plane of the monochromator and the plane surface which is being irradiated, θ_m is the Bragg angle for the ray of wave length λ_o which strikes the plane surface and diffracts from the plane whose spacing is d_m, θ is the Bragg angle for the ray of wave length λ_o diffracted by the polycrystalline sample, l is the distance between the x-ray source and the monochromator, F is the distance from the polycrystalline sample to the focus, and V is the distance from the monochromator to the polycrystalline sample.

If the x-ray source is of extent S, then the focus is of extent

$$S' = S \cos 2\theta \frac{\cos(\theta_m + \alpha)}{\cos(\theta_m - \alpha)}$$

which can be made very small by proper choice of α.

CRYSTAL STRUCTURES OF AMMONIUM AND POTASSIUM MOLYBDOTELLURATES

HOWARD T. EVANS, JR.,

Laboratory for Insulation Research, Massachusetts Institute of Technology.

In a previous report,[1] preliminary lattice constants were reported for ammonium and potassium molybdotellurates, and it was stated that crystals of these compounds are isostructural. The final unit cell and space group data show that they are not, but possess entirely different symmetries:

$(NH_4)_6TeMo_6O_{24} \cdot 7H_2O$, orthorhombic, mmm; $a_0 = 14.62$ Å, $b_0 = 14.91$, $c_0 = 14.26$; space group $Pnaa = C_{2h}^{10}$; Z = 4, density calc. 2.82, found 2.78.

$K_6TeMo_6O_{24} \cdot 7H_2O$, orthorhombic, mmm; $a_0 = 14.30$ Å, $b_0 = 14.95$, $c_0 = 14.26$; space group $Pcba = C_{2h}^{15}$; Z = 4, density calc. 3.15, found 3.05.

A set of Patterson maps prepared for the ammonium salt allowed only three possible models for the complex ion. Calculation of structure factors showed a reasonable agreement of observed and calculated intensities for only one of these models. The x, y and z parameters for the tellurium and molybdenum atoms in the ammonium and probably also the potassium crystals (with y and z interchanged) are: Te 0, 0, 0; Mo_I 0, 0.228, 0; Mo_{II} 0.113, 0.121, -0.168; Mo_{III} 0.113, -0.121, -0.168. The model accepted here is one originally proposed hypothetically by Anderson,[2] in which the molybdenum atoms lie in a hexagon about the tellurium atom at the center, and the oxygen atoms lie in two close-packed layers of twelve above and twelve below the plane of the hexagon.

[1] Evans H. T., Jr., *Am. Mineral.*, **32,** 687 (1947).

[2] Anderson, J. S., *Nature,* **140,** 850 (1937).

CRYSTALLOGRAPHY OF THE POLYMORPHIC FORMS OF BARIUM TITANATE[1]

HOWARD T. EVANS, JR., AND ROBINSON D. BURBANK,

Laboratory for Insulation Research, Massachusetts Institute of Technology.

Crystallographic measurements have been made on single crystals of barium titanate recently prepared in this laboratory. The habit, lattice dimensions and twinning of the cubic form, and the tetragonal modification formed by cooling the cubic crystals below the Curie point at 120° C. are described. The twinning of the tetragonal form on the (101) plane is demonstrated by means of Buerger precession photographs, and it is shown that all the observed domain structure in these crystals is generated by lamellar glide twinning on this plane.

New information on the hexagonal form is presented. The unit cell is hexagonal with $a_0 = 5.735$Å, $c_0 = 14.05$Å, space group $C6_3/mmc = D_{6h}^4$, and contains six units of $BaTiO_3$. It is shown that the structure contains close-packed BaO_3 layers as in the perovskite structure, but stacked in a different sequence. A six-layer repeat unit is found, with the sequence

[1] This work is sponsored jointly by the Office of Naval Research and the Army Signal Corps, on Contract NSori-78, T.O. 1.

ABCACB. In this structure, two-thirds of the TiO_6 octahedra are found to be joined in pairs by sharing a face, while the remaining octahedra are single, sharing corners with the double groups. The two titanium atoms in the double groups are strongly repelled and are separated by a distance of about 2.96Å. It is suggested that this feature may account for the difference in dielectric properties of the cubic and hexagonal forms. New polymorphs of barium titanate are predicted.

THE ELECTRONIC DIGITAL COMPUTER

H. H. Goldstine,
Institute for Advanced Study.

A SIMPLE GNOMONIC TRANSPORTEUR FOR *X*-RAY LAUEGRAMS*

Samuel G. Gordon,
Academy of Natural Sciences of Philadelphia.

The indexing of Lauegrams requires transposition of the Laue spots (which are at tan 2θ) to tan θ (stereographic trace of plane-pole in F-Laue, and gnomonic plane-pole in B-Laue) or to $90°-\theta$ (gnomonic plane-pole of F-Laue). The geometry involved is simple: to the line through the Laue spot and the center of the Lauegram draw the unit circle (5 cm. radius for $D=5$ cm. in camera), tangent to the line at the center of the Lauegram. From the Laue spot draw a line through the center of the circle. Erect perpendiculars to this line, tangent to each side of the unit circle. It is easily proven that the intersections of these tangents with that of the tangent through the Laue spot and the center of Lauegram are the points required, θ and $90°-\theta$. A simple transporteur may be constructed by swivelling a carpenter's square to a straight-edge, such that the center of rotation is 5 cm. below the straight edge used to connect the Laue spot and center of Lauegram; and the vertical arm moves tangent to it at the required distance. Such a device was described by Clark and Gross in 1937 for plotting $90°-\theta$. However the vertical arm can be adjusted to any distance from the center of rotation, giving reductions to 4, 3, 2.5 or 2 cm. as desired. A shorter vertical arm, on the opposite side of the center is used for plotting θ. Since the device is simply an angle bisector, it can be used for converting gnomograms to stereograms.

* See *Am. Mineral.*, **33**, 634 (1948).

PROGRESS IN SILICATE STRUCTURES

ADDRESS OF THE RETIRING PRESIDENT OF THE CRYSTALLOGRAPHIC SOCIETY OF AMERICA

J. W. Gruner,
University of Minnesota.

(*Printed in full in this issue*)

A TWO CURVED CRYSTALS MONOCHROMATOR FOR THE STUDY OF LOW ANGLE SCATTERING

A. Guinier and G. Fournet,
Laboratorie d'Essais, Paris, France.
(*Read by I. Fankuchen*)

A two crystals spectrometer has already been used by various authors[1] for the study of *x*-ray scattering at *very* low angles, the sample being placed between the two crystals. We now use a double monochromator in a different way, in order to decrease the ratio of the parasitic scattering to the studied scattering.

With a single curved crystal monochromator the reflected beam is very intense, but the lamella which receive the total direct beam issued from the tube give rise to scattered radiation of appreciable intensity. Therefore it is necessary in low angle scattering experiments to reduce the aperture of the reflected beam by a system of slits and so partly to lose the advantages of the curved crystal.

When the reflected beam is again reflected by a second crystal the parasitic scattered radiation practically disappears, even in directions close to the direction of the main beam. According to a suggestion of Dr. J. W. M. DuMond, we tried to place two curved quartz crystals in such a way that the monochromatic beam reflected by the first crystal could be reflected by the second. With JOHANN monochromators,[2] in spite of the imperfect focalization every ray of the beam is reflected, but only when the crystals are in *antiparallel position* and have the *same curvature*. But with JOHANNSONN[3] monochromators, the focalization being theoretically perfect, both parallel and antiparallel positions are convenient. Theory and experiment show that the intensity of the final beam is greater in the second device than in the first.

We found experimentally that the energy of the beam which can be used for the study of low angle scattering is nearly the same with two curved crystals as with a single crystal. The loss due to the double reflection is balanced by the increase in aperture of the beam. In our apparatus we can now register reticular spacings below 250 Å, because the distance from sample to film is only 100 mm. We hope with dissymetric monochromators[4] to increase this distance and to register 600 Å spacings.

The double monochromator is associated with a demountable rotating anode tube allowing a load of 60 m.a., 35 KV upon a 1 mm.^{2} focus. This powerful source allows the various adjustments of the second crystal to be made with a fluorescent screen, and has considerably reduced the exposure times. For example, a good small angle pattern of a 5% haemoglobin solution is obtained within 40 minutes.

[1] Fankuchen I., and Jellinek M., *Phys. Rev.*, **67**, 201 (1945).
DuMond J. W. M., *Phys. Rev.*, **72**, 83 (1947).
[2] *Zeit. Phys.*, **69**, 185, (1931).
[3] *Zeit. Phys.*, **82**, 507, (1933).
[4] Guinier, A., *Comptes Rendus*, **223**, 31, (1946).

IMPROVED GEIGER COUNTER SPECTROMETER

E. A. Hamacher and William Parrish,
Philips Laboratories, Inc.

A description of changes made in the Norelco spectrometer which markedly improves resolution by use of a new geometrical arrangement and intensity by use of mica window *x*-ray and Geiger tubes.

Resolution. The focal spot of the *x*-ray tube, 9×2.8 mm., with length perpendicular to the axis of specimen rotation[1] was 0.24 ×2.8 mm. in projection at 1½°. By rotating the focal spot 90° in manufacturing the *x*-ray tube, the length of the focal spot is made parallel to the axis of rotation and is 9×0.07 mm. in projection. A set of Soller slits 1×25 mm. between source and specimen and 1×50 mm. between specimen and receiving slit limits the divergence to 4.6° and 2.3°, respectively. Bragg focussing is used in the plane parallel to the Soller slit foils. The angular aperture of the incident beam is 42′ and covers a 20 mm. wide sample at 10°2θ. The CuKα doublet is resolved on reflection from (10$\bar{1}$1) of a single quartz crystal plate and the width at half height of each line is about 3′. In a quartz powder sample, the doublet is noticeably separated in the reflection from (11$\bar{2}$0), $2\theta = 36.58°$ in recorded data.

Intensity. The Lindemann glass windows have been replaced by 0.0005″ thick mica for x-ray and Geiger tubes. It has about the same absorption as 0.020″ pure beryllium and is much less than Lindemann glass for 0.7 to 2.5 Å. By eliminating the intermediate graded glass seal, the inactive length of the counters has been reduced from 35 mm. to 2.5 mm. The optimum pressure for the Lindemann glass counters was 30 cm. (Hg) since higher pressures gave no higher counting rates due to absorption in the long inactive length, whereas 60 cm. (Hg) or more may be used with the mica window. The use of chlorine[2] rather than methylene bromide for a quenching agent gives a much larger sensitive area. The data shown below are based on calculations of the per cent of the x-ray beam transmitted through x-ray and Geiger tube windows and inactive length, which is absorbed in the 100 mm. active length of the counter. This is a measure of the efficiency and hence expected increase in counting rate of the system for the same geometry and power input of the x-ray tube.

	MoKα	CuKα	FeKα	CrKα
Lind. 30 cm. Argon	7%	15	6	2
Mica 60 cm. Argon	14	55	48	34

[1] Friedman, H., *Electronics*, April **1945**.
[2] Liebson, S. H., *Phys. Rev.*, **72**, 18 (1947).

THE STRUCTURE OF TOURMALINE*

Gabrielle E. Hamburger and M. J. Buerger,
Massachusetts Institute of Technology.

Earlier work[1] has shown that the space group of tourmaline is $R3m$. The dimensions of the cell, referred to hexagonal axes were given as $a=15.93$, $c=7.15$. This cell (whose volume is equal to that of 3 primitive rhombohedral cells) contained 3 formula weights of composition

$$\begin{vmatrix}\mathrm{Na}\\ \mathrm{Ca}\end{vmatrix}\mathrm{R}_3\begin{vmatrix}\mathrm{Al}\\ \mathrm{Fe}\end{vmatrix}_6\mathrm{B_3Si_6O_{27}(O,OH,F)_4}$$

Intensity data were obtained for $(hkil)$ reflections for two comparatively simple tourmalines, namely for a black, Fe tourmaline from Andreasberg, and for a white, Mg tourmaline from de Kalb. In this study, the Weissenberg method was used with filtered cobalt and copper radiations, respectively, and the intensities were measured by the Dawton method.

From these data, implication diagrams $I3$ $(xy0)$ were prepared for each crystal. In addition to satellites, both of these contained one very strong set of equivalent peaks. It seemed certain that this set was to be attributed to Si, Al, or both. In the preliminary form of this abstract, it was attributed to both. Subsequent intensity computations have shown that it is the location of Si only.

The difference implication, $\{I3\ (xy0)_{\mathrm{Fe}}-I3\ (xy0)_{\mathrm{Mg}}\}$ was also prepared. This displayed only one strong peak, which was obviously attributed to the Fe, Mg location. With the Si's and Mg's located in this manner, these atoms were surrounded by oxygen atoms consistent with their coordinations and with space requirements. This creates a segment of the structure of composition $\mathrm{NaMg_3Si_6O_{21}(OH)_4}$. The $\mathrm{Si_6O_{18}}$ part of this segment is a ring of tetrahedra. The entire segment may be thought of as a fragment of the kaolin structure in which all octahedral positions are filled with Mg (instead of 2/3's of them being filled with Al). Na is located between these segments on the three-fold axis. The segments are joined together by Al octahedra which share some oxygens with the segment, but require 6 ad-

ditional oxygens in the general position. The Al octahedra spiral about the 3-fold screw axes sharing edges with each other. Boron is in planar triangular coordination.

Intensities of the (*hki*0) spectra computed for this structure are in excellent agreement with the observed intensities. The structure satisfies the Paulings rules, and the known wide range of tourmaline composition is explained by it.

The parameters for a tourmaline of composition $NaMg_3B_3Al_6Si_6O_{21}(OH)_4$ are as follows:

Atom	equipoint	x	y	z (approximate)
Na	3*a*	0	0	~7/9
Mg	9*b*	.133	.067	~1/6
B	9*b*	.117	.233	~ 0
Al	18*c*	.050	.367	~5/6
Si	18*c*	.192	.192	~5/9
$(OH)_1$	3*a*	0	0	~1/3
$(OH)_2$	9*b*	.233	.117	~ 0
O_1	9*b*	.058	.117	~ 0
O_2	9*b*	.142	.071	~2/3
O_3	9*b*	.102	.204	~2/3
O_4	18*c*	.200	.200	~1/3
O_5	18*c*	.279	.246	~2/3
O_6	18*c*	.058	.292	~ 0

* See *Am. Mineral.*, **33,** 532 (1948).

[1] Buerger M. J., and Parrish, William, The unit cell and space group of tourmaline: *Am. Mineral.*, **22,** 1139–1150 (1937).

HYPOTHETICAL DISORDER AND ITS USE IN CRYSTAL STRUCTURE DETERMINATIONS

David Harker,
General Electric Co.

Any crystal can be represented by the Fourier Series for its electron density:

$$\rho(x, y, z)=\frac{1}{V}\sum_h\sum_k\sum_l F_{hkl}e^{2\pi i(hx+ky+lz)},$$

where $F_{hkl}=F_{\bar{h}\bar{k}\bar{l}}$ (since $\rho(x, y, z)$ is real). The same structure shifted one-half unit translation along x is

$$\rho(x+\tfrac{1}{2}, y, z)=\frac{1}{V}\sum_h\sum_k\sum_l (-1)^h F_{hkl}e^{2\pi i(hx+ky+lz)}.$$

The average of these two structures is that of a crystal in which the two halves of the structure follow one another at random—a disordered structure. Its mean electron density is given by:

$$\begin{aligned}\rho_D(x, y, z)&=\tfrac{1}{2}\left[\rho(x, y, z)+\rho(x+\tfrac{1}{2}, y, z)\right]\\&=\frac{1}{V}\sum_h\sum_k\sum_l \tfrac{1}{2}\left[1+(-1)^h\right]F_{hkl}e^{2\pi i(hx+ky+lz)}\\&=\frac{1}{V}\sum_h\sum_k\sum_l F_{hkl}e^{2\pi i(hx+ky+lz)}.\end{aligned}$$

even

This structure is described by the Fourier coefficients with even h, i.e., it can be referred to a cell half as long in the x direction as the original one. The content of this half-sized cell consists of a superposition of the contents of the two halves of the true cell with the density scale divided by two.

It may happen in the early stages of a crystal structure determination that the disordered structure is more convenient to study than the ordered one. The final step in the determination then involves the "decollapse" of the structure into complete order. This process may not be unique, but the decision between the various possible ordered structures is made easily by means of the F_{hkl}'s not used for the disordered structure; e.g., by F_{hkl}'s with odd h in the example first described.

It is clear that disordering can be accomplished by superposition of thirds, fourths, etc., and that more than one axis can be used. The choice between various possible hypothetical disorderings is a matter of convenience. It happens frequently that the projection of a structure upon one of the crystallographically important planes can be described in terms of a smaller unit mesh than the true one; in such cases the use of a corresponding disordered structure is particularly convenient.

RELATIONS BETWEEN THE "PHASE INEQUALITIES", THE PATTERSON FUNCTION AND BUERGER IMPLICATIONS

David Harker,
General Electric Company.

To a crystal composed of real atoms can be related other periodic structures with the same unit cell. Thus, the crystal (C), the electron density of which is implied by the Fourier Coefficients F_{hkl}, can be related to the Patterson Function (P) with a density distribution implied by the Fourier Coefficients $|F_{hkl}|^2$. The P space contains "atoms" with coordinates x_p-x_q, y_p-y_q, z_p-z_q where p and q are the ordinal numbers of the atoms in the C space. Another function related to the C-space is the Buerger Function (B) described by the Fourier Coefficients B_{hkl}. The B space contains some, but far from all, of the "atoms" belonging to the P-space; namely, those corresponding to atoms in C-space related by the operations of the space group of the real crystal.

An example may make this clearer. A crystal with the space group $P2$ has atoms at $x_j, y_j, z_j, \bar{x}_j, \bar{y}_j, \bar{z}_j$, where j runs from 1 to $N/2$ (N is the number of atoms in the unit cell of the real crystal). The corresponding Buerger Function has N "atoms" at 0, 0, 0 and at $2x_j$, 0, $2z_j$; $2\bar{x}_j$, 0, $2\bar{z}_j$. The related Patterson Function has these "atoms" and many others with coordinates $x_p \pm x_q$, $y_p \pm y_q$, $z_p \pm z_q$ where p and q run over all the numbers from 1 to $N/2$ and the signs must be taken both plus or both minus. The unitary structure factors are (when written as sums over individual electrons):
for the crystal (C)

$$\widehat{F}_{hkl}=\frac{2}{Z}\sum_{j=1}^{z/2} e^{-2\pi i k y_j}\cos 2\pi(hx_j+lz_j),$$

for the Buerger Function (B)

$$\widehat{B}_{hkl}=\frac{1}{Z}\sum_{j=1}^{z/2}\left[1+\cos 2\pi(2hx_j+2lz_j)\right]=\widehat{B}_{h0l}=\tfrac{1}{2}+\tfrac{1}{2}\widehat{F}_{2h02l}$$

and for the Patterson Function (P)

$$|\widehat{F}_{hkl}|^2.$$

The Phase Inequality for a crystal of space-group P_2 is

$$|\widehat{F}_{hkl}|^2 \leqq \tfrac{1}{2}+\tfrac{1}{2}\widehat{F}_{2h02l} \quad \text{or}$$

or

$$|\widehat{F}_{hkl}|^2 \leqq \widehat{B}_{hkl}.$$

A section through P at $y=0$ will contain all "atoms" with $y \cong 0$, but these include all the atoms in the same section through B, and it is these latter that are useful in determining the structure of C. The $\widehat{B}_{hkl's}$ in the P_2 case do not vary with k and for each h, l combination can be approximated by the largest $|\widehat{F}_{hkl}|^2$ for any k. From these can be calculated values of $B_{hkl}=\widehat{B}_{hkl}f^2$. The series evaluated from these coefficients should be more valuable in locating atoms in C than are the series using $|F_{hkl}|^2$'s. Similar relations hold for all space-groups, except $P1$ and $P\bar{1}$.

ABSOLUTE INTENSITY SCALE FOR CRYSTAL DIFFRACTION DATA

DAVID HARKER,
General Electric Company.

It is well known that the intensities I_{hkl} of the rays diffracted by a crystal can be calculated from its structure by the formula:

$$I_{hkl}=K\Phi(\lambda, \theta)|F_{hkl}|^2, \tag{1}$$

where h, k and l are the Miller indices of the sheaf of planes in the crystal from which the ray hkl can be said to have been "reflected"; λ is the wave length of the radiation used, θ is the glancing angle of "reflection," $\phi(\lambda, \theta)$ is a function dependent in form on the experimental arrangements, F_{hkl} is the "crystal structure factor" and K is a constant for a given specimen and radiation.

The "crystal structure factor," F_{hkl}, is related to the atomic arrangement in a crystal by the formula:

$$F_{hkl}=\sum_{j=1}^{N} f_j e^{-2\pi i(hx_j+ky_j+lz_j)}, \tag{2}$$

where N is the number of atoms in a unit cell of the crystal, x_j, y_j, and z_j are the coordinates of the j^{th} atom—expressed as fractions of the unit translations of the cell—and f_j is the scattering power of the j^{th} atom. The values of f_j depend on $(\sin\theta)/\lambda$.

In the case of x-ray diffraction, it is possible to make the approximation $f_j=Z_j\widehat{f}$, where Z_j is the atomic number of the j^{th} atom and $\widehat{f}$ is the same function of $(\sin\theta)/\lambda$ for all atoms. If $Z=\sum_{j=1}^{N} Z_j$ is the total number of electrons in the unit cell, we can define $\widehat{F}_{hkl}=F_{hkl}/Z\widehat{f}$. $\widehat{F}_{hkl}$ can be called the "unitary crystal structure factor" and can be calculated from the atomic arrangement of the crystal by the formula:

$$\widehat{F}_{hkl}=\sum_{j=1}^{N} n_j e^{-2\pi i(hx_j+ky_j+lz_j)} \tag{3}$$

where $n_j=Z_j/Z$ is the fraction of the electrons in the unit cell which belong to the j^{th} atom. It is noteworthy that $\widehat{F}_{hkl}$ depends on the composition and structure of the crystal but not on the angle of diffraction or the wave length.

The intensities I_{hkl} and the known values of $\phi(\lambda, \theta)$ allow the calculation of the quantities $K|F_{hkl}|^2$ directly from the data, but, since the value of K is usually very inconvenient to measure experimentally, values of $|F_{hkl}|^2$ are obtained in most cases by calculation from the structure of the crystal. It will be shown in the following how the value of K may be obtained from the data with an accuracy depending on the validity of the relation $f_j=Z_j\widehat{f}$, even if the structure is not known.

The value of $|\widehat{F}_{hkl}|^2$ is obtained by multiplying (3) by its complex conjugate; the result is:

$$|\widehat{F}_{hkl}|^2 = \sum_{j=1}^{N} n_j^2 + \sum_{\substack{p=1 \\ p\neq q}}^{N} \sum_{q=1}^{N} n_p n_q e^{-2\pi i[h(x_p - x_q)+k(y_p - y_q)+l(z_p - z_q)]}. \tag{4}$$

The mean value of $|\widehat{F}_{hkl}|^2$ over a large number of "reflections",[1] $|\widehat{F}_{hkl}|^2$, is then given by

$$|\widehat{F}_{hkl}|^2 = \sum_{j=1}^{N} n_j^2 \tag{5}$$

with a probable error of about $\pm 1/Q$, where Q is the number of "reflections" used in taking the average.[2]

Formula (5) is wrong only if $h(x_p - x_q)$, $k(y_p - y_q)$ and $l(z_p - z_q)$ are all integers or zero for all "reflections" used in averaging. If one is careful to average many non-cozonal "reflections," this cannot happen.

Since $\widehat{F}_{hkl} = F_{hkl}/Z\bar{f}$, and writing $F'_{hkl} = KF_{hkl}$ for the "observed" structure factor, one obtains:

$$\overline{\left(\frac{|F'_{hkl}|^2}{Z^2\bar{f}^2}\right)} = K \sum_{j=1}^{N} n_j^2$$

or

$$K = \overline{\left(\frac{|F'_{hkl}|^2}{Z^2\bar{f}^2}\right)} \Big/ \sum_{j=1}^{N} n_j^2. \tag{6}$$

The last relation can be rewritten

$$K = \overline{\left|\frac{F'_{hkl}}{\sum_{j=1}^{N} f_j^2}\right|^2}. \tag{6'}$$

The factor K, which converts the observed relative values of the squares of the "crystal structure factor," $|F_{hkl}|^2$, to the absolute scale can be evaluated from either (6) or (6').

The Temperature Factor: In the foregoing, it has been assumed that no thermal motion exists in the crystal under consideration, but this is never the case. The effect of this thermal motion on the intensities of diffraction can be allowed for by making K a function of $(\sin\theta)/\lambda$ according to the formula:

$$K = K_0 e^{-2B[(Sin\theta)/\lambda]^2}$$

In this case, it is no longer possible to use formulas (6) or (6') to obtain K, unless the "reflections" used in averaging all lie in a narrow range of $(\sin\theta)/\lambda$, and this value of K is useful only in that range. However, the variation of K with $(\sin\theta)/\lambda$ is such that a plot of lnK against $[(\sin\theta)/\lambda]^2$ is a straight line, with a slope of $(-2B)$ and an intercept on the axis of ordinates at lnK_0. Thus, if the values of K are computed from equations (6) or (6') in various ranges of $(\sin\theta)/\lambda$ and the results plotted as just suggested, not only can the intensities be referred to an absolute scale, but the temperature effect on intensity can be evaluated.

[1] A bar over a quantity is used to indicate the average value of that quantity.

[2] This follows from the expression

$$\frac{1}{2P+1} \sum_{n=-P}^{P} e^{-2\pi i\, nx} = \frac{1}{2P+1}\left(\frac{\sin\pi(2P+1)x}{\sin\pi x}\right).$$

GROWING CRYSTALS FROM SOLUTION

A. N. Holden,
Bell Telephone Laboratories.

Large clear single crystals of many ionic salts can be grown from water solution in a reciprocating rotary crystallizer. Seed crystals are moved at about fifteen inches per second through slowly cooled supersaturated solutions in cylindrical jars, heated at the bottom to dissolve spurious seed crystals. Practicable rates of clear growth reach a maximum of 200 molecular layers per second in favorable cases. These rates are controlled by the specific crystallization rate on the growing surfaces at the prevailing supersaturation and temperature, rather than by diffusion to them through the adjacent unstirred solution film, as can be shown (1) by comparison of growth rates with dissolution rates, and (2) by agreement in order of magnitude of observed rates and rates calculated from a rough kinetic theory. There is no satisfactory refined theory of crystallization in two-component systems, nor any adequate body of experimental data to verify one.

INDEX OF REFRACTION STUDIES OF ISOMETRIC OPAQUE MINERALS

Arthur L. Howland and M. Darwin Quigley,
Northwestern University.

The determination of the index of refraction of opaque substances by the application of Brewster's law was studied by Quirke and McCabe as a means for establishing a measure of the rank of coal. The same method has been applied by the authors to metallic oxides and sulfides such as magnetite, sphalerite, galena, and pyrite to determine its usefulness for the identification of opaque and high index minerals. The procedure followed was to determine the polarization angle by means of an analyzing prism and photometer when a beam of unpolarized light was directed against cleaved or polished surfaces of a mineral. Satisfactory checks were obtained with the known indices of glass, diamond, and sphalerite, but it was found that the nature of the surface is of great importance and that films of moisture or grease, and the destruction of the surface layers by polishing have a marked effect in lowering the values obtained. Index measurements were also obtained from the opaque minerals magnetite (2.42), galena (4.71), and pyrite (6.22), in contrast to metallic conductors such as silver and copper, for which the polarization angle cannot be determined by the experimental procedure employed. These minerals, which can be assumed to be representative of metallic oxides and sulfides, behave like dielectrics in permitting the maintenance of a coherent light beam for an appreciable depth beneath the surface.

THE PIEZOELECTRIC EFFECTS IN SOME UNIPOLAR CRYSTALS

Hans Jaffe,
*The Brush Development Company.**

The piezoelectric d_{nm} constants of several crystals having a unique polar axis are given. It is seen that the constants connecting an electric field *in* the polar axis to compressional strains are in the average somewhat smaller than the constants connecting fields *perpendicular* to the polar axis with various shear strains. The hydrostatic *piezoelectric* constant, however, which is the algebraic sum of 3 compressional constants, is generally quite small. Lithium sulfate monohydrate is a notable exception; its constant d_{22} relating field in polar direction to compressional strain in the same direction, is much higher than its other constants and gives rise to an outstanding hydrostatic effect.

* Work supported in part by U. S. Signal Corporation under contract W 28-003 sc 1583.

A NEW PROCEDURE FOR CALCULATING RADIAL DISTRIBUTION CURVES FROM ELECTRON DIFFRACTION DATA

J. KARLE AND I. L. KARLE,
Naval Research Laboratory.

Radial distribution calculations have been rather inaccurate owing to the fact that experimental difficulties limit the amount of intensity data available for the integral ordinarily computed. The purpose of this paper is to indicate that the amount of intensity data usually obtained in scattering experiments is sufficient to accurately determine the structure of the scatterer by means of an inversion procedure and also to show how the calculation must be modified in order to accomplish this.

The integral required to determine the distribution of scattering matter $rf(r)$, is

$$f(r) = \sqrt{\frac{2}{\pi}} \int_0^\infty SI(S) \sin SrdS \tag{1}$$

where S is a function of the wavelength of the incident radiation and the angle of scattering and I is the experimentally determined intensity as a function of S. In practice the upper limit of integral (1) is S max determined by the maximum angle at which the intensity may be evaluated. The upper limit is ordinarily too small to give accurate results from (1). In order to overcome this difficulty for electron diffraction calculations, Degard,[1] Schomaker[2] and Finbak[3] have independently introduced a factor e^{-aS^2} into the integrand of (1) giving,

$$f_a(r) = \sqrt{\frac{2}{\pi}} \int_0^{S_{max}} SI(S)e^{-aS^2} \sin SrdS. \tag{2}$$

The value of a can be chosen so that the integrand of (2) converges rapidly. The merit of this calculation is that the equilibrium distances between atoms are accurately determined and spurious peaks are eliminated. This is analogous to the use of an "artificial" temperature damping in the Fourier synthesis of crystal structure. The function $f(r)$ may be obtained from $f_a(r)$ by making use of the following relation,[4]

$$f_a(r) = \frac{1}{\sqrt{2\pi}} \int_{-\infty}^{\infty} f(\rho)m(r-\rho)d\rho \tag{3}$$

where the m function is the Fourier transform of e^{-aS^2}.

In order to study the internal motion of molecules it is necessary to evaluate $f(r)$ rather than $f_a(r)$. In our method $f_a(r)$ is first calculated from (2) and then $f(r)$ is obtained from it using (3). In molecular scattering $f_a(r)$ often results in a series of well defined bell-shaped peaks. The introduction of an analytical $f(\rho)$ in the form of $e^{-h(r_0-\rho)^2}$ leads to an evaluation of integral (3), giving $f_a(r) = e^{-h(r_0-r)^2/4ah+1}/(4ah+1)^{1/2}$ which allows an immediate determination of $f(r)$ from $f_a(r)$.

The tests performed so far with this method indicate that with good intensity data, not only equilibrium distances but also the character of internal oscillations may be studied. Professor Verner Schomaker has very kindly made available to us a set of punched cards developed at the California Institute of Technology for performing the required numerical integrations.[5]

[1] Degard C., *Bull. Soc. Roy Sci. Liége*, **115**, (1938).

[2] Schomaker, V., presented to the *American Chemical Society*, Baltimore, April 1939.

[3] Finbak, Chr., *Tids. Kjemi, Bergvesen, Metallurgi*, **2**, 53 (1942).

[4] Titchmarsh, E. C., Introduction to the Theory of the Fourier Integral, Oxford, the Clarendon Press, page 51 (1937).

[5] Shaffer, P. A. Jr., Schomaker, V., and Pauling, L., *Jour. Chem. Phys.*, **14**, 659 (1946).

THE CRYSTAL STRUCTURE OF DECABORANE

J. S. Kasper, C. M. Lucht, and D. Harker,
General Electric Company.

The crystal structure of decaborane, $B_{10}H_{14}$, has been determined from single-crystal oscillation photographs, using CoKα x-radiation.

Crystals prepared by sublimation at room temperature, or above, show a high degree of polysynthetic twinning, giving rise to diffuseness of reflections for which h and k are odd. In the untwinned condition, the crystal is monoclinic,[1] but pseudo-orthorhombic, and it is convenient to choose the two-fold axis in the c direction. The space group is then $C_{2h}^4-C11\ 2/a$. With $a_0=14.37$ Å, $b_0=20.98$ Å, $c_0=5.69$ Å, $\beta=90.0°$, the cell contains eight molecules of $B_{10}H_{14}$, and the calculated density is 0.96.

The individual crystals, which make up the actual, highly twinned, crystalline edifice, are so short in the b-direction (a few unit translations, at most) that it is convenient to consider the system as a partially ordered crystal, the disordered state of which is described by a unit cell one-fourth the size of the one mentioned above. The dimensions of this small cell are: $a_0=7.18$ Å, $b_0=10.49$ Å, $c_0=5.69$ Å; and it contains $2B_{10}H_{14}$ or $(1/2\ B)_{20}$ $(1/2\ H)_{28}$. The "disordered" structure based on this cell explains *all* the sharp spots observed—its space-group is $D_{2h}^{12}-P_{nnm}$.

The boron parameters have been established by means of Fourier methods, including a three-dimensional synthesis of the complete unit cell. They have not varied more than $\pm.001$ in the last two refinements. Hydrogen atoms contribute significantly to many reflections, and it appears that all of them are resolved in Fourier sections. However, a total of 18 peaks, each possible for a hydrogen, has been obtained in the electron density functions for the molecule and the 14 hydrogen positions have not been assigned unequivocally at the present time. Consequently, only the boron parameters will be given. They are as follows (for the large unit cell of the ordered structure):

8B at 000; $\frac{1}{2}\frac{1}{2}0$ +

xyz $\quad \frac{1}{2}+x, y, \bar{z}$

$\bar{x}\bar{y}\bar{z}$ $\quad \frac{1}{2}-x, \bar{y}, z$

	x	y	z		x	y	z
B_I	.033	.328	0	B_I'	.217	.078	.500
B_{II}	.109	.276	.142	B_{II}'	.141	.026	.642
B_{III}	.109	.276	−.142	B_{III}'	.141	.026	.358
B_{IV}	.097	.202	0	B_{IV}'	.153	−.048	.500
B_V	.019	.210	.228	B_V'	.231	−.040	.728

The molecules are required by the space group to have only a two-fold axis, but appear to have two mirror-planes as well; thus, they exhibit the symmetry $C_{2v}-mm2$. From the coordinates listed above, the molecule of $B_{10}H_{14}$ has a novel, open-clam-shell type of structure which has not been postulated heretofore. Each boron atom is bound to five or six other atoms, but the bonds are not all equivalent. Tentatively, it appears that ten of the hydrogen atoms are each bound to a single boron atom; the four remaining ones may have a higher coordination number.

[1] Möller (*Zeit. Krist.*, **76**, 500–516, 1931) concluded incorrectly that the crystal class was orthorhombic. The correct space group, $C11\ 2/a$, is a sub-group of the one C_{mma}, given by Möller.

AN *X*-RAY CRYSTALLOGRAPHIC STUDY OF THE HYDRAZIDES OF SOME n-ALIPHATIC ACIDS

E. C. Lingafelter and L. H. Jensen,
University of Washington.

The hydrazides ($RCONHNH_2$) of hexanoic, heptanoic, and octanoic acids have been investigated by oscillation and equi-inclination Weissenberg photographs. The substances have the same structure, as predicted by Kyame, Fisher, and Bickford[1] from their melting point study. They are monoclinic (Aa or $A2/a$) with 8 molecules in the unit cell. The variation of d_{00l} with chain length indicates that the axis of the chains must be nearly normal to (001), while a consideration of the intensities of (00l) reflections indicates that the chains are probably not exactly normal to (001). The average cross section of the chains appears to be slightly less than that of the *n*-paraffin hydrocarbons. The relation of the structure to those of other paraffin-chain compounds is discussed.

[1] Kayme, Fisher, and Bickford, *Jour. Am. Oil Chemists Soc.*, **24**, 332 (1947).

AN APPARATUS FOR OBTAINING A POWDER DIFFRACTION PATTERN FROM A SINGLE CRYSTAL

F. W. Matthews and A. O. McIntosh,
Canadian Industries, Ltd.

A device which gives two complete simultaneous rotations to a single crystal is used to obtain diffraction patterns which simulate powder diffraction patterns. The relative intensity of the lines obtained is in reasonable agreement with those of the true powder pattern. The method may therefore be used for the identification of single crystals from published powder data. The method is useful in checking the identity of a crystal before proceeding with single crystal measurement. In metallurgical studies on coarse grained material powder measurements may be made in either the forward or back reflection region.

FERROELECTRIC ACTIVITIES OF BARIUM TITANATE

B. T. Matthias,
*Massachusetts Institute of Technology.**

Dielectric and optical investigations of single crystals confirm the ferroelectric behavior of barium titanate. Several modifications have been obtained, of which only the pseudocubic shows ferroelectric anomalies, although all have unusually high dielectric constants.

The pseudocubic crystals exhibit a domain structure. In each domain the polarization vector lies along one of the cube edges, and thus in first approximation each domain has tetragonal symmetry, the optic axis being the direction of polarization. The optical observations are complicated by the fact that compatibility of strain due to differently directed polarization, distorts each domain from ideal tetragonality.

Dielectric measurements confirm the optical observations, and in particular show that sufficiently large electric fields can orient the polar axis of all the domains into the field direction. The polarizability for small field strength is about three times higher perpendicular to the polar axis than parallel to it. The ideal single domain crystal is tetragonal below the Curie Point without the necessity of applying a field. Under special growing conditions, however, crystals can be obtained which correspond rather completely to a perfect uniaxial crystal.

As the anisotropy of the crystal can be changed, with respect to fixed axes in the sample, so greatly by an applied electric field, the peculiar piezoelectric resonance behavior of barium titanate ceramics can be understood.

* Now at Bell Telephone Laboratories.

COLLECTION AND PUBLICATION OF CRYSTALLOGRAPHIC DATA

W. C. McCrone,
Armour Research Foundation.

MORPHOLOGICAL AND OPTICAL CHARACTERIZATION OF ORGANIC CRYSTALS

W. C. McCrone,
Armour Research Foundation.

HIGH INTENSITY GEIGER-COUNTER SPECTROMETER WITH EXTENDED ANGULAR RANGE

William Parrish and E. A. Hamacher,
Philips Laboratories, Inc.

Description of the redesigned Norelco Diffraction Unit arranged for simultaneous use with various types of cameras and a new Geiger counter spectrometer-type goniometer designed to scan in the vertical plane. The x-ray tube is water-cooled and has four mica windows. It is run at about 7 times greater power input (for copper target) than the air-cooled spectrometer x-ray tube. This higher intensity allows a faster scanning speed, or greater precision for the same scanning speed due to faster averaging of the counting statistics. Full-wave rectification gives a greater linear range in the intensity measurements with the Geiger tube and allows the use of a Sorensen electronic voltage regulator on the input line.

The use of the vertically-mounted x-ray tube and goniometer makes it possible to obtain a continuous record of the back- and forward-reflection regions. As in the improved Norelco spectrometer (see abstract by Hamacher and Parrish) the length of the focal spot is parallel to the specimen axis of rotation. Vertical Soller slits limit the divergence of the beam in the horizontal plane and the slit system is designed with adjustable divergence, scatter and receiving slits.

The angular aperture of 38′ for the range 10°–70° 2θ covers a 20 mm. wide sample at 10° 2θ. Since focussing is inherently better in the back reflection region, the angular aperture can then be increased to 4° at 70° 2θ to again cover the same width sample. In this way, intensities are increased and more precise measurements are possible. To achieve this larger angular aperture, the focal spot must be viewed at 3° in order to avoid using radiation between 0° (grazing incidence) and 1° to the target face because the intensity falls off rapidly in this region. The focal spot, 9×1.5 mm., is 9×0.07 mm. in projection at 3° so that the resolution is comparable with that achieved in the improved Norelco spectrometer. With the present design of x-ray tube, scanning angles up to 150° 2θ are reached and new tube designs indicate this may be considerably increased. Greater dispersion results from the larger radius (15 cm.) and the higher intensity source makes it possible to use an even larger radius if desired. The circuits are rack-mounted and the goniometer is designed to be attached to existing generator units.

DESIGN AND OPERATION OF GRID-CONTROLLED FINE-FOCUS *X*-RAY TUBE*

R. Pepinsky,
Alabama Polytechnic Institute.

A demountable fine-focus grid-controlled x-ray tube has been developed for stroboscopic diffraction studies of periodic lattice distortions. The control grid provides a simple means for turning on and off the tube current and hence controlling the x-ray emission, while the fine focal spot affords a great enhancement in the net intensity of a parallel-collimated beam of small cross-section.

The electron gun, comprised of a linearly-extended spiral filament, reflecting electrode, control grid, and focussing shield, is near ground potential to facilitate application of control voltages, and the target is at high positive potential. The grid cut-off voltage is about 35 volts, and its capacity with respect to the other electrodes is low to facilitate application of very short (0.1 microsecond) pulses. With the reflector about 100 volts negative and the focussing shield 200 to 300 volts negative with respect to the filament, a current of some 200 microamps at an accelerating voltage of 35 KV can be concentrated into a sharply-defined focal spot approximately 0.15 mm. high by 0.8 mm. long. Viewed at 3° from the target surface, the projected length reduces to about 0.04 mm. The specific target loading is about 75 watts/mm.[2]

The fine focal spot permits the use of a single pinhole as a parallel-collimating device. An 0.005″ pinhole 12.5 cm. distant from the focus produces at the 3° grazing angle a beam of about 15′ divergence in the plane containing the long direction of the focal spot and the tube axis. This beam has the same intensity under DC excitation as that from a standard commercial diffraction tube, viewed at the same grazing angle, when the latter tube is operated at the same DC high voltage as the fine-focus tube but at 100 times the tube current.

The fine-focus tube thus provides a reduction by a factor of 100 in the input power required for a given average output intensity in a parallel-collimated beam of small cross-section. For periodically pulsed operation this results in extremely important reduction of the *peak* emission required from the cathode when the duty cycle (ratio of pulse length to repetition rate) is low and a beam of good *average* intensity is required.

Calculations are presented of permissible target loading under periodically pulsed excitation. These are based upon Bouwers'[1] calculations of loadings under short single pulse excitation, and upon the calculations and observations of de Graaf and Oosterkamp.[2] For low duty cycles at high repetition rates (50 to 100 KC) it is found that the *average* loading under pulsed operation can be as high as under DC excitation.

* Investigation conducted under contract with Signal Corps Engineering Laboratories.

[1] Bouwers, A., *Zeit. techn. Phys.*, **8**, 271 (1927).

[2] de Graaf, J. E., and Oosterkamp, W., *Jour. Sci. Inst.*, **15**, 293 (1938).

THE ELECTRONIC FOURIER SYNTHESIZER*

R. Pepinsky,
Alabama Polytechnic Institute.

Three new developments are reported in the electronic Fourier synthesizer under construction at Auburn:[1]

* The Fourier synthesizer is being developed under contract with the Office of Naval Research, Contract #N7onr-377.

[1] Pepinsky, R., *Jour. Appl. Phys.*, **18**, 601 (1947).

1. *Accurate* contour maps of electron densities or Patterson functions can be delineated directly on the presentation cathode-ray tube. This is accomplished by triggering coincidence circuits, set at predetermined voltage levels, directly from the synthesized voltage signal formerly applied for intensity modulation to the CR tube grid. The circuits produce 1-micro-second pips each time the synthesized signal crosses one of the preset levels, and these are applied to the CR tube grid in place of the entire synthesized signal.

As many of these contours as is desired can be delineated simultaneously on a map. These can be differentiated one from another by brightening or dotting various lines. The zero level of electron density can be set in through adjustment of the DC level of the synthesized signal.

The contouring technique was demonstrated on the model synthesizer previously shown at the CSA meeting at Annapolis, March 20, 1947.[2]

2. The restriction to centro-symmetric syntheses has been removed through the incorporation of sine as well as cosine terms. This was possible with addition of the required volume controls, switches and adding resistors, and by duplication of output portions of the 20 sine-wave oscillators only.

The possibility of non-centro-symmetric syntheses, combined with the obvious availability of one-dimensional syntheses, now afford rapid computation of general three-dimensional electron density and Patterson functions.

3. In combination with the synthesizer, a photoelectric procedure has been devised for computation of Fourier coefficients for two-dimensional functions, as defined by the relations:

$$\Omega_{H_1H_2}=\int_0^1\int_0^1 \Omega\cos 2\pi(H_1s_1+H_2s_2)ds_1ds_2+i\int_0^1\int_0^1 \Omega\sin 2\pi(H_1s_1+H_2s_2)ds_1ds_2.$$

This depends upon preparation of photographic transparencies corresponding to Ω, and the multiplication and integration of these over a unit of Ω with a "fringe" corresponding to $\cos 2\pi(h_1s_1+h_2s_2)$ or the corresponding sine. The fringes are available from the synthesizer, and the transparencies can be prepared by a radiographic technique.

The layout of the cosine and sine terms, on 42 panels ($19''\times36''$) of 40 terms each, and the general arrangement of the entire computer laboratory, are shown.

[2] Pepinsky, R., *Am. Mineral.*, **32**, 693 (1947).

OBSERVATIONS ON GEIGER COUNTER CHARACTERISTICS BY MEANS OF A GRID-CONTROLLED *X*-RAY TUBE*

R. Pepinsky and H. M. Long, Jr.,
Alabama Polytechnic Institute.

Control over the time of arrival of x-ray photons into a Geiger counter, as afforded by the grid-controlled x-ray tube reported in the preceding abstract, permits observations of importance in the theory and application of counter action.

1. Direct observation of dead and recovery times of counters, with simultaneous measurement of pulse heights and shapes in the recovery period. For example, under usual operating conditions the dead time in Norelco No. 62002 or 62003 counters is 100 microseconds; no photon arriving in a time less than this subsequent to a given counter discharge can be recorded as a pulse. Photons appearing later than 100 microseconds

* Development under contract with Signal Corps Engineering Laboratories, Bradley Beach, New Jersey.

after a count produce discharges which increase in height from zero at 100 microseconds to half maximum at 110 microseconds; and "full recovery," i.e., maximum pulse height, occurs at about 150 microseconds. A pulse height within the recovery period is related in a very definite way to the timing of the second photon.

2. Measurement of the time required for a photon-initiated discharge to reach the central wire, as a function of the distance of initial ionization from the wire. For the new Mica-window Norelco counters, e.g., and a beam parallel to the central wire and about 2 mm. distance from it, the counter pulse lags from 0.5 to 1.5 microseconds behind the arrival of the photon. This is presumably the time for collection of secondary electrons.

When the x-ray tube is periodically pulsed, the counter amplifying circuit can be gated off except during the times when discharges initiated only by x-ray pulses can appear. The background counts due to cosmic rays and radioactivity can then be very greatly reduced. In the present investigation a reduction by a factor of more than a hundred has been achieved.

Under self-quenching operation of the Norelco counters, scaling circuits with resolution times of less than 100 microseconds are unnecessary. For higher counting rates, resort is being had to counters of new design and to external quenching. Entirely reliable scalers with rates well in excess of a megacycle per second have been constructed, and it is recognized that properly-designed scaling circuits in themselves will not be the limiting factor in attainment of high resolution.

With the use of the entire fine focal spot as a source, as also described in the preceding abstract, it is possible to *meter* the photons issuing from one port of the x-ray tube by means of an auxiliary counter receiving a beam from an opposite port. The average deviation of the metered beam from a desired total number of photons can be reduced to any desired value by sampling a high enough number of counts in the monitoring beam. Direct measurements are presented of the statistics of this monitoring.

Circuitry for these observations is briefly described.

PREFERRED ORIENTATION AND SAMPLE PREPARATION FOR THE GEIGER-COUNTER SPECTROMETER

Annette Prévot and Guenter Schwarz,
The Johns Hopkins University.

We have been interested in the detection of small quantities of a light substance either pure or present in a mixture in low concentration.

The classical methods of sample preparation did not prove satisfactory for such a study. A holder, provided with a cavity to hold the sample, requires appreciable quantities of the substance. The use of a glass slide on which the sample mixed with a binder is spread causes a decrease in the absolute intensity of the diffracted beam due to the presence of the binder and an increase in the background due to scattering from the glass slide. The resultant increase in the statistical fluctuations makes it more difficult to distinguish weak lines from the background. In all standard methods, preferred orientation has to be prevented in order to obtain correct intensities of the diffracted lines.

Instead of avoiding preferred orientation we have been trying to produce it in order to favor one of the intense lines of the substance present in low concentration. The method we have used to create this preferred orientation has been to dissolve the substance under investigation and have the material recrystallize on the surface of the sample holder by evaporation of the solvent. The contribution to the background intensity due to the holder has been almost completely eliminated by supporting the sample on a very thin collodion film spread over a wire frame.

The method had been applied to dipentaerythritol (DiPE) either pure or mixed with pentaerythritol.

The study of mixtures led to the following results:

% of DiPE	Ratio of $\frac{\text{most intense line of PE}}{\text{most intense line of DiPE}}$ Cavity Holder	Crystallization
50%	2.0	0.3
5%	7.7	4

This technique has not given results sufficiently reproducible as to permit quantitative analysis of small amounts of DiPE, but must rather be considered as a method for the detection of impurities. Concentrations of DiPE as small as 1% can easily be detected. This corresponds to less than 0.1 mg of DiPE.

Some of the samples prepared from a 0.2% solution (absolute quantity of 20$_\gamma$ DiPE) still show a DiPE line; whereas a relative amount of about 2% DiPE can be considered as the limit of sensitivity when a powder specimen is packed in a cavity holder.

A GRAPHICAL METHOD FOR TRANSFORMING RHOMBOHEDRAL MILLER INDICES AND HEXAGONAL BRAVAIS-MILLER INDICES

Lewis S. Ramsdell,
University of Michigan.

In some cases published data for rhombohedral crystals list only the rhombohedral Miller indices. In presenting new data there is sometimes an advantage in using both the Miller and the Bravais-Miller indices. Easy transformation from either set to the other is possible with the reciprocal lattice. Since the direct representation of a rhombohedral reciprocal lattice is difficult, it is common practice to treat the rhombohedral cell as a doubly centered hexagonal cell, with lattice points at 000; 1/3, 2/3, 2/3; and 2/3, 1/3, 1/3. The characteristic extinctions of this centered cell eliminate two-thirds of the corresponding reciprocal lattice points. Such a lattice, with only the points corresponding to the permissible rhombohedral reflections present, can be used both as a rhombohedral and a hexagonal reciprocal lattice. By the suitable choice of lattice directions, the indices *hkl* or *hkī* can be determined directly for any point.

A COMPLETE STRUCTURE DETERMINATION

Barbara Rogers-Low,
Harvard Medical School.

THE USE OF MICROWAVE DIFFRACTION IN STRUCTURE ANALYSIS

Walter L. Roth,
General Electric Company.

Preliminary tests of the possibility of utilizing microwave diffraction from molecular models as an adjunct to crystal structure analysis have led to the following conclusions.

Commercial oscillators of 3750 Mc. and 24000 Mc. frequency (8 and 1.2 cm. wave length) generate sufficient power for studying diffraction phenomena. The use of superheterodyne reception provides sensitivity sufficient to detect the radiation scattered from

a small object, such as might be used to represent a single atom. Background radiation can be reduced with quarter-wavelength absorbers to an extent adequate for experimental work within the confines of an ordinary laboratory room. Diffraction patterns easily are observed by rotating a parabolic receiver about the diffracting cell, and measuring the intensity received as a function of angle. The intensity distribution in a cross section taken through a beam generated from a paraboloid or lens is not sufficiently constant to permit the vector addition of amplitudes from points within the unit cell by conventional methods, which require a wave front constant in both phase and intensity across the cell.

A new type of radar antenna has been designed, the basic feature being the incorporation of both phase and intensity control of the source. To be of practical use for the solution of molecular structure problems, the beam should be constant in amplitude to several per cent over an area of at least one square foot (corresponding to a unit cell). Calculations indicate that a beam with the required characteristics can be produced, but precision apparatus probably requiring several years development is necessary. Since the projected applications to molecular structure problems do not appear to warrant such extensive development, the project has been discontinued.

The experimental work was carried out largely by Miss Gabrielle Hamburger, with the assistance of Mr. Richard Koch who developed and assembled the necessary electronic circuits.

THE CRYSTAL STRUCTURE OF A METANILAMIDO-PYRIMIDINE

JOSEPH SINGER* AND I. FANKUCHEN,
Polytechnic Institute of Brooklyn.

The structure of 2-metanilamido-5-Br-pyrimidine has been worked out by two-dimensional Patterson and Fourier methods. The isomorphism of this compound with its iodine analogue was of assistance. The chlorine analogue has a different crystal structure. The lattice constants, as indexed for $P2_1/n$, are:

	a	b	c	β
Bromine:	9.53	5.64	21.9	92.5°
Iodine:	9.70	5.67	22.0	92.5°

About 75% of the $0kl$ structure factor signs were determined by successive trials in the usual way. The ring details remained unclear, however, until a subtraction-Fourier device was hit upon. A Fourier series using coefficients given by $(F_{0kl}^{obs} - F_{0kl}^{Br})$, where the temperature corrected Br contribution is subtracted from the observed F_{0kl}, gave sufficient detail to allow most of the remaining signs to be determined. Two trials resulted in a fairly clear Fourier projection and the intensity checks are good. The subtraction apparently works because the high order terms are emphasized. Absolute intensities are required. A second projection, $h0l$, is being worked on. At this point, several bond angles and bond lengths are already determined and lie within expected figures.

* At present with Franklin Institute, Philadelphia, Pa.

ANALYSIS OF TWINNED INTERGROWTHS OF CRYSTALS

C. B. SLAWSON,
University of Michigan.

All the crystal planes of two or more twinned individuals may be referred to the crystallographic axes of one of them. Every plane will have rational indices on the common axes. Equations are developed for transforming the indices. The forms resulting from some common twinning laws are presented in tabular form.

The juncture surfaces between twins may be (1) the twinning plane, which is crystallographically continuous, with no free energy at the interface, or (2) an interface of planes with unlike indices and free energy at the interface. The second type of juncture occurs in contact twins at the points of discontinuity if the twinning plane is step-like, and in all penetration twins. These suture junctions are surfaces of weakness and also commonly the locus of flaws and inclusions.

The potential twinning plane may be (1) a single layer of atoms which may be considered as common to both individuals, or (2) a double layer of atoms both of which may be common to each individual. An example of the single layer type would be a simple cubic structure twinned across the octahedron with the bonds inclined to the twinning plane while the tetrahedral-bonded diamond or sphalerite would be of the double layer type with the bonds between the layers normal to the twinning plane. One would therefore not expect to see twinning in the first type and would expect it to be common in the second type, as is the case with diamond, sphalerite, and fluorite. This results from the energy distribution on the twinning plane of the double layer type.

ELECTRON DIFFRACTION STUDIES OF MANGANESE PRECIPITATION IN MAGNESIUM ALLOYS

Lorenzo Sturkey,
Dow Chemical Company.

Manganese occurs either as an impurity or as a deliberately added constituent in practically all commercial magnesium alloys. Concentrations range from a few hundredths of a per cent in cell magnesium to something over one per cent in alloys containing no aluminum. It has been shown that many of the properties—especially grain size and corrosion characteristics—are directly connected with the composition and amount of manganese precipitation. Electron diffraction studies have been made using selective etching techniques[1] to study this precipitation, with the following results:

(*a*) *Magnesium plus 1–2% Mn (either with or without Ce)* contains α-Mn precipitation.

(*b*) Mg 1 Zn, 0–0.4 Fe, 0–0.3 Al, 0–0.4 Mn (rolled sheet): Mn is precipitated in one of the various Mn-Al compounds, depending upon the Mn to Al ratio in the alloy. β-Mn occurs at the composition containing 0.3% Al and 0.40% Mn with a 2% increase in the lattice constant of β-Mn.

(*c*) Cell magnesium, which contains other metallic elements as impurities only, shows Mn precipitation either as a Mn-Al phase or a Mn-Al-Cu phase when Al and Cu are present, even in quantities less than 0.01%.

(*d*) *Commercial Mg-Al-Zn alloys containing from 0.1–0.3% Mn:* Mn is present in the cast metal as $MnAl_6$ crystals unless the melt has been superheated. Single crystal patterns of a "cross-grating" nature from these $MnAl_6$ crystals are frequently obtained and may be used for structural and crystal habit information.

Superheated melts showing grain refinement when cast contain a different Mn precipitation of such a nature as to increase nucleation of magnesium crystals. Rolling or heat-treatment after casting usually results in additional $MnAl_6$ precipitation.

[1] Heidenreich, Sturkey, and Woods, *Jour. Appl. Physics*, **17**, 127 (1946).

FORMATION OF KCl CRYSTALS FROM AN AQUEOUS SOLUTION AT VARYING RATES OF EVAPORATION

Helmut Thielsch,
Lehigh University.

Crystallization of a substance can be described in terms of nucleation and crystal growth. However, depending upon the rates of the two phenomena, principally the latter,

distinctly different crystal patterns (crystal habit) may be produced. These have been studied in aqueous solutions in which the rates of nucleation and crystal growth were varied by changing the rates of evaporation of the water phase. This was accomplished with the aid of an efficient vacuum system.

Thus tests made on KCl aqueous solutions showed[1] that slow rates of crystallization will produce relatively few crystals having well developed cubic faces. This, of course, is in agreement with the theories of Stranski, Kossel and Volmer[2] who predict such formation under (or near) equilibrium conditions. The ions will deposit in tangential fashion building up orderly plane upon plane.

Above a definite rate of evaporation the KCl ions deposit in a linear dendritic pattern. This is due to temperature gradients from the released heat of fusion (or crystallization) which prevents crystal growth on the faces of the crystallites. Still faster rates of evaporation will produce a region in which crystallization occurs in an irregular dendritic pattern. Here ionic movement or migration may be restricted by extreme concentration currents. However, the resulting structure is still cubic in nature.

With maximum rates of evaporation the ions are not able to fall into a regular lattice arrangement. Instead, they "freeze" virtually in the positions which they held last in the liquid solution. This is the familiar amorphous state.

Only the first arrangement is thermodynamically stable. In the other three ion migration or reorientation will occur when the specimen is heated or is allowed to remain in a moist atmosphere for several days. These conditions will supply sufficient energy to the KCl ions allowing their rearrangement into the stable cubic lattice pattern.

Impurities present in the aqueous solution which are either insoluble, or due to their quantity or lower solubility will form nuclei ahead of the principal (KCl) substance, will act as seed crystals. The presence of these will increase the rate of crystallization tending to support growth in dendritic patterns instead of the equilibrium cubic planar structure. Moreover, the "foreign" atoms or ions will interfere with the migration phenomena, making it less likely for these dendrites to rearrange. This, however, depends on the amount and kind of impurities present and the "reorientation" energy supplied.

[1] Thielsch, H., *Jour. Chem. Phys.*, **13,** 249 (1945).

[2] Volmer, M., "Kinetic der Phasenbildung," Verlag von Theodor Steinkopff, Dresden und Leipzig (**1939**).

PUNCHED CARD METHODS OF FOURIER ANALYSIS

L. H. Thomas,
Watson Scientific Computing Laboratory.

The summation of numerical Fourier series may be done by standard punched card methods, at a speed depending on the rate of the slowest operation, multiplication. There are three methods of carrying out the multiplications required.

I. Using tables on cards of multiples of sines and cosines requires the minimum of equipment. A key-punch, sorter, and tabulator suffice; though a considerably smaller file of cards is required if a reproducer and summary punch is available. The equivalent of about 3000 multiplications per hour to six digit accuracy can be attained.

II. Multiplying by progressive digiting requires only tables on cards of sines and cosines; and key-punch, sorter, tabulator, and reproducer and summary punch. About the same speed of 3000 six digit multiplications an hour is possible for sums of 30 or more products.

III. Multiplying by machine is more flexible but requires a multiplying punch. With the new "603" multiplier, 6000 six digit multiplications can be done per hour. For all these methods a collator is useful but not essential.

There are available at the Watson Laboratory tables on cards for doing crystal structure Fourier analysis by method I. These consist of tables of A cos $(mn(2\pi/3))$ and A sin $(mn2\pi/3)$, $n=0, 1, 2, 3$ on the same card; for $m=0, 1, 2, 3$ and $A=-499000$ to 500000 by 1000 and from 1 to 999 by 1, values given to seven figures; 12000 cards: and corresponding cards for A cos $(mn2\pi/5)$ and A sin $(mn2\pi/5)$; 20000 cards. A complete three dimensional $60\times60\times30$ Patterson to five digit over-all accuracy can be done with these cards by the method of sub-series in five to seven weeks.

Tables on cards are being computed and will soon be available of cos z and sin z to six decimals and of sin z/z to five decimals with $z=2\pi rs/400$, $s=1, 2, \cdots 600$; $r=1, 2 \cdots 200$, for doing Fourier analysis by method II or method III.

OBSERVATIONS ON PIEZOELECTRIC CRYSTALS

Karl S. Van Dyke,
Wesleyan University.

Considerable thought has been given to tabulating the piezoelectric, dielectric and elastic properties of crystals for piezoelectric application. A scheme for systematic portrayal of the constants of the several properties by crystal classes, and for presenting the numerical values of the constants for ready use in piezoelectric equations of the bilinear type, has been developed. Calculations of the tables, or matrices, of constants has been carried out as part of a research program supported by a Signal Corps contract and has been completed for several commonly used crystals. The constants are given for all four of the forms of the basic equations (solved for any two of the four variables: stress, strain, field and electric displacement), taking the basic data from the literature. The data completed so far are incorporated in Part II of a report of January 20, 1948 to the Signal Corps as a volume entitled *A Manual of Piezoelectric Data* under the author's name. Data on additional crystals will be given in a second volume in July 1948.

Two other parts of this Signal Corps supported research may be of special interest to crystallographers. These are both treated in a Master's Degree thesis by Clyde P. Glover, appear in earlier reports to the Signal Corps and have been presented to the American Physical Society. One of these is the peculiar characteristic etching of a Z-cut plate of quartz by hydrofluoric acid when a field of five to ten thousand volts per millimeter is applied across the etching surface, following a technique used by Choong in China. Growth rings appear on the surface of the quartz, usually as nearly concentric triangles showing a preference for growth on major rhombs. The etching alternates within and between the triangular annuli among two characteristic types. These same two types of quartz are distinguishable in the selective blackening of quartz under x-ray illumination. The boundaries between regions under the two types of development coincide. Again, measurement of the optical density of x-irradiated quartz and of the coincident elastic defect, both as functions of the radiation time, shows the two phenomena to be different functions of the radiation, and the elastic defect to saturate at about half the irradiation which saturates the blackening.

PHOTOELASTIC PROPERTIES OF CRYSTALS

C. D. West and A. S. Makas,
Polaroid Corporation.

Elastic behavior of a solid can be visualized by specifying the dimensions of the triaxial strain ellipsoids which result from the deformations of an initial unit spherical element by applications of unit stresses; these dimensions are given through the elastic compliances s_{ik}. Similarly, photoelastic behavior of a transparent solid is visualized by specifying the

changes in the triaxial index ellipsoid which result from applications of unit stresses; these are given through the photoelastic compliances π_{ik}. From these two sets of material constants are derived the dimensionless photoelastic strain constants p_{ik} which show the optical effects accompanying unit strains. Data taken from the literature illustrate the very wide range of these three sets of constants for type materials (see Table 1, which includes for comparison the flow birefringence constant of a liquid containing highly anisotropic molecules). In general one gets the maximum birefringence per unit stress from the weakest solids, but the maximum per unit strain from the strongest solids.

TABLE 1. ELASTIC AND PHOTOELASTIC CONSTANTS UNDER SHEAR STRESS

Material	Elastic Compliance $1/G=2(s_{11}-s_{12})$ in 10^{-13} cm²/dyne	Photoelastic Compliance $2B/n^3=(\bar{\pi}_{11}-\bar{\pi}_{12})$ in 10^{-13}cm²/dyne	Photoelastic Strain Constant $\frac{1}{2}(\bar{p}_{11}-\bar{p}_{12})$
Diamond	3.58	0.78	0.225
MgO	9.82	1.24	0.126
CaF_2	16.8	1.42	0.086
LiF	27.0	1.44	0.053
Silica Glass	32.4	1.91	0.059
K alum	137	5.0 (av.)	0.037 (av.)
Bakelite, 21° C.	645	20.8	0.0323
Bakelite, 110° C.	358,000	558	0.00156
13% Aq. Gelatine Gel	72,500,000	44,600	0.000615
Range	(10^7)	(10^4)	(10^3)
Nitrobenzene in laminar flow, 20° C., $\eta=0.02$ poise		2,300	—

A more extensive survey of photoelastic behavior of solids would soon remove any illusion of regularity and reveal it be a highly capricious phenomenon—the $\bar{\pi}$ constant corresponding to a known s constant can be large or small in magnitude, positive or negative in sign, without any immediately obvious reason.

Isotropic bodies and trigonal and hexagonal crystals have one easily measured constant of stress birefringence $(\bar{\pi}_{11}-\bar{\pi}_{12})$; cubic and tetragonal crystals have two such constants $(\bar{\pi}_{11}-\bar{\pi}_{12})$ and $\bar{\pi}_{44}$ resp. $\bar{\pi}_{66}$, and the greater the difference between these two constants, the higher is the photoelastic anistropy of the crystal. We have measured approximate constants for cubic crystals which illustrate high photoelastic activity and anistropy as follows:

TABLE 2. PHOTOELASTIC ANISTROPY OF CUBIC CRYSTALS

Crystal	λ (mmu)	n	$\bar{\pi}_{11}-\bar{\pi}_{12}$	π_{44}
AgCl	560	2.08	−5.62	+8.89
Tl(Cl, Br), or KRS-6	560	2.36	(0)	−13.1
Tl(Br, I), or KRS-5	610	2.62	(−4)	−27.2

A known photoelastic anistropy can be utilized in locating crystallographic directions in a crystal block, in interpreting pressure figures observed polariscopically, and the like. An annealed plate of polycrystalline AgCl in tension reveals some grains with positive,

others with negative birefringence—this is understandable only in view of the opposite signs of its two constants as tabulated. The same plate in transverse torsion or bending also reveals birefringence which now is confined to the vicinity of such grain boundaries as are not perpendicular to the plane of the plate—this likewise new phenomenon can also only be understood in terms of photoelastic anistropy. Such photoelastic effects observed in polycrystalline plates of the cubic system one should be able to duplicate without difficulty in cemented models formed from unlike plastics (isotropic bodies) and study more conveniently in this way. A knowledge of photoelastic constants would seem to be necessary for interpreting the complex permanent birefringences observed in cubic crystals to result from plastic deformations.

CRYSTALLIZATION OF POTASSIUM NITRATE

V. C. Williams, L. O. Stine, and R. M. Garrels,
Northwestern University.

Potassium nitrate was crystallized from aqueous solutions in a small vacuum crystallizer under constant pressure and constant stirring conditions. Temperature-time curves for the crystallization were obtained, and data on crystal size procured by photographic sampling at regular time intervals. A plot of average crystal size against time gave a linear relationship; extrapolation to the time of zero size was made for comparison with the cooling curves. The time at which crystallization began, as indicated by this extrapolation, occurs several minutes before any heat effects, indicating that the linear growth does not occur until equilibrium is reached, and that growth prior to equilibrium is very rapid. Equilibrium was reached at an average size of approximately 0.1 millimeter; after this size was attained little further free nucleation occurred. The rate of cooling of the supersaturated solution was 1.5 times the rate after equilibrium was attained; rough calculations from the data available in the literature indicate a heat of crystallization of approximately 30–35 calories per gram. This is roughly one-half the heat absorbed during solution under nearly corresponding conditions; that is, from crystals to saturated solutions. The number of nuclei present at equilibrium in these experiments was about one per cubic millimeter, or 100,000 per 100 cubic centimeters of solution. The experiment was originally designed to secure data on the change of heat of crystallization with size, on the hypothesis that the very small sizes, because of increased surface energy, should show smaller heat effects. The variation was not detected, but difficulty in securing formation of enough nuclei may have obscured the effect.

INFORMATION CONCERNING THE WATER UPTAKE OF COLLAGEN AS EVIDENCED BY ITS LOW ANGLE *X*-RAY DIFFRACTION PATTERN

Barbara A. Wright,
Research Division, United Shoe Machinery Corp.

A series of low angle *x*-ray diffraction patterns of collagen were photographed under controlled conditions of humidity, temperature, and tension. A specially designed specimen holder was attached to our North American Philips low angle *x*-ray diffraction camera. Relative humidities from 2% to 100%, and temperatures from 20° C. to 100° C. can be maintained in this holder and various controllable amounts of tension can be applied to the sample. All patterns in this series were taken on the same sample of kangaroo tail tendon stained with phosphotungstic acid. These patterns show variations both in the fundamental collagen spacing and in the relative intensities of the observed orders as a function of relative humidity. No changes in the pattern were produced by variations in temperature from 20° C. to 70° C. A marked reduction of the over-all intensity of the diffraction

pattern occurs above this temperature range only at high humidities. Possible alterations in the collagen molecular structure which could account for these observations will be discussed.

SOME CRYSTALLINE HEMOGLOBINS

Dorothy Wrinch,
Smith College.

The classical study of crystalline hemoglobins by Reichert and Brown provides several instances of cubic and hexagonal crystals, many instances of such "pseudo-symmetries." Since x-ray studies afford many examples in which such "pseudo-symmetries" indicate a direct approach to the atomic pattern,[2] these instances may well provide pointers to the structural principle in which the protein essence resides. A preliminary analysis of two such instances follows:

I. Oxyhemoglobin of Albino of Mus norvegicus (p. 230).[1]

Orthorhombic. Axial ratio: $a:b:c=0.7829:1:0.7332$. Since $a:b:c=1/\sqrt{2}\times1.05:0.95:1/\sqrt{2}\times0.985$, a companion cell may be taken with unit displacements $[110]_c$, $[002]_c$, $[1\bar{1}0]_c$ in the cubic system $x_cy_cz_c$ from which the actual cell differs in its cell ratios by not more than ±5 per cent. Since $2x=x_c+y_c$, $2y=z_c$, $2z=x_c-y_c$, we may rewrite these relations and interpret the recorded forms as follows:

$(200)=(110)_c$, $(020)=(001)_c$, $(002)=(1\bar{1}0)_c$;
unit prism (110); $(220)=(111)_c$, $(2\bar{2}0)=(11\bar{1})_c$;
brachydome (011); $(022)=(1\bar{1}1)_c$, $(0\bar{2}2)=(1\bar{1}\bar{1})_c$.

Thus the companion cell has the single cubic form $w(111)_c$. Trillings in parallel on the unit prism as composition face are recorded. These the companion cell identifies as (w/3) trillings.

II. Oxyhemoglobin of Ursus americanus (p. 259).[1]

Monoclinic. Axial ratio: $a:b:c=1.2239:1:1.1429$, $\beta=75°5'$. The forms recorded are $(\bar{1}11)$, $(1\bar{1}0)$, (010), (001) and in twins $(2\bar{3}0)$. Since $a:b:c=\sqrt{6}/2\times1.03:1.03:\sqrt{6}/2\times0.97$, a companion cell may be taken with unit displacements $[111]_c$, $[\bar{1}10]_c$. $[111]_c$ in the cubic system from which the actual cell differs in its cell ratios by not more than ±3 per cent and in angle by $4°33'$, affording the following interpretations:

$(400)=(11\bar{2})_c$, $(020)=(\bar{1}10)_c$, $(004)=(112)_c$:
$(\bar{2}22)=(\bar{1}12)_c$, $(22\bar{2})=(\bar{1}1\bar{2})_c$, $(1\bar{1}1)=(100)_c$, $(\bar{1}\bar{1}\bar{1})=(0\bar{1}0)_c$:
$(2\bar{3}0)=(12\bar{1})_c$, $(23\bar{0})=(2\bar{1}\bar{1})_c$: $(44\bar{0})=(\bar{1}3\bar{2})_c$, $(\bar{4}40)=(\bar{3}12)_c$.

The measured angles correspondingly pass into angles of the cubic system.
(1) $78°30'=\bar{1}10$–$001\wedge1\bar{1}0$–$001=(13\bar{2})_c$–$(112)_c\wedge(31\bar{2})_c$–$(112)_c=\cos^{-1}(1/5)=78°28'$:
(2) $79°=1\bar{1}0\wedge001=(31\bar{2})_c\wedge(112)_c=\cos^{-1}(1/\sqrt{21})=77°24'$:
(3) $46°47'=\bar{1}11\wedge00\bar{1}=(\bar{1}12)_c\wedge(\bar{1}1\bar{2})_c=\cos^{-1}(2/3)=48°11'$.
Twins, in trillings with c as common axis and composition face $(2\bar{3}0)$ are recorded. These are translated into (w/3) trillings with common axis $[111]_c$ and composition faces $(2\bar{1}\bar{1})_c$, $(\bar{1}2\bar{1})_c$, $(\bar{1}\bar{1}2)_c$.

These two cases, and many others which can be analyzed in similar fashion, suggest the following conclusions. The hemoglobin crystals contain a dominant cubic theme,[2] to which

[1] The Crystallography of Hemoglobins. Carnegie Institution of Washington (1909).
[2] Wrinch, Dorothy, *Am. Mineral.*, **32**, 695 (1947).

the close approach of the crystal lattices to compound cubic lattices is due. This theme is associated with the submultiple cube, thus being closely definable in scale and in orientation. However the cubic theme is disturbed, in definite ways, by a minor non-cubic theme (since the crystal lattices are in fact not compound cubic lattices) though not so far as to be unrecognizable. It must be presumed, if these conclusions prove correct, that the dominant major theme comprises cubic skeltons of protein molecules and that the minor theme is the distribution of substituents or side chains on the molecular skeltons.

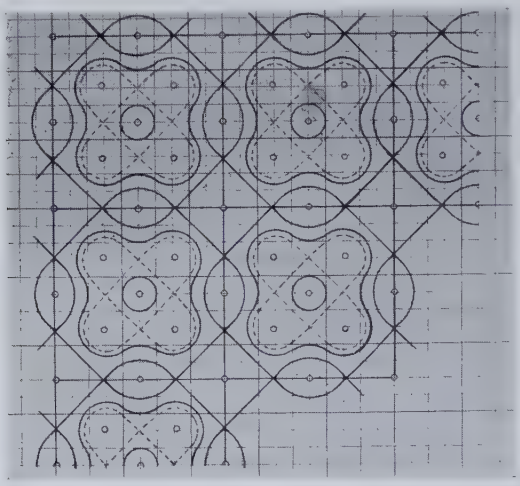

FIG. 1

AN APPLICATION OF FOURIER TRANSFORMS TO A CRYSTAL STRUCTURE ANALYSIS

DOROTHY WRINCH,
Smith College.

In an ASXRED Monograph,[1] a discussion of Fourier transforms has been given, with a view to their wider use in *x*-ray structure analysis. This note traces an application of these ideas to a crystal for which a complete structure analysis has been given,[2] namely pentaerithrytol $C(CH_2OH)_4$ which crystallizes with space group $I\bar{4}$ and $a=6.10$ Å, $c=8.73$ Å. While the procedures can be applied to the three-dimensional molecule, only the F_{hk0}'s will be considered. The extension to three dimensions introduces no new principle.

We adopt a crude representation for the molecule and take 9 points for its tetragonal projection, viz. $x_iy_i=00$, $\pm(10)$, $\pm(01)$, $\pm(20)$, $\pm(02)$ on a square lattice of metric k, thus adopting, for the C-C and C-O bonds indifferently, a length $a=k\sqrt{6}/2$. Then:

$$T(XY)=1+2\cos^2\pi X+2\cos 4\pi X+2\cos^2\pi Y+2\cos 4\pi Y$$
$$=4(\cos 2\pi X+1/4)^2+2(\cos 2\pi Y+1/4)^2-7/2.$$

Thus T has a square lattice with unit displacements $XY=10,01$ (cp. Fig. 1). The map has just one important "parameter" $X_1=\cos^{-1}(-1/4)=0.290$. On the diagonals of

[1] Wrinch, Dorothy, Fourier Transforms and Structure Factors (**1946**).
[2] Llewellyn, F. J., Cox, E. G., and Goodwin, T. H., *J. Chem. Soc.*, 883 (**1937**).

the square, it marks the minimum $T=-7/2$, on the edges the col $T=11/4$, on the line $Y=1/2$ the col $T=-5/4$. The general topology of the transform is then determined. To draw contours to any degree of fineness it is necessary and sufficient to compute $\cos^2 \pi X + \cos 4\pi X$ correspondingly: the points in which the contours hit the diagonals; edges and the lines $Y=1/2$ are then known.

With the transform drawn to any convenient scale, the scale in reciprocal space is fixed. If the unit cell has edge (say) 10 cm., then on our map 10 cm. means $d^*=1/k$. With $a=1.5°$ Å, for example, 10 cm. would mean $d^*=1/1.225$ Å. With suitable values of k in mind (e.g. 1.225 Å), we compare the map with the map of F_{hk0} on the same scale, placing the origin on any node of the transform. Rotating one relative to the other changes the mutual orientation of the molecule and the crystal. Our objective, of course, is to find—with some small latitude in k—the orientation which will place large F's in regions in which $|T|$ is large, whether positive or negative and small F's in regions where $|T|$ is small. This we find is achieved in large measure by orienting the intensity map at $\tan^{-1}(4/3)$ to the axes of the molecules, with the identification $XY=20$, $hk=86$. We therefore write: $h=4X-3Y$, $k=3X+4Y$; $25x=4x_t-3y_t$, $25y=3x_t+4y_t$; thus obtaining for the atomic positions

carbon $(x_ty_t=10)$ $xy=0.16, 0.12$: oxygen $(x_ty_t=20)$ $xy=0.32, 0.24$.

These may be compared with the atomic positions derived from the Patterson map and with those finally adopted after the complete structure analysis,[2] viz.

carbon $xy=0.161, 0.123$; oxygen $xy=0.314, 0.247$:
$xy=0.162, 0.123$; $xy=0.317, 0.247$.

It should also be recorded that, when we assign to each F the sign of the region of the transform in which it finds itself, 46 of the 48 signs are those adopted in the structure analysis.[2] The two F's in question are $F_{400}=5.3$ and $F_{730}<2.8$ and $F_{000}=148$. We could then, of course, proceed in the usual manner, no longer focussing attention on the atomic positions yielded by the extremely crude representation of the molecule through the transform and so obtain a Fourier synthesis in atomic space practically indistinguishable from the distribution found in the structure analysis.

In this example of the actual use of Fourier transforms, the following points may be emphasized. (*A*) The representation used for the molecule is extremely crude in that (1) atomic scattering factors are neglected, i.e. atoms are represented by points, (2) carbons and oxygens are not distinguished, i.e. each point has the same weight, (3) C-C and C-O bonds are given a common length. (*B*) The resulting transform is then extremely simple and can be computed within the hour. (*C*) Despite the crudeness of the transform the xy parameters for the atoms are found within 3 per cent and the signs adopted for the F's are correctly assigned in almost all cases. It may therefore be claimed that, regarded as a preliminary to the stage of the refinement of parameters, the use of a Fourier transform can be both efficient and swift.

CRYSTAL CHEMISTRY OF THE ELEMENTS FROM ACTINIUM TO AMERICIUM

W. H. Zachariasen,
Argonne National Laboratory and Department of Physics,
University of Chicago.

During and after the war crystal structure studies have been carried out on a number of compounds of actinium, thorium, uranium, neptunium, plutonium and americium.

Most of the investigated compounds correspond to the tetravalent or trivalent states. The

structures deduced for these compounds indicate that the binding is predominantly ionic in character. Table 1 shows the ionic radii of the trivalent and tetravalent ions for coordination number six. The radii were deduced from observed distances in oxygen and fluorine compounds using ionic radii of 1.40 Å for O^{-2} and 1.33 Å for F^{-}. The monotonic decrease of ionic radius with increasing atomic number represents experimental proof that the added electrons enter the 5*f*-shell.

A similar decrease in the size of the $(XO_2)^{+2}$-radical is observed in passing from uranyl to neptunyl to plutonyl compounds.

In the subnormal valence states the variation of crystal radius with increasing atomic number shows irregularities which are not understood at present.

Table 1. Ionic Radii

Number of 5*f*-Electrons	Thoride Series	Actinide Series
0	Th^{+4} 0.95 Å	Ac^{+3} 1.11 Å
1	Pa^{+4} (0.91)	(Th^{+3} 1.08)
2	U^{+4} 0.89	(Pa^{+3} 1.06)
3	Np^{+4} 0.88	U^{+3} 1.04
4	Pu^{+4} 0.86	Np^{+3} 1.02
5	Am^{+4} 0.85	Pu^{+3} 1.01
6		Am^{+3} 1.00

CRYSTAL CHEMICAL RELATIONS IN INORGANIC PIEZOELECTRIC MATERIALS

Samuel Zerfoss,
Naval Research Laboratory.

Increased interest in specialized electronic gear has resulted in a renewed search for new synthetic piezoelectric materials. The war-time production of large single crystals of $NH_4H_2PO_4$ is a notable example. The Crystal Section of the Naval Research Laboratory has undertaken a comprehensive laboratory survey of piezoelectric materials and has completed the testing of all the likely water soluble inorganic compounds which were obtainable in the necessary form. The purpose of this paper is not to present the detailed experimental data of that investigation but to summarize some of the general relations observed. Wooster[1] has listed the simple crystal chemical relationships found to exist in piezoelectric inorganic salts. He showed for example that the majority of the piezoelectric materials contain a radical which does not possess a center of symmetry. The more complete data of the present investigation are used in an attempt to extend these relationships and to account for the various exceptions.

[1] Wooster, Crystal Physics, Cambridge (**1938**).

BOOK REVIEWS

KLOCKMANN'S LEHRBUCH DER MINERALOGIE, Thirteenth Edition, revised by Paul Ramdohr. Octavo, XII+674 pp., with 606 text figures and one fold-in table. Ferdinand Enke Verlag, Stuttgart, Germany, 1948.

This widely used German text book first appeared in 1892. Due to its popularity, there have been frequent revisions. Professor Klockmann was the sole author of the first ten editions. Klockmann was professor of mineralogy and petrography at the Claustahl School of Mines (1887–1899) and at the Technische Hochschule in Aachen (1899–1924). The eleventh edition, issued in 1936, was revised by Dr. Ramdohr, professor of mineralogy at the University of Berlin, who had earlier been on the staffs of the institutions in Claustahl and Aachen. Subsequent editions were also revised by Ramdohr.

That the study of mineralogy still makes a strong appeal in war-stricken Germany is clearly shown by the fact that the twelfth edition appeared during the war, in 1941, and the present edition in the difficult post-war period, in 1948.

The earlier editions of the Klockmann mineralogy were in the main like other German texts, such as, Naumann–Zirkel, Bauer, and Tschermak–Becke. Mineral associations and the important occurrences and economic uses of minerals were, however, always stressed. Under the authorship of Professor Ramdohr, the book has been expanded and much of the material given a modern treatment. The mineral classification followed in the twelfth and thirteenth editions is essentially that used by H. Strunz in his Mineralogische Tabellen (Leipzig, 1941).* It is to be regretted that the excellent tables for the determination of minerals by means of their physical properties, which were an important feature of the Klockmann editions, are no longer included. In its present form the Klockmann-Ramdohr Lehrbuch der Mineralogie is the best text designed to meet the needs of students of mineralogy, chemistry, geology, and mining, and of mineral collectors and laymen, which has been published in Germany in the last decade.

Edward H. Kraus,
University of Michigan

* Reviewed by A. F. Rogers, *Am. Mineral.*, **33**, 95–96 (1948).

FESTSCHRIFT FOR PAUL NIGGLI

On June 26, 1948, Paul Niggli, world-renowned Swiss mineralogist, crystallographer, geologist, and educator, celebrated his sixtieth birthday. In his honor for that occasion there has been published a notable series of scientific papers by his "students, coworkers, and Swiss colleagues." The collection, which numbers forty-seven articles, under fifty-one authors, appears as volume 28 of the *Schweizerische mineralogische und petrographische Mitteilungen*. The articles embrace the subjects, crystallography, crystal structure, petroleum geology, geochemistry, petrography, petrogenesis, economic geology, metamorphic geology, paleontology, geophysics, structural geology, descriptive mineralogy, paragenesis, chemical mineralogy, optical mineralogy, and glacial geology. To enumerate a few titles of papers, we may select the following: L. Weber: "Die Verzerrungen des Oktaeders"; L. Déverin: "Oolithes ferrugineuses des Alpes et du Jura"; W. Q. Kennedy: "Crustal layers and the origin of ore deposits"; R. Staub: "Aktuelle Fragen im alpinen Grundgebirge"; R. L. Parker: "Zur Kristallographie von Tinzenit"; and M. de Quervain: "Das Korngefüge von Schnee." Most articles are in German, but others are in French, Italian, and English. The titles reflect, in their wide variety, the manifold interests and accomplishments of Professor Niggli, whose publications are enumerated at the close of the work. This impressive tabulation, which lists his first paper in 1908, contains a total of 247 titles, of which

more than a dozen are books and many others are complete volumes of investigations published by the Geological Commission of Switzerland.

This memorable tribute to the scientific endeavors and achievements of Professor Niggli comes at a fitting time. Long widely known in Europe as an outstanding scholar of the earth sciences and allied fields, and as an inspiring teacher who has personally guided the doctoral dissertations of forty-two students from all over the world, Professor Niggli received formal recognition of the esteem of American mineralogists in 1947 when he was awarded the Col. Washington A. Roebling medal of the Mineralogical Society of America. On this occasion, the sixtieth year of Paul Niggli and the fortieth of his career, his American friends join in expressing their congratulations and well wishes.

E. Wm. Heinrich,
University of Michigan

NEW MINERAL NAMES

Bredigite

C. E. Tilley and H. C. G. Vincent, The occurrence of an orthorhombic high-temperature form of Ca_2SiO_4 (bredigite) in the Scawt Hill contact-zone and as a constituent of slags: *Mineralog. Mag.*, **28,** 255–271 (1948).

The pseudo-hexagonal orthorhombic form of Ca_2SiO_4, designated as α^1-Ca_2SiO_4, has been found at Scawt Hill, Antrim Co., Ireland, associated with larnite, gehlenite, and spurrite in one assemblage, with melilite, larnite, perovskite, and magnetite in another. Also observed in the limestone contact zone of the island of Muck, Inverness-shire, and in a spiegeleisen slag that contained melilite, monticellite solid solution, CaS, and glass. An analysis of a sample separated from the slag is given. It contained a little sulfide and glass and had G. 3.42. The analysis, recalculated after deducting impurities, shows good agreement with Ca_2SiO_4, with 3.4% MnO, 6.9% BaO, and 6.8% MgO. Bredigite is optically positive with $\gamma=c$, $\alpha=b$, $\beta=a$, 2V 30°, but variable down to 10°; indices: $\alpha=1.712$, $\beta=1.716$, $\gamma=1.725$; $\alpha=1.725$, $\beta=1.728$, $\gamma=1.740$ (from melilite-magnetite assemblage, probably contains Fe); $\alpha=1.713$, $\beta=1.717$, $\gamma=1.732$ (from slag). Basal sections have hexagonal outlines in cross-section and show simple and cyclic twinning and traces of prismatic cleavage.

Some samples showed partial inversion to $\gamma-Ca_2SiO_4$. Bredigite dissolves readily in the weakest acids, leaving a silica pseudomorph.

Named for M. A. Bredig, physical chemist, for his studies of the polymorphism of Ca_2SiO_4 (see *Am. Mineral.*, **28,** 594 (1943).

Michael Fleischer

Rashleighite

Arthur Russell, On rashleighite, a new mineral from Cornwall, intermediate between turquoise and chalcosiderite. *Mineralog. Mag.*, **28,** 353–358 (1948).

The name rashleighite is given to a mineral of the turquoise-chalcosiderite series. Two complete analyses are given; they show Al_2O_3 21.63, 20.84; Fe_2O_3 20.29, 21.29; Al_2O_3/Fe_2O_3 1.69, 1.53. Two occurrences are described. At the Bunny tin-tungsten mine, St. Austell, Cornwall, it occurs in ore veinlets in greisen, associated with quartz, kaolimite, tourmaline, fluorite, topaz, cassiterite, and wolframite. At the Castel-an-dinas tungsten mine, St. Columb Major, Cornwall, it occurs with quartz, wolframite, wavellite, and lithiamica. The name is for Phillip Rashleigh, 1729–1811, Cornish mineralogist.

Discussion: An unnecessary name for ferrian turquoise.

M.F.

Wisaksonite

J. H. Druif, On the occurrence of a new mineral species in the deposits of the river Pekoeringan, district Masamba, Celebes: *Communications of the General Agricultural Experiment Station*, Buitenzorg, Java, No. **69,** 8 pp. (1948).

The mineral occurs as minute grass- to emerald-green tetragonal crystals. These are isotropic or nearly so, optically positive, n above 1.800. Insoluble in HCl, no data on chemical composition. Heavy, d. "probably about 4." Found in heavy mineral concentrates from river sand, associated with much colorless and pink zircon, allanite, biotite, green amphibole, some epidote, sphene, and aptite, and traces of chloritoid, glaucophane, tourmaline, and corundum. Sometimes observed in regular intergrowth with zircon. The name is for Wisaksono Wirjodihardjo, the first Javanese Acting Chief of the Institute for Soil Research at Buitenzorg.

Discussion: This is another example of the unfortunate practice of naming a mineral on the basis of practically no data. Druif says, "At the first glance one feels almost compelled to identify this mineral as *green zircon*. . . . However, when the fact of the absence of double refraction becomes revealed, this supposition cannot be upheld any longer." Druif was apparently unaware of the fact that zircon of low density and low birefringence has been studied repeatedly; some recent references are Chudoba and Stackelberg, *Z. Krist.*, **95,** 230–246 (1936); **97,** 252–262 (1937); Leitz, *Z. Krist.*, **98,** 201–210 (1937); Stott and Hilliard, *Mineralog. Mag.*, **27,** 198–203 (1946). There seems little reason to suppose that the material here given a new name is anything but low-density zircon.

M.F.

Basaluminite Hydrobasaluminite

F. A. Bannister and S. E. Hollingsworth, Two new British minerals. *Nature*: **162,** No. 4119, 565 (1948).

White, plastic material, hitherto thought to be allophane, was found to be an aluminum sulfate. Analyses of air-dried material by C. O. Harvey gave SO_3 15.6, 14.2; Al_2O_3 43.0, 41.3; Fe_2O_3 0.3, 0.2; P_2O_5 trace, 1.0; H_2O by difference 38.7, 39.7%. This corresponds, deducting about 5% allophane, to $2Al_2O_3 \cdot SO_3 \cdot 10H_2O$, and the mineral is named basaluminite. Its composition is close to that of felsobanyite, but its x-ray powder pattern, with longest spacing 9.2 Å, differs from that of felsobanyite. Basaluminite is fine-grained, anisotropic, with mean n about 1.510.

Samples of the plastic material, preserved in contact with water, gave an x-ray pattern with longest spacing 12.9 Å. The water content of this fully hydrated material, named hydrobasaluminite, is not known. It loses approximately 50% by weight at 16° C. in ten days before constant weight is reached and the powder pattern of basaluminite only is given.

The mineral occurs coating of joint-faces and as a fissure breccia in quarries in the Northampton Ironstone, especially at the Lodge Pit, Irchester Ironstone Co., two miles south of Wellingsborough.

M.F.

NEW DATA

Wehrlite

K. Sztrokay, Über den Wehrlit (Pilsenit): *Ann. Hist.-Nat. Musei Natl. Hungarici*, **39**, 75–103 (1946).

Optical study by reflected light was made on three samples from the type locality, Borszony (Deutsch-Pilsen). The specimens were found to contain tellurbismuth (Bi_2Te_3), tetradymite (Bi_2Te_2S), a similar phase, assumed to be Bi_2TeS_2, also bismuthinite (Bi_2S_3) hessite (Ag_2Te), and a little native Bi, petzite, gold, and molybdenite.

Discussion: The results do not agree with the *x*-ray work of Peacock (Warren and Peacock, *Univ. of Toronto, Geol. Ser.* No. **49**, 55–70 (1945)). Further work is necessary before the species can be considered discredited.

M.F.

Charles H. Behre, Jr., professor of economic geology, at Columbia University, has been granted a leave of absence for the year 1948–49 to continue the study of the genesis, distribution and geologic control of the mineral deposits of Mexico. T. S. Lovering of the U. S. Geological Survey and Donald M. Davidson of the E. J. Longyear Company lectured in the Department of Geology in October and November on ore genesis and its influence in search for minerals.

The U. S. Geological Survey has prepared for *x*-ray diffraction workers tables of *d* spacings based on the solution of the Bragg equation $n\lambda = 2d \sin\theta$. It is entitled: "Circular **29**: Tables of *d* spacings for angle 2θ." Spacings are tabulated for CuKα, CuKα_1, CuKα_2, FeK$_\alpha$ FeKα_1, and FeKα_2 in steps of 0.05° θ. Wave lengths used are those agreed upon in July, 1946, by the *X*-ray Analysis Group of the Institute of Physics (Great Britain). The tables are available free on application to the Director, U. S. Geological Survey, Washington 25, D. C. The data has been compiled by George Switzer, Joseph M. Axelrod, Marie L. Lindbergh, and Esper S. Larsen, 3d.

Attention is called to a new German journal of mineralogy and the revival of an old one. The new one is *Heidelberger Beiträge zur Mineralogie und Petrographie*. O. H. Erdmannsdorffer, Univ. Heidelberg, is editor and Springer-Verlag of Heidelberg, publisher. Vol. 1, No. 1, is dated Nov., 1947, and its price is given as *RM* 14.60. The revival is *Tschermak's mineralogische und petrographische Mitteilungen*. Vol. 1, No. 1 of Ser. 3 is dated June, 1948. The editors are F. Machatschki and H. Leitmeier, Univ. Vienna. No price is given. Published by Springer-Verlag, Wien I, Molkerbastei 5.

In the first issue of the new *Tschermak's Mitt.*, the deaths are reported of:

Max Haitinger, Vienna, died Feb. 19, 1946.

Emil Dittler, Mineralog. Inst., Univ. Vienna, died Nov. 9, 1945.

A comprehensive 20-page authors, name, and subject index of the first 73 issues of Industrial Diamond Review, 1940–1946 (vols. 1–6) has been prepared and is for sale at 3/- each. Address: N. A. G. Press, Ltd., 226 Latymer Court, Hammersmith, London, W. 1.

James G. Manchester, a summer resident of Hampton Bays, Long Island, New York, and Past President of the New York Mineralogical Club, died July 28, 1948, at the age of 76. His publications include a very attractive book on The Minerals of New York City and

Its Environs (Bulletin of the New York Mineralogical Club, vol. 3, No. 1, 1931), a booklet on The Minerals of the Erie Cut, Bergen Hill, New Jersey, and a number of papers.

Dr. A. Lacroix of the Museum d'Histoire Naturelle, Paris, France, a Correspondent of The Mineralogical Society, died March 16, 1948.

The Department of Geology and Geography of the University of Tennessee is sponsoring a symposium on the mineral resources of the Southeast. Sessions will be held on the campus at Knoxville, on March 3, 4, and 5. Papers on the major metallic and non-metallic mineral products of the Southeast will be presented by invited speakers.

Professional Paper 180, The minerals of Franklin and Sterling Hill, Sussex County, New Jersey, by Charles Palache has been reprinted and is for sale by the Superintendent of Documents, Government Printing Office, Washington 25, D.C. Price 75 cents.

Alexander N. Winchell has accepted an appointment as visiting professor in the School of Geology of the University of Virginia for the present school year. He will continue to do some consulting work. His address until next June will be University Station, Charlottesville, Virginia.

Bulletin 95 of the U. S. Department of the Interior, Bureau of Mines, A Glossary of the Mining and Mineral Industry, by Albert H. Fay, has been reprinted from the 1920 edition without change and can now be purchased from the Superintendent of Documents, U. S. Government Printing Office, Washington 25, D. C., for $1.75. The book lists many mineralogical and petrological names and terms.

The fourth Annual Spring Meeting of the Crystallographic Society of America will be held at University of Michigan, Ann Arbor, Michigan, April 7, 8, 9, 1949. Rooms and meals will be available at the Michigan Union which will handle reservations. The closing date for titles of papers to be presented at this meeting is January 15 and for abstracts March 1, and should be sent to Dr. Howard T. Evans, Jr., Laboratory for Insulation Research, Massachusetts Institute of Technology, Cambridge 39, Mass. At least one of the sessions will be devoted to a symposium on some special topic of general crystallographic interest.

INDEX TO VOLUME 33

Leading articles are in **bold face** type; notes, abstracts and reviews are in ordinary type. Only minerals for which definite data are given are indexed.

GEORGE BANTA PUBLISHING COMPANY, MENASHA, WISCONSIN